JPRS L/10408

24 March 1982

Translation

HOLOGRAPHY AND OPTICAL INFORMATION PROCESSING IN GEOLOGY

Ed. by

S.B. Gurevich and O.A. Potapov

FBIS FOREIGN BROADCAST INFORMATION SERVICE

NOTE

JPRS publications contain information primarily from foreign newspapers, periodicals and books, but also from news agency transmissions and broadcasts. Materials from foreign-language sources are translated; those from English-language sources are transcribed or reprinted, with the original phrasing and other characteristics retained.

Headlines, editorial reports, and material enclosed in brackets [] are supplied by JPRS. Processing indicators such as [Text] or [Excerpt] in the first line of each item, or following the last line of a brief, indicate how the original information was processed. Where no processing indicator is given, the information was summarized or extracted.

Unfamiliar names rendered phonetically or transliterated are enclosed in parentheses. Words or names preceded by a question mark and enclosed in parentheses were not clear in the original but have been supplied as appropriate in context. Other unattributed parenthetical notes within the body of an item originate with the source. Times within items are as given by source.

The contents of this publication in no way represent the policies, views or attitudes of the U.S. Government.

APPROVED FOR RELEASE: 2007/02/09: CIA-RDP82-00850R000500040054-3

JPRS L/10408

24 March 1982

HOLOGRAPHY AND OPTICAL INFORMATION PROCESSING IN GEOLOGY

Leningrad GOLOGRAFIYA I OPTICHESKAYA OBRABOTKA INFORMATSII V GEOLOGII in Russian 1980 (signed to press 19 Nov 80) pp 1-181

["Holography and Optical Information Processing in Geology", edited by Professor S.B. Gurevich and Candidate of Technical Sciences O.A. Potapov, Leningrad Physicotechnical Institute imeni A.F. Ioffe, USSR Academy of Sciences, 500 copies, 181 pages; for related material, see JPRS L/9206 23 Jul 80 No 13/80 (FOUO) USSR Report: Cybernetics, Computers and Automation Technology, pp 76-93]

CONTENTS

[I - USSR - N FOUO]

ANNOTATION

This collection of works is based on reports that were read at the Second All-Union Seminar on Geophysical Holography and Opticoelectronic Methods of Processing Geological and Geophysical Information, which was held in Gelendzhik in 1979.

The main theme of the collection is the use of the principles of holography in geophysical investigations, the processing of large masses of geological and geophysical information, and the creation of new instruments and devices for the opticoelectronic processing of geological and geophysical materials. Along with summary reports with this theme, there are discussions of specific methods and results. The material presented in the articles is of great value for the development of projects provided for in the national economic plan and the interdepartmental coordinating plan for geophysical holography, and it enables specialists in geophysics and geology to become acquainted with the new possibilities offered by holography and optical information processing methods in problems of searching for and surveying useful minerals, and also has the purpose of attracting the attention of specialists in other areas of science and technology to these important problems.

APPROVED FOR RELEASE: 2007/02/09: CIA-RDP82-00850R000500040054-3

FOREWORD

The complexity of the problems to be solved during geological surveying work aimed at various types of mineral raw materials requires an increase in the effectiveness of geophysical surveying methods that is based on the use of contemporary achievements in physics, mathematic and the technical sciences. Good prospects in this field are related to the use of the principles of holography and the processing of the information obtained by opticodigital computer complexes.

The first projects in this field, which were carried out in various organizations belonging to the USSR Ministry of Geology, the Ministry of the Gas Industry, the Ministry of Higher and Secondary Specialized Education and the USSR Academy of Sciences, indicates the possibility of using the basic principles of holography in the solution of geophysical surveying and geological problems. The results that have been obtained make it possible to hope for success in the utilization of geophysical holography and the opticoelectronic processing of original data for the solution of practical problems.

This collection of works consists of reports that were given at the Second All-Union Seminar on Holography and the Opticoelectronic Processing of Geological and Geophysical Information, which met at Gelendzhik in 1979 under the auspices of the Southern Branch of the USSR Academy of Sciences' Institute of Oceanology. The materials published in it will help attract specialists to problems, the solution of which is of great national economic importance.

UDC 550.834

GEOPHYSICAL HOLOGRAPHY AS A NEW FIELD IN THE INVESTIGATION OF GEOLOGICAL OBJECTS

Leningrad GOLOGRAFIYA I OPTICHESKAYA OBRABOTKA INFORMATSII V GEOLOGII in Russian 1980 (signed to press 19 Nov 80) pp 4-8

[Article by O.A. Potapov from collection of works "Holography and Optical Information Processing in Geology", edited by Professor S.B. Gurevich and Candidate of Technical Sciences O.A. Potapov, Leningrad Physicotechnical Institute imeni A.F. Ioffe, USSR Academy of Sciences, 500 copies, 181 pages]

[Text] The author elucidates on the problems that it is necessary to solve in the near future for the purpose of improving the accuracy and effectiveness of the study of geological objects by geophysical methods. He describes the structure of the basic directions of the work being done in the field of geophysical holography, which has been called upon to take up the challenge of solving part of the complex problems involved in geological explorations for the purpose of finding various types of mineral raw materials. He also points out the importance of creating highly efficient opticodigital complexes for the accelerated processing of ever-increasing volumes of information.

The rapid development of the USSR's national economy requires the creation of a strong material and raw material base, in connection with which a special urgency is attached to integrated geological and geophysical investigations aimed at the solution of the important national economic problems formulated by the 25th CPSU Congress for the purpose of improving the quality and effectiveness of geological prospecting for gas, oil and other types of mineral raw material.

For the successful solution of the problems set before the branch in the area of supplying the USSR's national economy with mineral resources--fuel and energy raw materials, in particular--it is necessary to expand the utilization of progressive geophysical methods in geological surveying work and provide a considerable improvement in the scientific and technical level and effectiveness of geophysical investigations that is based on the use of the latest achievements in physics, mathematics and the technical sciences. One of the important and promising areas for the further development and improvement of geophysical research is the development and introduction into production work of methods and systems for the excitation, registration and processing of wave fields (seismic wave fields, in particular) for the purpose of modeling (visualizing) studied objects on the basis of an analysis of an entire wave field and its amplitude and phase characteristics. This

branch of science has received the name "geophysical (seismic, acoustic, electromagnetic) holography."

Geophysical holography is a new and higher stage in the development of wave methods for exploration geophysics, which are distinguished by their extremely good resolution. This concept encompasses a broad circle of theoretical and experimental problems in geophysical research: the development of a theory for the recovery of objects exposed to a wave field; the creation of efficient, nonexplosive sources of wave energy; the development of techniques, equipment and technology for field observations, systems for processing and interpreting the information that is obtained, and facilities for the visualization of objects that are being studied. It is obvious that when developing the fundamental principles of geophysical holography, we must take into consideration and use (with the appropriate modifications) the methods and achievements of optical holography. At two interdepartmental conferences on geophysical holography that were held in 1978 and 1979 on the instructions of the Presidium of the USSR Academy of Sciences, the importance, promise, great national economic value and the high economic effect expected from the introduction of achievements in the field of geophysical holography were emphasized. In these conferences an extensive, integrated program for the development of projects in this field was prepared with the participation of many ministries and departments. This program was used as the basis for the formulation and discussion of the interdepartmental coordinating plan of work to be done during the 1980-1990 period and the "Physics--to the Depths of the Earth" program.

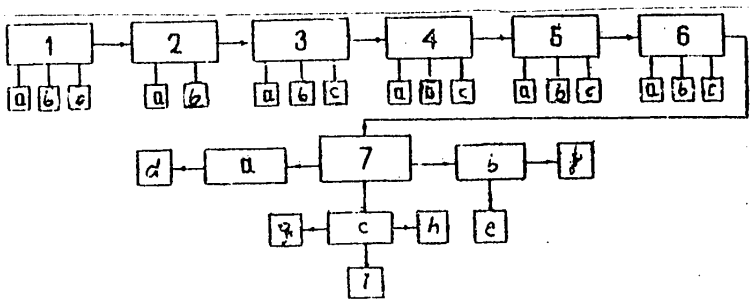

Figure 1. Structure of the basic directions of work being done in the area of geophysical holography: 1. development of theoretical principles of the use of seismic (a), acoustic (b) and electromagnetic (c) fields; 2. modeling of processes: mathematical (a) by computer calculations, physical (b), utilizing the principles of optical holography; 3. development of sources of seismic (a), acoustic (b) and electromagnetic (c) energy; 4. development of equipment for recording seismic (a), acoustic (b) and electromagnetic (c) fields; 5. creation of efficient field visualization devices: analog (a), digital (b) and three-dimensional (c) representations; 6. development of methods for observing and recording wave fields: land (a), sea (b) and aerial (c) variants; 7. processing of large amounts of information: creation of high-speed (a) systems for rapid field processing on the basis of opticodigital devices (d), creation of expedition-level computer complexes (b) based on opticoelectronic (e) and opticodigital (f) systems, creation of regional-level computer centers (c) using powerful computers (g), special high-speed optical processors (h) and optical displays (i).

From the structure of the basic directions of work being done in the field of geophysical holography that is presented in Figure 1, it follows that in the overall cycle of necessary developments, an important place is given to the creation of highly efficient optical, opticoelectronic and opticodigital equipment, both for the recording of wave fields and the solution of physical modeling problems and for the processing of data gathered during field observations. This is no accident, since the practical utilization of even normal geophysical profile observations demonstrates that the opticodigital area has acquired great urgency in relation to the processing of large masses of information [1-3], as has the creation of specialized seismoholographs [4]. The simplicity of such devices, as well as their portability, low cost and economy of operation makes this area one of primary importance.

Based on the work experience that has been amassed to date, it is possible to say that the solution of problems in geophysical holography by computers may give more accurate results, but it requires the use of powerful computers and the development of peripheral equipment, and will be accessible only in large, regional, departmental computer centers after the creation of the appropriate software, specialized processors, displays and other devices to use with a computer. At the present time it is a well-known fact that despite the explicit successes that have been achieved, the development of facilities for the automated processing of geophysical and (in particular) geological information on the basis of computers continues to lag behind the growing branch requirements. Scientific and technical progress in geology and exploration geophysics is making ever greater demands on the speed, efficiency and timeliness of the processing of large masses of data and is forcing us to look for new ways to solve the problems with which we are faced. In connection with this, it is advisable to develop and build expedition-level high-speed opticodigital systems that have a large optical (holographic) memory capacity and the capability to carry out parallel procedures, and that are distinguished by a rational distribution of the processing operations between electronic and optical computers. The presence in such complexes of a coherent optical processor, the appropriate matching devices and systems for the operational input and output of half-tone information will insure the rapid processing of geological and geophysical materials of different types.

The projects in progress at the present time make it possible to state that we have all the capabilities for the realization in the near future and the introduction into production work of highly efficient opticodigital complexes that are able to operate under both stationary conditions at expedition bases and field conditions, as well as on board scientific research ships. The cooperation of several organizations subordinate to the USSR Ministry of Geology, the Ministry of Higher and Secondary Specialized Education, the USSR Academy of Sciences and other departments is contributing to the successful realization of the program of projects that has been planned in this field. The work is being coordinated by the USSR Ministry of Geology's "Soyuzgeofizika" Scientific Production Association. The practical realization of the plan for geophysical holography as a whole requires the enlistment in this work of additional organizations that have mastered the contemporary achievements in the fields of physics, mathematics, cybernetics, instrument building and production technology.

BIBLIOGRAPHY

1. Potapov, O.A., "The Problem of Processing Large Masses of Geological and Geophysical Information and Ways of Solving It," in "Golografiya i opticheskaya obrabotka informatsii v geologii i geofizike" [Holography and the Optical Processing of Information in Geology and Geophysics], Leningrad, 1979, pp 5-18.

2. Potapov, O.A., Vorob'yev, O.A., and Dubyanskiy, V.I., "The Holographic Optico-digital Processing of Seismic Surveying Data," ibid., pp 95-101.

3. Potapov, O.A., "Opticheskaya obrabotka geofizicheskoy and geologicheskoy informatsii" [Optical Processing of Geophysical and Geological Information], Moscow, Izdatel'stvo "Nedra", 1977, p 184.

4. Potapov, O.A., and Dubyanskiy, V.I., "The State of Seismic Holography and the Opticoelectronic Processing of Seismic Recordings," REGIONAL'NAYA, RAZVEDOCHNAYA I PROMYSLOVAYA GEOFIZIKA: EKSPRESS-INFORMATSIYA/VNII EKONOMIKI MINERAL'NOGO SYR'YA I GEOLOGICHESKIKH RAZVEDOCHNYKH RABOT, Moscow, No 13, 1979, pp 29-40.

UDC 550.834

ARCHITECTURE OF AN OPTICODIGITAL COMPUTER COMPLEX WITH A COMMON MAIN MEMORY

Leningrad GOLOGRAFIYA I OPTICHESKAYA OBRABOTKA INFORMATSII V GEOLOGII in Russian 1980 (signed to press 19 Nov 80) pp 9-15

[Article by A.M. Kuvshinov, O.A. Potapov and R.G. Tazitdinov from collection of works "Holography and Optical Information Processing in Geology", edited by Professor S.B. Gurevich and Candidate of Technical Sciences O.A. Potapov, Leningrad Physicotechnical Institute imeni A.F. Ioffe, USSR Academy of Sciences, 500 copies, 181 pages]

[Text] The authors discuss the problem of organizing optico-digital complexes for the accelerated processing of geological and geophysical information. They propose a system with a common main memory that meets the contemporary requirements for the organization of computer systems. They also present specific plans for connecting a coherent optical processor to a YeS-22 computer.

The need for efficient processing of large masses of seismic information makes the practical realization of opticodigital computer complexes (OTsK) ever more urgent. An analysis that we made of methods of combining optical (OVM) and digital (TsVM) computers enabled us to draw the conclusion that the most realistic way of integrating a TsVM and an OVM at the present time is the creation of multimachine, directly connected computer systems [1]. After a discussion of the two types of directly connnected systems--through a common area in the main memory and through the input-output channels--we selected coupling through the input-output channels.

Basically, the choice of this principle for the physical organization and practical realization of the OTsK was the result of the contemporary level of development of OVM's and memory systems that would make satisfactory OVM's and TsVM's as far as operating speed and capacity are concerned. At the present time, a YeS-series TsVM has a main memory (OP) with a capacity of 0.25-0.5 Mbytes, although on the basis of its architecture it can have an OP with a capacity of 16 Mbytes [2].

In connection with the already begun industrial production of solid-state, large-capacity memory elements that are small in size but have the required capacity, the possibility of using them to create a large-capacity OP appeared to be quite real.

There are examples of the construction of an OP based on solid-state elements that has a capacity of 1 M bits and is contained on a single plate [3-5].

A high-speed, large-capacity OP makes it possible to build an OTsK according to a better principle of physical organization; namely, the principle of directly connected systems with a common OP.

In this case the jointly used part of the OP plays the role of a "post office box" for the exchange of information between the computers. One of them places some information in the "post office box" and signals the other that this has been done. After receiving the signal about the readiness of the information, the second computer can then use it in its work.

The advantage of the coupling of the OVM and the TsVM through the memory line over coupling through input-output lines consists of the following elements:
the information exchange speed is increased and the exchange program is simplified;
during multiprogram work the TsVM does not waste its memory resources on the storage of large masses of information;
when there is down time, the OVM and TsVM can use the common OP for their own needs, thereby increasing their own productivity;
when checking the results of the optical processing of information, the TsVM does not have to take into consideration all of the prepared information, but can consider only a few nodal points by checking the results of filtration, while in the case of coupling through input-output lines, the TsVM is obligated to take all the prepared information into its own memory. This operation makes it possible to achieve a considerable reduction in the amount of time needed to select the required optical filters;
it is necessary to synchronize the operation of the TsVM and the OVM, which makes it possible to operate the OVM with analog-to-digital (ATsP) and digital-to-analog (TsAP) converters with any operating speed without reducing the TsVM's computing power.

Our proposed plan for an opticodigital computer complex constructed on the principle of directly connected systems with a jointly used part of the OP is shown in Figure 1. The complex contains a general-purpose YeS-1022 TsVM, additional internal storage of the dynamic type, based on solid-state elements (DOZU) and having a control unit (BUDOZU), and an optical computer. The YeS-1022 TsVM is in its standard form. The OVM consists of a laser (OKG), an optical information input device (OUVv) with a control unit (BUOUVv), a coherent optical processor (KOP) with a control unit (BUKOP) and an optical memory (OOZU), an optical output device (OUV) with a control unit (BUOUV), and a microcomputer or microcontroller of the "Elektronika S5) type.

The coherent optical processor consists of a set of lenses, as well as spatio-temporal (PVMS) or spatial (PMS) light modulators. The KOP's control unit translates digital information into control signals for the light modulators. The optical memory is used to store a set of standard filters. The OUVv, with its control unit, carries out spatial modulation of a coherent light flow in accordance with the information entered in the KOP. The optical output device, with its control unit, converts light information at the KOP's outlet into an eight-bit digital code. The microcomputer controls information input and output.

When matching the optical and digital parts of the complex, we took into consideration the bit configuration of the YeS-1022's memory lines and the amount of information that can be processed simultaneously in the OVM. For the YeS-1022 and most

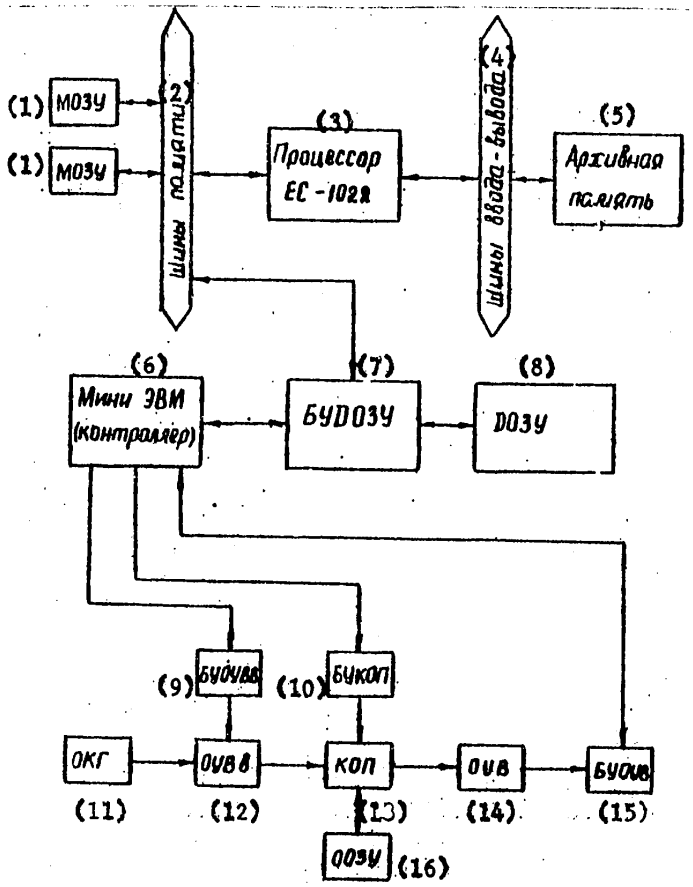

Figure 1.

Key:
1. Magnetic core storage
2. Memory lines
3. YeS-1022 processor
4. Input-output lines
5. Archive memory
6. Minicomputer (controller)
7. Additional internal storage control unit
8. Additional internal storage
9. Optical information input device control unit
10. Coherent optical processor control unit
11. Laser
12. Optical information input device
13. Coherent optical processor
14. Optical information output device
15. Optical information output device control unit
16. Optical memory

microcomputers, the word length of an exchange with the OP is 2 bytes [2,6], which organization was also used for the DOZU. The DOZU's capacity is determined by the number of independent reference points and the dynamic range of the optical input-output devices. When each point is encoded by a single byte, which provides a dynamic range of 48 decibels and an independent point mass of 3,000 x 300, the DOZU's capacity is 1 Mbyte.

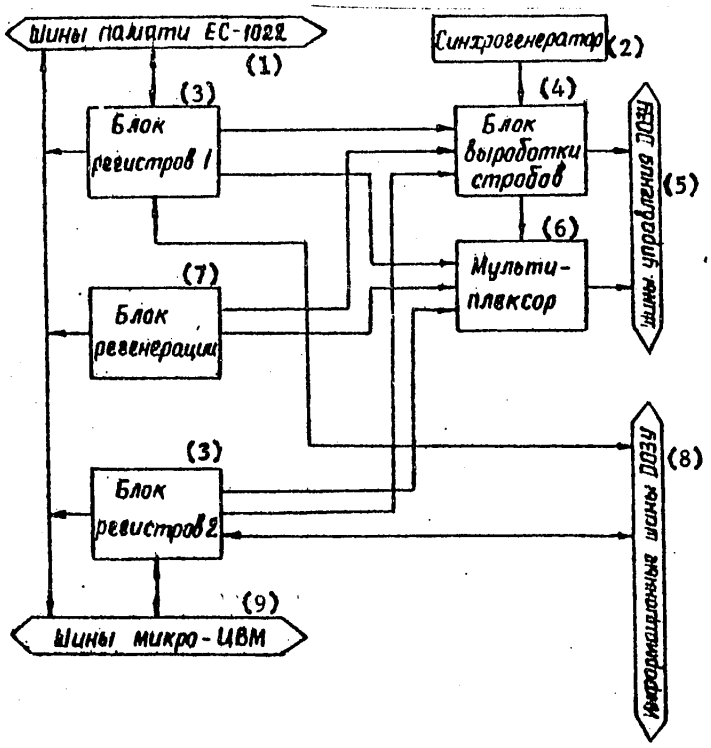

Figure 2.

Key:
1. YeS-1022 memory lines
2. Synchrogenerator
3. Register block #.
4. Strobe light operating unit
5. DOZU control lines
6. Multiplexor
7. Regeneration unit
8. DOZU information lines
9. Microcomputer lines

Since a microcontroller of the "Elektronika S5" type can address an OP using only 64 Kbytes [6], it is necessary to add to the BUDOZU an additional register that switches the DOZU's memory areas.

For the actual development, we used the most common YeS-1022 computer model and K565RUZ solid-state memory circuits of the dynamic type, which have a capabity of 16K bits. For matching with both processors, the DOZU was divided up on plates. Each plate has a capacity of 32 Kbytes, and there are 32 of them in the DOZU.

The DOZU's operation is controlled by the BUDOZU, the structure of which is shown in Figure 2.

The DOZU control unit must operate in two directions: the YeS-1022's memory lines and the microcomputer's lines. This is done by two units--register block 1 and register block 2. A strobe light operating unit controlled by a synchrogenerator is used to gate the K565RUZ microcircuits. The multiplexor switches information from about the DOZU's address from three directions: both processors and the regeneration unit.

The regeneration unit is needed to store recorded information in the DOZU, since the K565RUZ microcircuit is of the dynamic type. When operating with either computer, the other computer's lines are blocked. Both processors have the same priority for access to the DOZU. The regeneration unit has the highest priority. The regeneration period is no more than 2 ms, which provides the DOZU with 96 percent accessibility.

The OTsK operates in the following sequence. The TsVM computes the original information from the archive memory (magnetic tape) and enters it in the DOZU. Upon completion of information entry in the DOZU, the TsVM records a code with respect to a certain address (A_0) that contains information about the completion of work and to what unit this information should be transferred. When it receives an "Access" signal from the TsVM, the microcontroller takes the control information from A_0 and begins to extract the information from the DOZU and send it to the proper device. The distribution of addresses in the DOZU is strictly defined and corresponds to the optical pattern.

After the optical processing cycle is completed, the information enters the DOZU through the BUOUV. The microcomputer does the addressing. When the entry in the DOZU is completed, the microcomputer can repeat the optical processing cycle, using another optical filter, or transfer the processed information to the TsVM. The presence of the conventional code in A_0 and the reception of a signal to block the YeS-1022's memory lines serves as the TsVM access signal.

It should be mentioned that during the processing of information recorded on photographic film, the OTsK can operate discretely; that is, the OVM carries out the necessary filtration without the participation of the TsVM. In this case visual evaluation of the filtration is required. When the evaluation is positive, the results of the OVM's filtration can be published as results both through the common OP into the YeS-1022 and into the archive memory with subsequent processing in the TsVM. The proposed OTsK structure reduces to a minimum the interdependence of the OVM and the OTsM and, at the same time, makes it possible for them to exchange information at a high speed.

BIBLIOGRAPHY

1. Potapov, O.A., Vlasov, Ye.N., Kuvshinov, A.M., and Kiryukhin, V.V., "Principles of the Organization of an Opticodigital Computer System for the Processing of Geophysical Information," EKSPRESS-INFORMATSII, Moscow, VIEM [expansion unknown], No 10, 1980, pp 1-11.

2. Drozdov, Ye.A., et al., "Elektronnyye vychislitel'nyye mashiny edinoy sistemy" [Electronic Computers in the Unified System Series], Moscow, Izdatel'stvo "Mashinostroyeniye", 1976.

3. Kouker, "A 16 Kbit ZUPV [expansion unknown] That Simplifies the Realization of the Memory of Large Computers and Microcomputers," ELEKTRONIKA, No 9, 1977 (translated from English).

4. Titov, Yu.M., et al., "A Semiconducting Memory Module for a Microcomputer," in "Mikroelektronika i poluprovodnikovyye pribory" [Microelectronics and Semiconducting Instruments], Moscow, Izdatel'stvo Sovetskoye Radio, No 4, 1979.

5. Kou, Oldkhem, "The First 16-Kbit ZUPV's: Design and Organization," ELEKTRONIKA, No 4, 1976 (translated from English).

6. Val'kov, V.M., "Mikroelektronnyye upravlyayushchiye vychislitel'nyye kompleksy" [Microelectronic Control Computer Complexes], Leningrad, Izdatel'stvo "Mashinostroyeniye", 1979.

UDC 550.834

DEVICES FOR ENTERING INFORMATION FROM AN OPTICAL COMPUTER AND THEIR COUPLING WITH AN ELECTRONIC COMPUTER

Leningrad GOLOGRAFIYA I OPTICHESKAYA OBRABOTKA INFORMATSII V GEOLOGII in Russian 1980 (signed to press 19 Nov 80) pp 16-31

[Article by A.M. Kuvshinov, V.V. Kiryukhin, A.I. Orlov, O.A. Potapov and L.S. Ryazanov from collection of works "Holography and Optical Information Processing in Geology", edited by Professor S.B. Gurevich and Candidate of Technical Sciences O.A. Potapov, Leningrad Physicotechnical Institute imeni A.F. Ioffe, USSR Academy of Sciences, 500 copies, 181 pages]

[Text] The authors discuss the problems involved in matching electronic and optical computers when organizing opticodigital complexes for the accelerated processing of geological and geophysical information. They propose and describe an optico-mechanical device that has been developed and is characterized by a comparatively low (in comparison with solid-state coordinate-sensitive elements) operating speed, but a large dynamic range and accuracy in information transmission.

The basic technical problems that have to be solved for the creation of optico-digital systems consist of the development of optical information input-output devices and units for coupling the optical and digital parts of the system. Since coherent optical computers (OVM) are the ones most widely used in seismic research, the problem is reduced to the development of facilities for exchanging information between a laser installation and a digital computer.

The result of the processing of information in coherent computers is presented in the form of the distribution of the brightness of the light flow from the laser in the mapping plane (when determining the signal spectrum) or in the image plane (during optical filtration). In order to enter a light signal in an electronic computer (EVM) it is necessary to compute the resulting light pattern, transform the light signal into a digital code, and match and synchronize the information reception and transmission channels.

Before we determine the requirements that must be satisfied by optical information output devices and units for coupling them with an EVM, let us mention the basic features and specific nature of the output of seismic data. As has already been mentioned, the result of the processing in an OVM is presented in the form of a light pattern. This special feature imposes special limitations on the choice of

the image scanning method with respect to the arguments during quantification. In this case it is practically impossible to scan an image by moving it mechanically or to make calculations with the help of a light beam formed by an optical system. This special feature can, of course, be eliminated if the distribution of the brightness in the laser unit's output is recorded on a phototransparency and the photographic image is then entered in the EVM. The problem of entering a photographic image in an EVM is now solved quite simply, since devices for the computer input and output of photographic images have been developed. Among them we can mention the complex of optical half-tone information input-output devices developed at the IAE SO AN SSSR [Institute of Automation and Electrometry, Siberian Department, USSR Academy of Sciences] and the SKB [Special Design Office] of NP [possibly Observation Instruments]--the "Zenit" and the "Romb"--as well as the complex of equipment for the automatic input and output of information from photographic film and photographic paper that is used with the Minsk-32 EVM [1]. However, it should be mentioned that the output of information from an OVM onto photographic film is an undesirable operation, since its realization takes time and the additional transformation of the information is a source of error.

The second special feature is that incandescent lights, gas-discharge tubes and cathode-ray tubes are used as illuminators in existing input systems. In laser units, the light flow has a rigorously fixed wavelength. It is necessary to take this fact into consideration when selecting the devices to be used to convert the radiant energy into an electrical signal and to carry out the energy calculation.

A third special feature is the specific nature of the actual seismic information that is being processed; namely, its frequency and dynamic range and the duration and multichannel nature of the recordings. The basic requirements that must be satisfied by output devices (OUV) for information from OVM's and their coupling units are determined on the basis of the three special features listed above. Let us evaluate the basic parameters of an optical output system, among which we will include: number and arrangement of the elements during quantification of an image with respect to an argument, shape and dimensions of the reading aperture, the number of signal quantification levels. Starting with these parameters it may be possible to select a specific OUV plan, as well as determine the operating speed and the accuracy of the transformations.

The number of image scanning elements during quantification should be determined by the well-known theorem of references [2] and, in addition, should meet the accuracy requirements for the realization of the computation algorithms in a digital computer. The aperture's dimensions will be selected on the basis of the condition of obtaining the maximally possible signal amplitude at the OUV's outlet in order to provide the required signal-to-noise ratio for the given image reading error.

With a linear dimension along a line of image taken from the OVM of X = 36 mm for a seismic signal with duration T = 6 s and an upper frequency f_u = 120 Hz, according to the theorem of references we obtain a spatial quantification step $T_X \leqslant 0.025$ mm, while the number of reference points is N = 1,440.

All the basic algorithms in a digital EVM are realized with an accuracy of 2 ms. Therefore, in order to insure the required accuracy in the computations, the number of scanning points during quantification will be determined by the following formula:

$$N = T/\Delta t, \tag{1}$$

where Δt = 2 ms.

The computed N = 3,000 reference points for T = 6 s of the realization of a seismic signal does not contradict the value obtained in accordance with the theorem of references. It is obvious that the condition of insuring the accuracy of computations (1) is more rigorous, so we should accept N = 3,000, while the value of T_X will by 0.012 mm. In order to eliminate information losses and mixing of the tracks, it is necessary to have the number of scanning elements n with respect to the second spatial coordinate (with respect to a frame) equal the number of tracks in the time profile being processed. The total number of scanning elements is then n' = N·n. In order to eliminate information losses, it is necessary that the height (b) of a reading element be equal to the step of the recording of the seismic traces of the seismic section taken from the EVM. It is necessary to select the width (A) of a reading element on the basis of the calculation of the permissible error in the readout of the image. Let us evaluate the error in the image readout for a signal with a harmonic shape. For this case, the distribution of the intensity of the coherent source's emissions in the OVM's output plane will be determined by the expression

$$J(x) = \frac{J_m}{2}[1 - \cos w_x x], \tag{2}$$

where I_m = maximum value of the image's intensity.

When reading an image with an element of width A, the reading error at a given point will be determined by the expression

$$\Delta J = \frac{J_m}{2}\cos w_x x\left[\frac{2}{\delta w_x}\sin\frac{w_x}{2}A - 1\right], \tag{3}$$

while the relative reading error $\delta(x)$ is

$$\delta(x) = \frac{\cos w_x x\left(\frac{2}{\delta w_x}\sin\frac{w_x}{2}A - 1\right)}{1 - \cos w_x x}\cdot 100\%. \tag{4}$$

The families of the dependences of the maximum relative error δ on the frequency and the reading element's width are presented in Figure 1. With the graph in Figure 1 it is possible to determine that when the reading element's dimension A is chosen to be equal to the quantification step T_X (that is, A = 0.012 mm), the magnitude of the reading error will not exceed δ = 3 percent for signals with spectrums within the limits 0-120 Hz.

The second stage in image quantification is quantization of the brightness. In connection with this, the number of quantization levels, which determines the word length of the image encoding, is of substantial importance. Quantization of the brightness of an image's elements is usually done in such a manner, on the one hand, as to preserve the image's dynamic range and, on the other, that the quantization required for this number of levels is minimal. During quantization, the entire range of changes in brightness, from B_{min} to B_{max}, is divided into separate segments ΔB_i, where i = the number of the interval. The brightness value within each quantization interval is replaced by a fixed value.

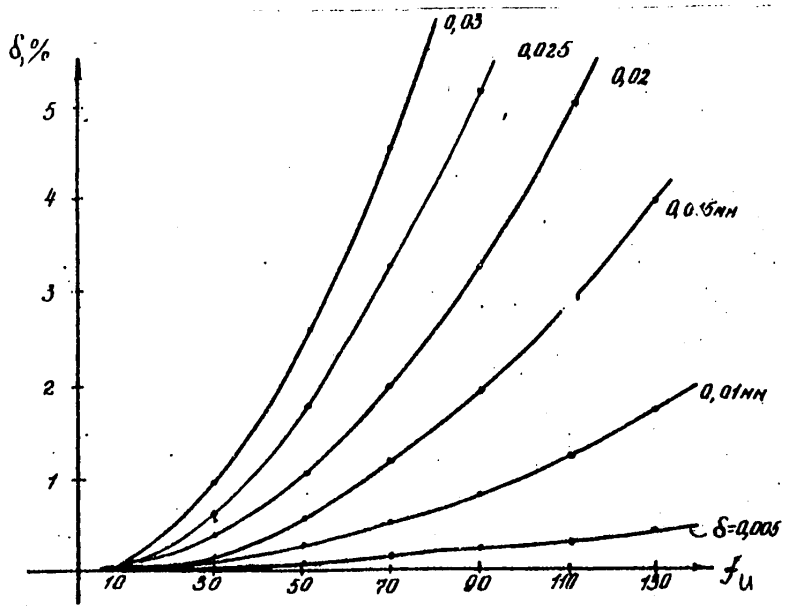

Figure 1. Dependence of reading error on width of the reading element.

The dynamic range of the image at the OVM's output does not exceed the input signal's dynamic range. Let us determine the number of quantization levels from the expression

$$D = 20 \lg \frac{B_{max}}{B_{min}}, \quad (5)$$

where D = the dynamic range. When spatiotemporal light modulators, which make it possible to preserve the dynamic range of input signals of up to 60 dB [3], are used for the input into the OVM, by using the following well-known expression we can determine the encoding word length:

$$\frac{B_{max}}{B_{min}} = (2^m - 2). \quad (6)$$

where m = encoding word length. From formula (6), m = 10 when D = 60 dB.

For the entry of information from photographic film in the OVM, it is required that m = 7.

On the basis of the calculated value of the word length, it is possible to select the specific type of analog-to-digital converter.

Thus, for signal duration T = 6 s, f_u = 120 Hz, n = 300 and D = 60 dB, what will be taken out of the OVM is a mass of independent reference points measuring 3,000 x x 300, with subsequent 10-bit encoding of each signal value.

An important characteristic of the OUV, which determines the accuracy of the information transformation, is the static characteristic of the converter that

transforms the light signal into an electrical one. This characteristic, in turn, is basically determined by the photoelectronic converter's energy characteristic. Without discussing in detail the power matching of the laser unit and the OUV, the technique of which requires a special discussion, let us determine the basic requirements that must be met by the photoelectronic converter's characteristics and parameters, as well as the basic power relationships. The equipment accuracy of the conversion of a radiant beam into an electrical signal will depend both on the degree of linearity of the energy characteristic and on the relationships between the useful signal that has been received at the converter's input and its internal noise. Let us write the linearity requirement in the following form:

$$K_{\Lambda} = \frac{I_{max}/I_{min}}{\Phi_{max}/\Phi_{min}}. \tag{7}$$

where K_{Λ} = required coefficient of linearity of the energy characteristic; I_{max}, I_{min} = currents in the photoelectronic converter's circuit for the corresponding light flows Φ_{max} and Φ_{min} at its input.

K_{Λ} is usually taken to be equal to 0.98-1.02. In view of the fact that between the values of the light flow Φ and brightness B there exists a proportional relationship and that from the values of B it is possible, by using well-known formulas, to convert to Φ, the following relationship should be satisfied:

$$\frac{\Phi_{max}}{\Phi_{min}} \geqslant \frac{B_{max}}{B_{min}}. \tag{8}$$

The second condition for accurate operation is determined by the relationship

$$\Phi_{thr\ r} \leqslant \Delta\Phi_i, \tag{9}$$

where $\Phi_{thr\ r}$ = threshold flow of the photoelectronic converter with respect to the radiation source; $\Delta\Phi_i$ = change in the flow corresponding to a single quantization level.

When determining $\Phi_{thr\ r}$ it is possible to use the technique explained in [4], keeping in mind in connection with this that the radiation source is monochromatic and the fact that the photoelectronic converter operates under conditions of constant background illumination caused by the specific nature of the readout of signals from the OVM.

Depending on dimension A, which determines the necessary resolution during scanning (or the number of independent reference points), we choose the scanning method and the assembly layout that realizes this method.

The most promising scanning method involves the use of solid-state, matrix photoconverters. Such photoconverters are notable for high reliability and small size, as well as a large dynamic range. Of special interest is the use of instruments with charge communication (PZS).

A PZS is a series of simple MDP (metal-dielectric-semiconductor) structures [5,6]. The metal electrodes are several micrometers (6 x 3) in size and are arranged on a common semiconducting substrate, at a minimum distance from each other, so that they form a linear or matrix regular system. Each PZS element is capable of transforming an element of a light pattern having the same dimensions. When a matrix

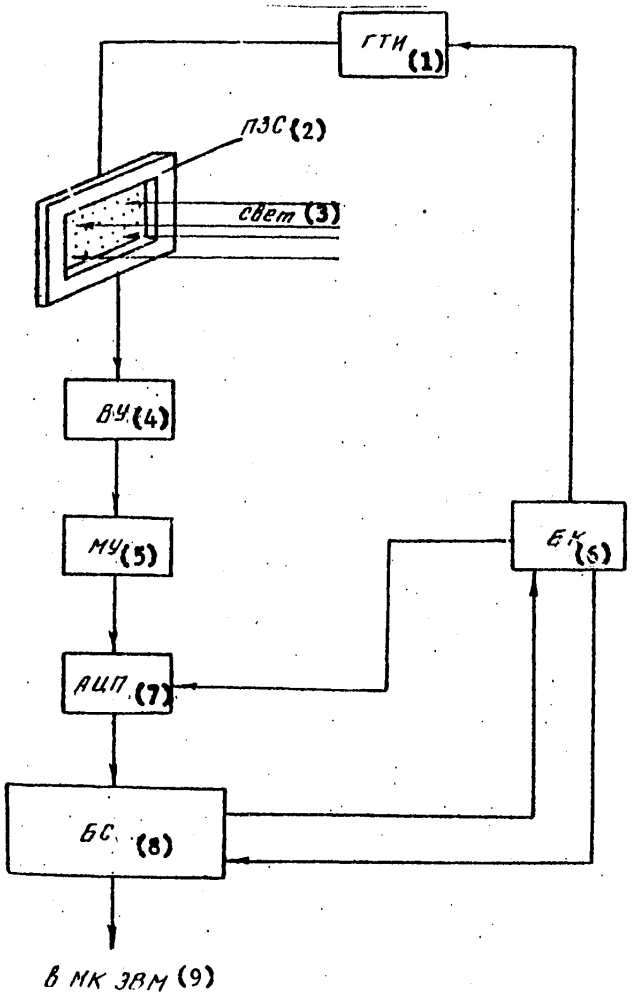

Figure 2. Diagram of optical output device based on a PZS.

Key:
1. Time pulse generator
2. Instrument with charge communication
3. Light
4. Output device
5. Scale amplifier
6. Command unit
7. Analog-to-digital converter
8. Sampling unit
9. To computer's multiplex channel

photoreceiver irradiates a PZS, the entire light pattern is instantly transformed into a pattern of charge packets.

The device for output from the PZS operates in the following manner (Figure 2). Light striking the PZS is converted into charge packets that are sent sequentially, by timing pulses, from the matrix into the output device (VU). The VU converts the charge packets into a voltage level, which enters the scale amplifier (MU) and then the ATsP [analog-to-digital converter]. From the ATsP, the information--in digital

form--is sent to the coupling unit. The command unit (BK) controls the timing pulse generator and the ATsP.

PZS's have the following photoreception characteristics:
1) light sensitivity--500 μA/lm;
2) threshold light sensitivity--10 lux·s;
3) area of spectral sensitivity Λ--1.1 + 0.4 μm;
4) resolution--10 lines/mm;
5) integration time--tenths of a millisecond;
6) dynamic range--1,000:1 (60 dB).

An important advantage of matrix PZS's is that during an exposure, the entire light pattern is converted into a pattern of charge packets and then--with the help of the timing pulses--self-scanning takes place. This makes it possible to reduce the conversion time to tenths of a millisecond. Most ATsP's operate at speeds lying within these limits, so the questions involved in matching PZS's and ATsP's pose no difficulties.

Matrix PZS's having 10^2-10^5 photosensitive elements covering an area of 500-1,000 μm^2 have already been developed. They make it possible to record information with a density of $(1\text{-}2)\cdot 10^5$ bits/cm^2.

Let us mention here that the existing matrices with 232 x 288, 512 x 520 and 496 x x 475 scanning elements are not capable of converting the entire light pattern at an OVM's output instantanteously, since the required number of scanning elements is 3,000 x 300. Therefore, additional technical facilities are needed in order to read the entire light pattern. The most acceptable way of solving this problem is:
1) assemble a mosaic consisting of several PZS matrices;
2) read fragments of the optical pattern with the help of coherent light guides on several PZS matrices;
3) move one PZS fragment mechanically and then carry out fragment-by-fragment reading.

At the present time, we know that line (linear) PZS's based on 1,738 scanning elements have been developed.

By using such gauges, it is possible to create a combined optical-mechanical reading device in which scanning with respect to one coordinate is carried out electrically with the help of the PZS gauge, while with respect to the other it is done with the help of a mechanical assembly.

Thus, such a device can join together two important advantages: the high resolution of the opticomechanical output device and the high operating speed of the PZS's output device.

At the present time we know of examples of the use of television camera tubes (PTT)--vidicons, in particular--to read the light pattern at an OVM's output. The principle of the construction of an OUV based on a vidicon is explained in [7]. Figure 3 is a block diagram of an OUV based on a vidicon. The device operates in the following manner: the complete television signal (PTS) goes from the vidicon to a scale amplifier (MU) and then into the analog key (K). From the analog key, the image signal that has been separated from the PTS is sent to the ATsP, where it is transformed into a digital code.

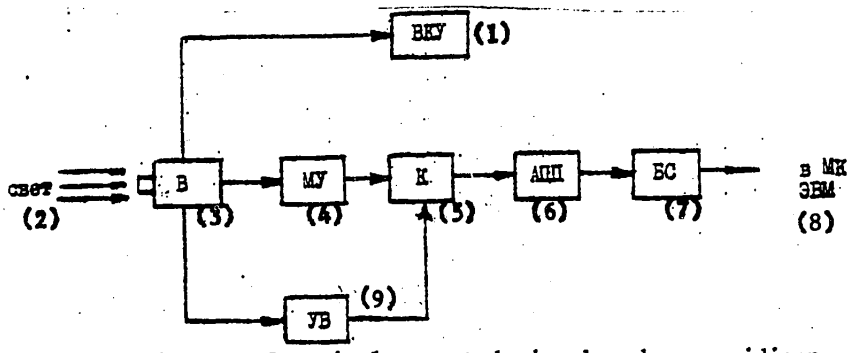

Figure 3. Diagram of optical output device based on a vidicon.

Key:
1. Video monitoring unit
2. Light
3. Vidicon
4. Scale amplifier
5. Analog key
6. Analog-to-digital converter
7. Coupling unit
8. To computer's multiplex channel
9. Sampling unit

Vidicons use the grating method of scanning an image, with synchronized, staggered scanning that is continuous with respect to the lines and discrete with respect to a frame; the grating is rectangular in shape. In addition to the image signal, a PTS contains a frame-synchronized pulse, a frame-quenching pulse, a line-synchronizing pulse and a line-quenching pulse. In order to separate the signal image (which contains the information about the light pattern) from the PTS and in order to quantify the image with respect to a line, a sampling unit (UV) that opens the analog key at certain moments of time is used. The transformation process can be monitored visually on the video monitoring unit (VKU).

Modern vidicons have sensitivity, resolution and a signal-to-noise ratio that are adequate for most cases of image input into a computer and are also small and have comparatively low signal nonuniformity over the target's working field.

At the same time, an output device based on a PTT has substantial shortcomings, the main one of which is the presence in the PTS (in addition to the video signal) of synchronization and quenching signals, which make analog-to-digital conversion difficult and require the use of additional equipment. Such an output device requires a high-frequency reference generator (up to 12 MHz) for line quantification of the image, as well as a high-speed ATsP, which involves considerable difficulties.

In addition to this, vidicons have a light-sensitive port with a small area (up to 1 cm^2), with a maximum resolution of up to 44 lines/mm. This does not make it possible to read the full output light pattern. The speed reduction method is used to match a vidicon with an ATsP [7]. This method makes it possible to take one reading from each line when a frame is scanned. In connection with this, the readout rate is reduced to 15,625 Hz. Such a speed matches that of most ATsP's, which perform up to 20,000 transformations per second. The readout time for an optical image fragment equal in area to the light-sensitive port is 24 s. A high rate of information readout from the OVM can be achieved by using uni- or two-dimensional coordinate-sensitive radiation receivers [8,9]. However, such receivers have poor

resolution (up to 5-10 lines/mm) and a small dynamic range. At the same time, when the signal is presented in the form of a silhouette image or a binary matrix code, such converters can be very useful. In this case they determine the coordinate of the image's boundary, proportional to the signal's amplitude, where there is an abrupt change in the transmission coefficient.

The most realistic possibility for the complete reading of a light pattern from an OVM, with high spatial resolution, is still the use of plane opticomechanical scanning circuits. We have developed an OUV with plane opticomechanical scanning and a grating scanning method. The coordinate table is moved by a step drive. In the device there is no system for monitoring the accuracy of the reading element's linear movement, since precision-machined screws and nuts with no play are used. The output device operates in the following manner (Figure 4): the computer sends an inquiry through the coupling unit to the scanning assembly's command unit (BK). The BK implements the functions for program control of the scanning assembly. From the BK the command enters the horizontal-displacement step motor control unit (BUShDG) and the motor (ShDG) makes a discrete movement of the reading element along the first line. At the end of the first line, the BK sends a signal to the vertical-displacement step motor control unit (BUShDV) and that motor (ShDV) moves the reading element to the next line, after which the process is repeated.

Light from each element of the pattern passes through a light guide into an FEU [photoelectric multiplier], which carries out a linear transformation of the light into an electrical signal. The electrical signal enters the scale multiplier (MU) and then the analog-to-digital converter (ATsP). The MU matches the FEU and the ATsP. The ATsP transforms the sequence of voltage levels into a digital code. In order to avoid erosion of the image, when the motor is moving the reading element the BK sends a "Transformation Prohibited" signal to the ATsP.

From the ATsP, the code carrying the information about the intensity of the light flow from a light pattern scanning element goes into the coupling unit (BS).

It should be mentioned that the OUV we developed is intended for use with a "Kogerent" laser unit, with a YeS-1022 EVM acting as the control computer.

The coupling unit's basic purpose is to implement the direct interaction of the EVM's multiplex channel with the optical output device. With its help, the most nearly complete interaction of OVM and EVM hardware and software is achieved. The coupling unit must satisfy the following basic requirements:
1) establish communications by means of standard input-output interface lines (signals);
2) carry out the exchange of the sequence of signals for address, command and data transmission;
3) insure the informational data transmission rate and monitor the data.

Carrying the optical information, the digital code from the ATsP enters the signal converter (PS), which matches the the ATsP's signals with the buffer memory (BP). When acted upon by control signals from the control unit (BU), the information passes from the BP through the communication unit with channel (BSK) and is transmitted byte-by-byte through the multiplex channel (MK) into the EVM's main memory for storage and programmed processing. Upon completion of the reading process, the output device's BK sends the BU a "Stop" signal that is encoded in the command

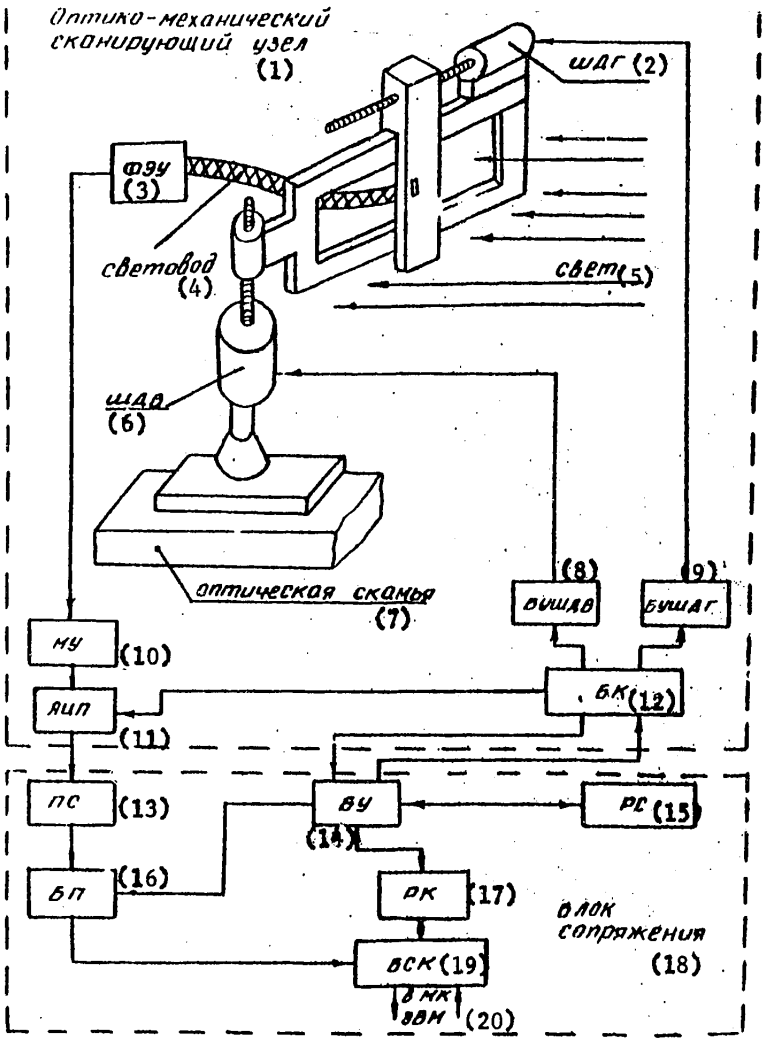

Figure 4. Diagram of opticomechanical output device and coupling unit.

Key:

1. Opticomechanical scanning assembly
2. Horizontal-displacement step motor
3. Photoelectric amplifier
4. Light guide
5. Light
6. Vertical-displacement step motor
7. Optical bench
8. Vertical-displacement step motor control unit
9. Horizontal-displacement step motor control unit
10. Scale amplifier
11. Analog-to-digital converter
12. Command unit
13. Signal converter
14. Control unit
15. RS [possibly shift register]
16. Buffer memory
17. Command register
18. Coupling unit
19. Communication unit with channel
20. To computer's multiplex channel

register (RK) and sent to the EVM. After this, the programmed processing of the information that has been obtained begins.

It should be mentioned that the optical output device developed by us matches a "Kogerent" OVM very well. The entire mechanism is mounted on a small micrometric table and installed on the bed of an optical bench. Although the reading time for a complete light pattern is significant (12 min), in connection with this the EVM does receive the entire mass of seismic data. This makes it possible to test and develop algorithms for the processing of seismic information with the required 2-ms accuracy.

BIBLIOGRAPHY

1. Grishin, M.P., Kurbanov, Sh.M., Markelov, V.P., et al., "An Equipment Complex for the Automatic Input and Output of Experimental Half-Tone Information With the 'Minsk-22' Electronic Computer," AVTOMETRIYA, No 4, 1971, pp 27-32.

2. Kotel'nikov, V.A., "Teoriya potentsial'noy pomekhoustoychivosti", [Theory of Potential Noise Stability], Moscow, Izdatel'stvo "Gosenergoizdat", 1956.

3. Mari, Zh., Dzhonson, Zh., and Azan, Zh.-P., "Image Reproduction Devices Based on the Pockels Effect and Their Utilization," in "Dostizheniya v tekhnike peredachi i vosproizvodeniya izobrazheniy" [Achievements in Image Transmission and Reproduction Technology], Moscow, Izdatel'stvo "Mir", Vol 1, 1978.

4. Yakushenkov, Yu.G., "Osnovy teorii i raschet optiko-elektronnykh priborov" [Theoretical Principles and Design of Opticoelectronic Instruments], Moscow, Izdatel'stvo "Sovetskoye radio", 1971.

5. Seken, K., and Tompset, M., "Pribory s perenosom zaryada" [Instruments With Charge Transfer], Moscow, Izdatel'stvo "Mir", 1978 (translated from English).

6. Nosov, Yu.R., and Shilin, V.A., "Poluprovodnikovyye pribory s zaryadovoy svyaz'yu" [Semiconducting Instruments With Charge Communication], Moscow, Izdatel'stvo "Sovetskoye radio", 1976.

7. Potapov, O.A., and Aftandilov, G.A., "A Device for the Input of Optical Information in an Electronic Computer That Is Based on an Applied Television Installation (PTU)," REGIONAL'NAYA, RAZVEDOCHNAYA I PROMYSLOVAYA GEOFIZIKA. EKSPRESS-INFORMATSIYA VNII EKONOMIKI MINERAL'NOGO SYR'YA I GEOLOGICHESKO-RAZVEDOCHNYKH RABOT, Moscow, Branch Center for Scientific and Technical Information, All-Union Scientific Research Institute of the Economics of Mineral Raw Materials and Geological Exploration Work, No 13, 1979, pp 1-13.

8. Zotov, V.D., "Poluprovodnikovyye ustroystva vospriyatiya informatsii" [Semiconducting Information Reception Devices], Moscow, Izdatel'stvo "Energiya", 1976.

9. Gos'kov, P.I., "Monitoring and Measuring Devices Based on Scanistors," in "Optiko-elektronnyye pribory v sistemakh kontrolya i upravleniya" [Optico-electronic Instruments in Monitoring and Control Systems], Moscow, 1978.

UDC 550.834

POWER (ILLUMINATION ENGINEERING) CALCULATION OF OPTICOELECTRONIC SYSTEMS FOR PROCESSING GRAPHIC INFORMATION

Leningrad GOLOGRAFIYA I OPTICHESKAYA OBRABOTKA INFORMATSII V GEOLOGII in Russian 1980 (signed to press 19 Nov 80) pp 32-35

[Article by Yu.G. Yakushenkov from collection of works "Holography and Optical Information Processing in Geology", edited by Professor S.B. Gurevich and Candidate of Technical Sciences O.A. Potapov, Leningrad Physicotechnical Institute imeni A.F. Ioffe, USSR Academy of Sciences, 500 copies, 181 pages]

[Text] The author discusses a general approach to the calculation of the power characteristics of opticoelectronic systems. He also derives formulas that are refined enough for engineering use.

The purpose of a power calculation is to establish sufficiently optimal relationships among the separate parameters of opticoelectronic systems (OES). The common power calculation technique [1] reduces to the formulation of a generalized power calculation of the type

$$\Delta \Phi_{in} / \Phi_t = \mu,$$

where $\Delta\Phi_{in}$ = a signal (flow of radiation) at the OES's input that exceeds the OES's sensitivity threshold Φ_t by a factor of μ, and the subsequent solution of this equation in developed form; that is, in the form of a function of the OES's parameters relative to one of them.

When calculating and planning an OES for the processing of graphic information and, in particular, the processing of seismograms and other forms of geophysical information representations [2], this technique has certain positive features.

The basic formula for calculating the flow arriving at an OES's input aperture is [1]:

$$\Phi_{in} = \tau^{\ell} L \frac{A_{rad} A_{in}}{\ell^2},$$

where τ = transmission coefficients of the optical mediums on the path ℓ from an emitter with area A_{rad} and brightness L to an input aperture of area A_{in}.

If the emitter covers the OES's entire instantaneous angular field, as determined by the area of an element of resolution q (the sensitive area of a radiation

receiver, for example), it is then the case that

$$\Phi_{in} = \frac{1}{4}\tau L q \frac{A_{in}}{f'^2},$$

where f' = focal length of the OES's objective.

During scanning of a field of view (seismogram, photographic film or any other graphic information carrier), if an element of resolution with area q is struck in turn by radiation from sections of the field with brightnesses L_1 and L_2, the difference signal $\Delta\Phi_{in}$ is:

$$\Delta\Phi_{in} = \frac{1}{4}\tau (L_1 - L_2) q \frac{A_{in}}{f'^2}.$$

Considering the spectral nature of $\tau = \tau(\lambda)$ and $L = L(\lambda)$, for the OES's working spectral range $\lambda_1,\ldots,\lambda_2$ we obtain

$$\Delta\Phi_{in} = \frac{1}{4} q \frac{A_{in}}{f'^2} \int_{\lambda_1}^{\lambda_2} \tau(\lambda)[L_1(\lambda) - L_2(\lambda)]d\lambda. \quad (1)$$

In the general case, when the emissions of separate sections of a field or a carrier of graphic information are determined to be both intrinsic and scattered or reflected emissions from a foreign source, the values of spectral densities $L(\lambda)$ are defined as the sum of the intrinsic L_{1c} and L_{2c} and reflected or scattered L_{1o} and L_{2o} components. For Lambertian emitters,

$$L_1(\lambda) = \varepsilon_1(\lambda)\frac{M_1(\lambda)}{\pi} + \rho_1(\lambda)\frac{E(\lambda)}{\pi},$$

$$L_2(\lambda) = \delta_2(\lambda)\frac{M_2(\lambda)}{\pi} + \rho_2(\lambda)\frac{E(\lambda)}{\pi}, \quad (2)$$

where $\delta_1(\lambda)$, $\delta_2(\lambda)$ = spectral radiating capacities (radiation coefficients); $M_1(\lambda)$, $M_2(\lambda)$ = spectral densities of the emissions; $\rho_1(\lambda)$, $\rho_2(\lambda)$ = spectral brightness coefficients (or reflection factors); $E(\lambda)$ = illumination or irradiation created by the foreign source (such as the Sun, which illuminates brightness fields L_1 and L_2, or a laser brightening a phototransparency or seismogram).

The next stage of the calculation consists of determining the signal-to-noise ratio at the outlet of the OES's radiation receiver:

$$\mu = \Delta V_c / V_n, \quad (3)$$

where $\Delta V_c = \Delta\Phi_{in} S_v$ = amplitude of the difference signal at the receiver's outlet that corresponds to flow $\Delta\Phi_{in}$; S_v = voltage sensitivity of the receiver; V_n = noise level as adduced at the receiver's outlet.

Expressing the receiver's sensitivity S_v in terms of its detecting capability,

$$D^* = \frac{S_v\sqrt{A_{nu}\Delta f}}{V_n},$$

where A_{nu} = area of the receiver's sensitive layer; Δf = effective transmission band of the OES's electronic channel, we obtain

$$S_v = \frac{D^* V_n}{\sqrt{A_{nu}\Delta f}} \cdot \tag{4}$$

From this, with due consideration for the fact that D* = D*(λ), after substituting (1) and (4) into (3), we obtain

$$\mu = \frac{q A_{in}}{4 f'^2 \sqrt{A_{nu}\Delta f}} \int_{\lambda_1}^{\lambda_2} \tau(\lambda)[L_1(\lambda) - L_2(\lambda)] D^*(\lambda) d\lambda. \tag{5}$$

By assigning the necessary value of μ, from this it is possible to determine the requirements for both the individual OES assemblies and the graphic information carrier. As an example let us discuss the case of the processing of graphic information presented in the form of a phototransparency with seismograms recorded by the broad track or variable density method, brightened by an illuminating system that creates illumination E(λ) on the transparency.

In this case the first components determining the intrinsic radiation in formulas (2) are much smaller than the second ones, which are determined by external illumination E(λ); consequently,

$$L_1(\lambda) \approx \rho_1(\lambda) E(\lambda)/\pi,$$
$$L_2(\lambda) \approx \rho_2(\lambda) E(\lambda)/\pi.$$

Substituting these values into (5), we obtain

$$\mu = \frac{q A_{in}}{4\pi f'^2 \sqrt{A_{nu}\Delta f}} \int_{\lambda_1}^{\lambda_2} \tau(\lambda) E(\lambda) \Delta\rho(\lambda) D^*(\lambda) d\lambda,$$

where $\Delta\rho(\lambda) = \rho_1(\lambda) - \rho_2(\lambda)$.

If the brightness coefficients ρ(λ) (scattering and reflection factors) in range $\lambda_1,\ldots,\lambda_2$ can be taken as constants, by removing the value Δρ from under the integral sign in (6) it is possible to determine the requirements for the transparency's dynamic range or for the density of the recording, as defined by gradient Δρ:

$$\Delta\rho = \frac{4\pi\mu f'^2 \sqrt{A_{nu}\Delta f}}{q A_{in}} \left[\int_{\lambda_1}^{\lambda_2} \tau(\lambda) E(\lambda) D^*(\lambda) d\lambda\right]^{-1}.$$

BIBLIOGRAPHY

1. Yakushenkov, Yu.G., "Osnovy optiko-elektronnogo priborostroyeniya" [Principles of Opticoelectronic Instrument Building], Moscow, Izdatel'stvo "Sovetskoye radio", 1977, 272 pp.

2. Potapov, O.A., "Opticheskaya obrabotka geofizicheskoy i geologicheskoy informatsii" [Optical Processing of Geophysical and Geological Information], Moscow, Izdatel'stvo "Nedra", 1977, 184 pp.

UDC 550.834

SOME QUESTIONS ON THE DESIGNING OF LIQUID CRYSTAL MATRIX SCREENS

Leningrad GOLOGRAFIYA I OPTICHESKAYA OBRABOTKA INFORMATSII V GEOLOGII in Russian
1980 (signed to press 19 Nov 80) pp 36-44

[Article by A.B. Beklemishev from collection of works "Holography and Optical Information Processing in Geology", edited by Professor S.B. Gurevich and Candidate of Technical Sciences O.A. Potapov, Leningrad Physicotechnical Institute imeni A.F. Ioffe, USSR Academy of Sciences, 500 copies, 181 pages]

[Text] The author discusses the effect of the ratio of the resistances of the interelectrode insulation and the electrode on the voltage levels active in the elements of a matrix. He shows that for realistic values of this ratio, the effective voltages are lower than the set ones by 10-30 percent. He also presents a convenient and effective formalism of matrices of temporal characteristics for evaluating the capabilities of a matrix screen that takes into consideration the sum total of the direct and inverse electro-optical transitions for the voltages active in a screen's elements.

As is well known [1,2], when designing liquid-crystal (ZhK) matrices it is necessary to take into consideration the reversible medium's electro-optical characteristics, the control system's output voltages (EUS) and the methods used to set them in the matrix. To a considerably lesser degree, one must also deal with the question of the necessity of allowing for the electrodes' actual resistances and the levels of the substrates' interelectrode insulation (MEI).

In this article we discuss several questions related to the creation of multielement matrices controlled on a line-by-line basis from direct-current sources, using as an example the bistable "nematik-kholesterik" [translation unknown] and "guest-host" systems [1].

Figure 1 depicts a fragment of a matrix containing four elements and an alternative way of connecting them. According to the nature of the interaction of the EDS [electromotive force] source and the matrix's elements, the latter are subdivided into three types: selected (addressed with a zero potential with respect to the corresponding line and column); semiselected (addressed with a zero potential with respect to either the line or the column); unselected (not addressed with a zero potential, but connected to the voltage source with respect to line and column). Since the information entering the matrix is quite variegated (digits, letters,

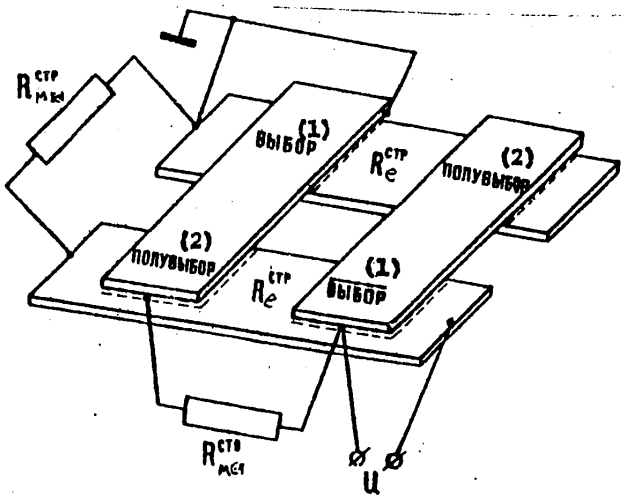

Figure 1. Fragment of a liquid-crystal matrix.

Key: 1. Selection 2. Semiselection

symbols, graphs and so on), during the frame-addressing phase each element is repeatedly semiselected and unselected, while (in addition) some relatively small part of the matrix's elements is selected in certain line-addressing phases.

In Figure 1, R_e = resistance of a transparent electrode made of tin oxide; R_{MEI} = = resistance of the interelectrode insulation. The superscripts are "CTP" for lines and "CTO" for columns, while "U" is the voltage of the source.

The matrix's operating mode is as follows. Before beginning operation, voltage U is fed into all the lines and columns of the matrix and converts a thin (~20 μm) film of the ZhKM [liquid-crystal matrix] that is located between the lines and columns from its original nontransparent state into transparency. The optical system is constructed in such a fashion that in this case the screen looks dark. The working cycle consists of a frame-scanning phase that is composed of successive and identical line-scanning phases. In the first (and each subsequent) line-scanning phase, an addressing zero potential is fed into one line of the matrix, while into all the columns there is fed some combination of zero and nonzero potentials that are formed automatically in the EUS. Thus, both electrodes of the element designated as "selection" in Figure 1 are grounded, while only one of the electrodes of the "semiselection" element is grounded. In connection with this, elements outside the addressed line can also be of two types: "semiselection" and "nonselection." Voltage U is applied to the electrodes of an element of the latter type.

The selected elements of an addressed line are "tripped," forming a given combination of colored squares against the dark background. The steady-state values of the electro-optical responses of the selected (B), semiselected (П) and unselected (H) elements are depicted in Figure 2. As the response it is convenient to consider (for example) the threshold dependence of the transparency of an element of the matrix on the voltage; that is, if the line-addressing phase equals or exceeds the setting time, the responses for elements of the indicated types, one would think, could be represented, respectively, as $\Psi(0)$, $\Psi(U/2)$ and $\Psi(U)$. In connection with this, the levels of responses $\Psi(U/2)$ and $\Psi(U)$ are ignorable.

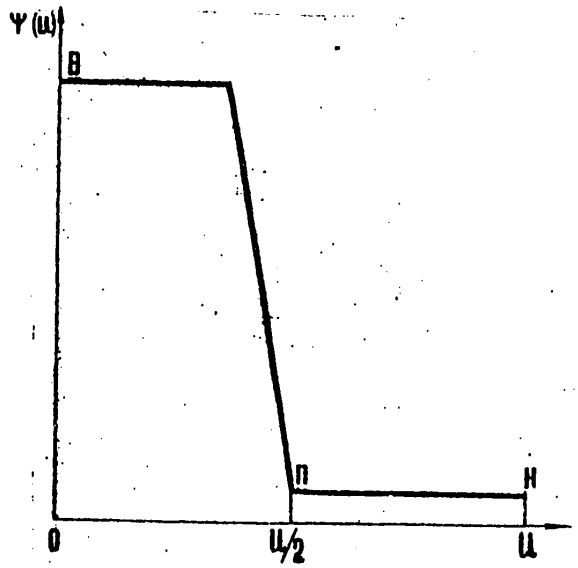

Figure 2. Function of electro-optical response (B = selection; П = semiselection; H = nonselection).

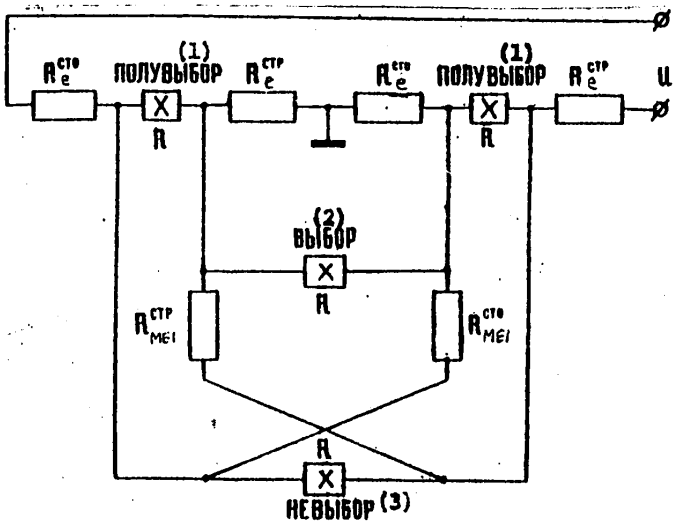

Figure 3. Electrical connection diagram.

Key: 1. Semiselection 2. Selection 3. Nonselection

However, let us attempt to discuss the electrical diagram corresponding to the given fragment (Figure 3). The resistive elements R here are elements of the three mentioned types.

Practically usable ZhKM's have a specific resistance on the order of 10^8 Ω·cm. If the distance between a line and a column is 0.02 mm, while an element aperture is 0.5 mm^2 (real estimates for large-format matrices), then

Obtaining R_{MEI} levels of the same or higher orders is an extremely difficult task. Practical estimates show that when $R_e \approx 10$ kΩ, $R_{MEI} = 20$ kΩ-10 MΩ. The specific level of the R_{MEI} values depends on the electroerosion and subsequent etching techniques [3]. Thus, the voltage in an element of each type can be represented by the values

$$u^B = \frac{1}{2 + \frac{R_{MEI}}{R_e}} \cdot u \qquad \text{for "selection,"}$$

$$u^H = \frac{1 + \frac{R_{MEI}}{R_e}}{2 + \frac{R_{MEI}}{R_e}} \cdot u \qquad \text{for "nonselection,"}$$

$$u^П = -\frac{1}{2}(u^B + u^H) = -\frac{1}{2}u \qquad \text{for "semiselection."}$$

It is easy to see that, in practice, the voltages acting on the "selection" and "nonselection" elements are far from the original estimates. For instance, for $R_{MEI} = R_e$, we obtain (for example)

$$u^B = \frac{1}{3}u, \quad \text{while} \quad u^H = \frac{2}{3}u.$$

It is useful (obviously) to evaluate the nature of the regularities:

$$\frac{u^B}{u} = f_1\left(\frac{R_{MEI}}{R_e}\right) \quad \text{and} \quad \frac{u^H}{u} = f_2\left(\frac{R_{MEI}}{R_e}\right).$$

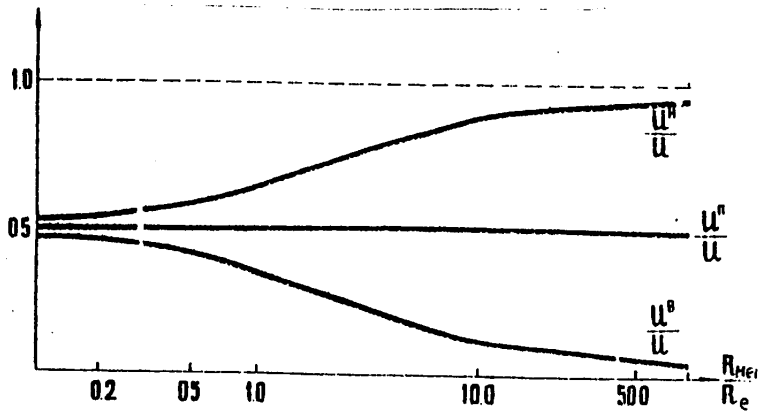

Figure 4. Dependence of voltages in "selection," "semiselection" and "nonselection" elements on value of ratio R_{MEI}/R_e.

The graphs of these functions are shown in Figure 4. Here we can see that functions $f_{1,2}$ undergo significant changes in the band

$$0{,}2 \leqslant \frac{R_{MEI}}{R_e} \leqslant 50.$$

From the graphs it is easy to derive the voltages that are acting on the matrix element under discussion from the normally known values of U, R_{MEI} and R_e. For instance, when U = 20 V, R_e = 20 kΩ.

R_{MEI}, kΩ	4	I0	20	200	I000
U^B, V	9,2	8	6,6	2	0,4
U^H, V	I0,8	I2	I3,4	I8	I9,6

The obvious conclusion drawn from what has been said is that the choice of a ZhKM must be made with due consideration for the real values of R_{MEI}/R_e. In any case, one must not count on ideal values of U^B and U^H equaling, respectively, 0 and U, since in connection with this the condition $R_{MEI} >> R_e$ must be fulfilled.

In the case where $R_{MEI} << R_e$, the diagram under discussion loses all its useful properties, since the following equality is realized:

$$U^B = U^H = U^П$$

Thus, let us assume that the values of R_{MEI} and R_e have been established as the result of measurement of the substrates' resistive characteristics. Their ratio gives the position of the ordinate in the graph (Figure 4) that determines the values of U^B and U^H.

At the present time, the characteristics of $\Psi(U)$ have been studied for a considerable number of ZhK compounds and materials have been published that describe the transformation of functions $\Psi(U)$ for changes in temperature and the distance between the planes of the lines and columns [1,2].

Therefore, it is usually not difficult to choose a group of ZhKM's that provide the given contrast $\Psi(U^B)/\Psi(U^H)$.

The further search for the optimum ZhKM in the group is carried out with the help of a matrix of temporal characteristics (MVKh) that includes a complete listing of the times of direct and inverse electro-optical transitions for the voltage jumps that were determined above: $U^B \not\rightleftarrows U^П$, $U^B \not\rightleftarrows U^H$, $U^П \not\rightleftarrows U^H$.

For the purpose of simplifying the designations, henceforth we will drop the letter "U." The MVKh has the following form:

-	T(П → В)	T(Н → В)
T(В → П)	-	T(Н → П)
T(В → Н)	T(П → Н)	-

Each element of the MVKh is the time T of the setting of functions $\Psi(B \not\rightleftarrows П)$; $\Psi(B \not\rightleftarrows H)$; $\Psi(П \not\rightleftarrows H)$.

Each of the MVKh's elements is material. Actually, T(H → B) and T(П → B) determine the tripping time; that is, they give the minimum value of the line-addressing phase.

It is useful to have the tripping time as short as possible in order to shorten the frame formation time, increase the rate of information arrival and renewal in the ZhKM, and simplify the buffer ZU's [memory unit] and the interface as a whole.

$T(B \rightarrow H)$ and $T(B \rightarrow \Pi)$ determine the relaxation time; that is, they give the maximum value of the frame-scanning phase for given ZhKM's and operating conditions.

In connection with this, ratios $T(B \rightarrow \Pi)/T(\Pi \rightarrow B)$ and $T(B \rightarrow H)/T(H \rightarrow B)$ give an evaluation of the maximally possible number of lines in a matrix. No less significant are the values of $T(H \rightarrow \Pi)$ and $T(\Pi \rightarrow H)$. It is usually necessary to have the value of $T(\Pi \rightarrow H)$ on the same order of magnitude as $T(B \rightarrow \Pi)$. Otherwise, a selected element will "go out" when acted upon even once by a "nonselection" voltage.

Thus, of the six MVKh elements, only two (represented in the matrix by dashes) must be maximally small values.

Let us, for example, design a ZhKM with 128 lines. This means that when depicting the most informative (in the sense of filling the screen) flow of digits and/or letters, 110 lines should be addressed in each frame (the other 18 are spaces when there is a 7 x 5 sign format). Consequently, it is necessary to insure that $T(B \rightarrow H)/T(H \rightarrow B) > 110$. Otherwise, only part of the screen will reproduce the required information and the person perceiving it will be unjustifiably fatigued by the flickering.

We should keep in mind the fact that the process of setting the function $\Psi(U)$ is far from always being monotonic, particularly when the levels of the control voltages are comparatively low [2].

By evaluating the functions $\Psi(U)$ for the recently most popular materials, which are based on cyanobiphenyls, it is possible to detect substantial deviations that are related to the presence of oscillatory components. In connection with this, the basic change in the function $\Psi(U)$ takes place quite rapidly, whereas complete setting is achieved in an amount of time that is an order or more of magnitude longer.

Therefore, sometimes it is advisable to set the duration of the line-addressing phase in accordance with the duration of the basic change in function $\Psi(U)$, making the necessary corrections in the MVKh and the contrast evaluation.

As experience has shown, in connection with this it is particularly important not to forget the dependence of the values of $T(B \rightarrow \Pi)$ and $T(B \rightarrow H)$ on the duration of the line-addressing phase. As is known [4,5], when it is shortened, the value of ratio $T(B \rightarrow H)/T(H \rightarrow B)$ can not only be reduced by an order of magnitude or more, but can even turn out to be less than unity. As a result, the ZhKM will prove to be incapable of reproducing information.

In summing up what has been said, let us mention that, with due consideration for the resistances of the electrodes and the interelectrode insulation, it is possible to evaluate the actual voltage levels acting on the elements of a liquid-crystal screen. Formalization of the temporal characteristics in the form of a matrix is a convenient and effective means for evaluating the possibilities for depicting information on a screen that is being designed.

BIBLIOGRAPHY

1. Blinov, L.M., "Elektro- i magnitooptika zhidkikh kristallov" [Electro- and Magneto-Optics of Liquid Crystals], Moscow, Izdatel'stvo "Nauka", 1978.

2. Kapustin, A.P., "Elektroopticheskiye i akusticheskiye svoystva zhidkikh kristallov" [Electro-Optical and Acoustical Properties of Liquid Crystals], Moscow, Izdatel'stvo "Nauka", 1973.

3. Alekseyev, M.I., and Beklemishev, A.B., "Using Electroerosion in the Production of Liquid-Crystal Matrices," ELEKTRONNAYA TEKHNIKA, Series 4, No 1, 1979, pp 87-90.

4. Makeyeva, Ye.N., Beklemishev, A.B., and Kurdyumov, G.M., "Some Characteristics of Alloyed Liquid-Crystal Materials," ELEKTRONNAYA TEKHNIKA, Series 6, Materials edition 4 (129), 1979, pp 110-115.

5. Makeyeva, Ye.N., Beklemishev, A.B., Urupov, A.K., and Serebrennikova, G.A., "Using Liquid-Crystal Compounds in Geophysical Opticoelectronics," "Tezisy dokladov IV Vsesoyuznoy konferentsii po zhidkim kristallam" [Summaries of Reports Given at the Fourth All-Union Conference on Liquid Crystals], Ivanovo, Izdatel'stvo IGU [Ivanovo State University], 1977.

UDC 550.834:621.384

ON THE USE OF SEMICONDUCTING PHOTORECEIVERS FOR THE ACCELERATED INPUT OF OPTICAL INFORMATION

Leningrad GOLOGRAFIYA I OPTICHESKAYA OBRABOTKA INFORMATSII V GEOLOGII in Russian 1980 (signed to press 19 Nov 80) pp 45-56

[Article by A.V. Dutov from collection of works "Holography and Optical Information Processing in Geology", edited by Professor S.B. Gurevich and Candidate of Technical Sciences O.A. Potapov, Leningrad Physicotechnical Institute imeni A.F. Ioffe, USSR Academy of Sciences, 500 copies, 181 pages]

[Text] The author proposes a parametric method for connecting photodiode sensors for the accelerated input of information in opticoelectronic seismogram processing systems.

He presents some results of an experimental investigation of the conversion of optical signals for different photoreceiver connection methods.

In the solution of the problem of processing the large masses of information that are generated when seismic surveying methods are used to prospect for gas- and oil-bearing structures, particular interest has been aroused by hybrid opticoelectronic systems, the effectiveness of which is related to the information capacity of the light field as an information carrier, the high speed at which information in analog form is processed, and the accuracy with which information in digital form is handled [1].

Since these light fields are at least two dimensional, the problem of the high-speed input of optical information into the digital part of the system is solved either by increasing the scanning speed in scanning-type devices or by multichannel reading. When contemporary requirements--the creation of systems for the preliminary processing of information under field conditions--are taken into consideration, the most promising photoreceivers are assumed to be converters based on charge-coupled devices (PZS). However, increasing the scanning speed in PZS rulers entails a proportional decrease in sensitivity, while the use of PZS matrices involves a reduction in resolving power as a consequence of the multiple reflection of the light beams from the sensor's multilayer structure [2]. In a number of cases, therefore, an increase in input speed can be achieved either by combining high-sensitivity photodiodes with opticomechanical scanners, the scanning speed of which has reached television standards [3], or by the creation of photodiode rulers for multichannel reading. Both approaches involve an increase in the sensors' total light-sensitive area

and, correspondingly, the photodiodes' capacity. As a result, the basic shortcomings of photodiode sensors become apparent: the maximum spatial method of connecting these photoreceivers and the dependence of the amplitude of the pulses at the sensor's output on the dynamic band of the light signals.

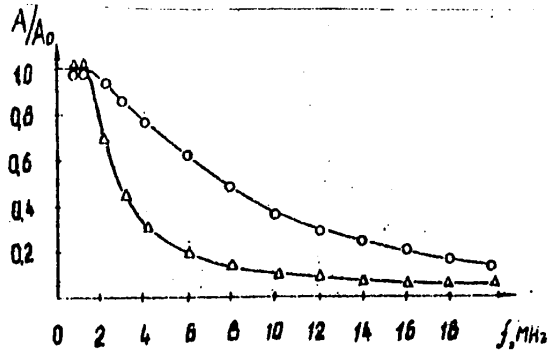

Figure 1. AChKh of high-sensitivity photodiodes for small values of R_H: o = FD-11K; Δ = FD-7G.

The amplitude-frequency characteristic (AChKh) of two sensitive photodiodes, as shown in Figure 1, can serve as an example illustrating the possibility of evaluating unambiguously the time lag of a converter when photodiode connection is used. The AChKh's have been read for those values of load resistance R_H that are normally used when working with high-frequency elements (50-75 Ω) and make it possible to reach a conclusion about the possibility of using these instruments on frequencies exceeding the frequencies corresponding to the textbook operating speed values ($5 \cdot 10^{-6}$ s) by almost an order of magnitude. However, as a result of the fact that photodiodes are high-ohm elements in the electrical circuit, reducing R_H entails a corresponding reduction in the output signals' values.

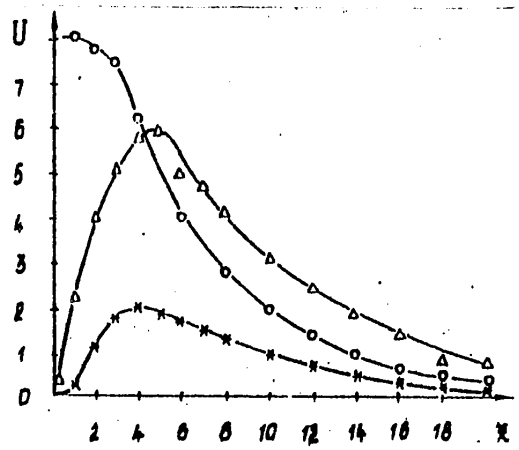

Figure 2. FD-11K photodiode saturation curves for R_H = 10 k : o = constant component; Δ = variable component at frequency of 30 kHz; * = variable component at frequency of 100 kHz; z = 1/ε, where ε = irradiation.

Besides this, inherent in the photodiode connection method are limitations related to the power of the light pulses being received. In connection with this, it has recently been established [4] that the high-frequency sensitivity of photodiodes can be saturated at levels of optical radiation that are considerably lower than those required for the creation of a constant saturation current. Figure 2 shows the dependences that have have found for the change in the amplitude of the variable component of a sinusoidal signal and the magnitude of the constant component at the photodiode's output on the value of the relative attenuation of the light flow (in comparison with its value Φ_H, which corresponds to saturation of the watt-ampere characteristic). They enabled us to convince ourselves experimentally that for certain relationships between R_H and photodiode capacitance $C_{\phi\partial}$, these limitations exist even for comparatively low light signal frequencies.

Photoparametric systems, some varieties of which--based either on a change in photodiode conductivity when acted upon by a light flow Φ or on a corresponding change in $C_{\phi\partial}$--have been known for quite a long time [5,6], are free from these flaws to a certain degree. However, the necessity of using two identical photoreceivers in the first case [5] and the narrow band of changes in perceivable light flows in the second [6] has caused their use to be limited, and in the literature there is almost a complete lack of information on the sensitivity and operating speed of photoparametric systems in comparison with systems using other methods of connecting the photoreceivers.

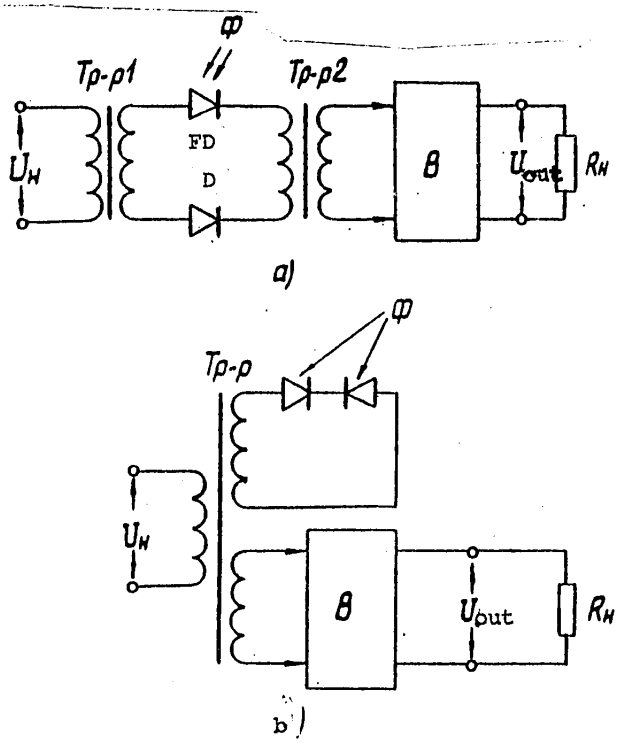

Figure 3. Schematic diagrams of photoparametric systems: a. series; b. parallel; FD = photodiode; D = high-frequency diode; B = amplitude detector (rectifier); U_H = pump voltage.

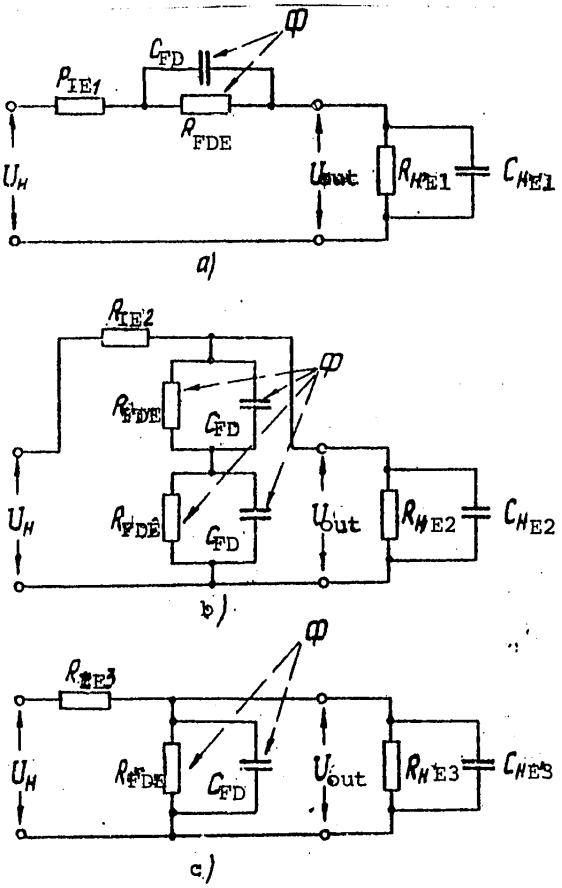

Figure 4. Equivalent circuits: a. of series-connected parametric system; b. of parallel-connected parametric system; c. of system with photodiode connection of the converter; R_{IE}, R_{FDE}, R_{HE}, C_{HE} = equivalent values, respectively, of the power source's resistance, the photodiode's back resistance and the load resistance and capacitance.

Here we present two elementary systems for the photoparametric conversion of light flows, the schematic diagrams of which are shown in Figure 3.

The role of the first transformer in the series-connected system is limited by the matching of the high-resistance circuit from the diodes connected in opposition with the output circuits of the pumping voltage generator. The second high-frequency transformer in the series-connected system, as is the case with the transformer in the parallel-connected one, is needed to generate the variable component of the photodiode's flow on frequency f_H, which corresponds to the first harmonic of pumping voltage U_H.

All of the characteristics presented below were read with the help of diode fullwave rectifiers charged to a resistance of 10 kΩ and the filter's capacitance. The value

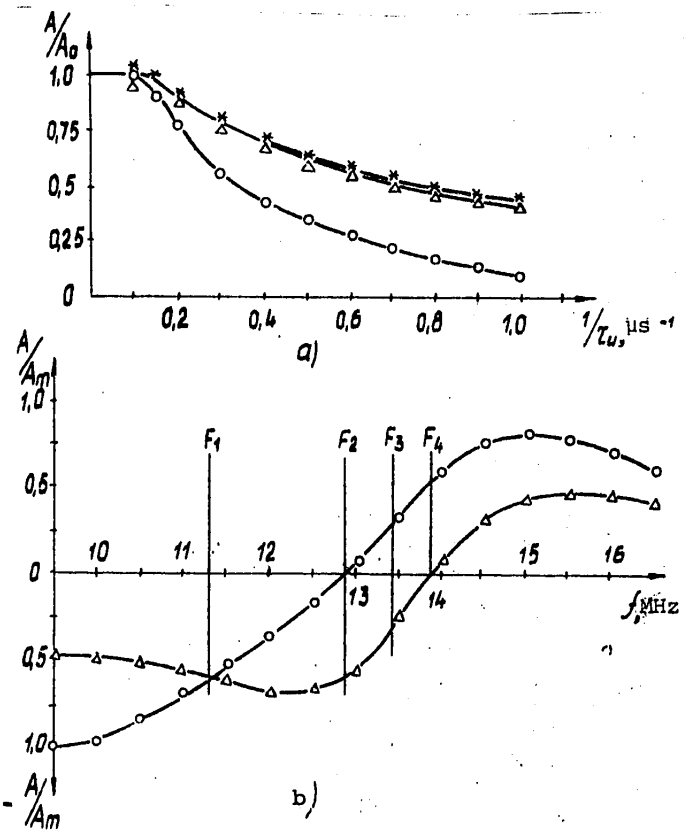

Figure 5. AChKH's of: a. * = ZL-119 light diode; Δ = series-connected photoparametric system; o = photodiode method; b) parallel-connected photoparametric system; Δ = for low illumination of the photodiodes; o = for high illumination of the photodiodes.

of R_H for the systems that have been presented can change within quite broad limits, although the highest output signal values are achieved for small photodiode current flow angles; that is, when the condition $R_H > 100 \cdot R_{\phi\partial}$ is fulfilled [7], where $R_{\phi\partial}$ is the back resistance of an open photodiode. (For example, for an FD-11K, $R_{\phi\partial} \approx 10$ Ω, so for a transformation rate that equals unity, it should be the case that $R_H >$ > 1 kΩ.)

Omitting the common and quite trivial and awkward computations from the field of electrical engineering, let us proceed to a discussion of the equivalent circuits in Figure 4, which model the operation of the series- and parallel-connected parametric systems, as well as the operation of the converter when the photodiode is connected (Figure 4c), in the area of high frequencies of changes in light flows; that is, for those modes when, under the obligatory condition $f_H > f_{cb.c}$ (where $f_{cb.c}$ is the frequencies of the light signals' higher harmonics), the value of $1/2\pi f_H C_{FD}$ turns out to be comparable with the value of $R_{\phi\partial}$ and, at the same time, for the series-connected system the value of $1/2\pi f_H C_D$ remains comparable with the value of a

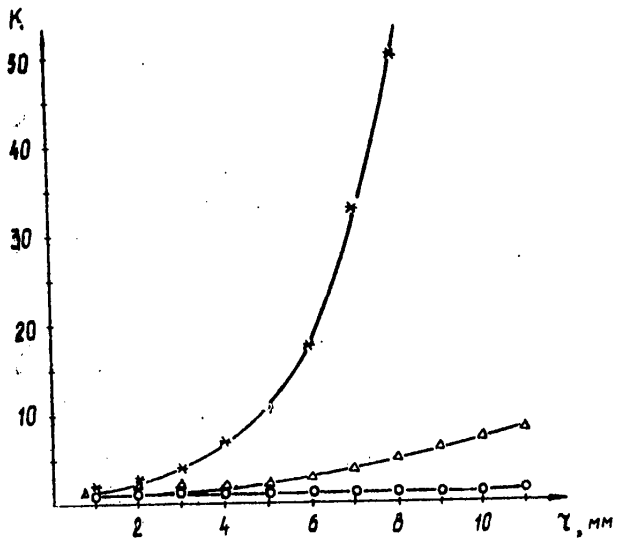

Figure 6. Characteristics of perceivable contrast in seismograms: * = for series-connected photoparametric system; Δ = photodiode mode; o = valve mode.

darkened photodiode. Let us mention here that the fulfillment of the latter condition, as it applies to the problem of obtaining the maximum values of the output signals at the system's output, is possible only if $C_{FD} >> C_D$.

Directly from Figure 4 we can see the obvious potential possibility of increasing the operating speed in the system (Figure 3a) in comparison with the system with photodiode connection of the sensor, since in the former, capacitance C_{HE} is connected in series with capacitance C_{FD}. This possibility is confirmed by the AChKh's of the corresponding systems, which are presented in Figure 5a. The AChKh's were read with the help of an opticoelectronic pair consisting of an FD-25K photodiode and a ZL-119 light diode that were excited by light pulses ranging in duration from 100 μs to 1 μs, with an on-off time ratio of at least 5. The light diode's AChKh was determined with an FEU-62 photomultiplier.

Directly from Figure 4b it is obvious that there are no inherent analogous possibilities in the parallel-connected system. However, when operating with a pumping frequency that is close to the antiresonance frequency, this system is of considerable interest for the solution of the problem of increasing the noise stability of the reading process [8]. The AChKh's of such a system (read with the help of FD-25K photodiodes) are presented in Figure 5b, and they make it possible to form an opinion about the special features of the operating modes of a system with pumping frequencies corresponding to cross-sections F_1, F_2 and F_4, as well as cross-section F_3 (the most interesting mode), in which output signals of the system that are different in magnitude and polarity correspond to the two values of the light flow.

The sensitivity characteristics of photoparametric systems are better than the analogous characteristics of systems with photodiode and valve connection of the photoreceivers. This is determined by the total unidirectional change of both the

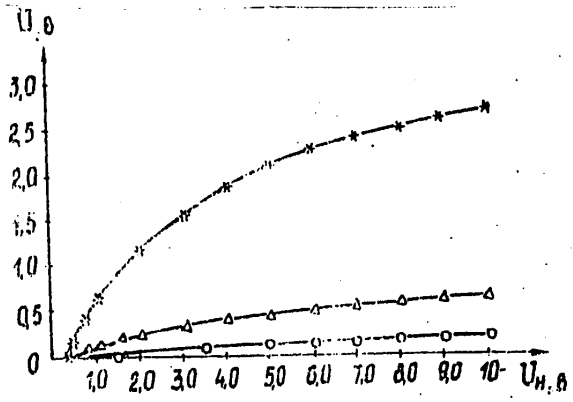

Figure 7. Parametric characteristics of a series-connected system with a high-sensitivity p-i-n photodiode.

conductance and susceptance of the photodiodes when the amount of illumination of the light-sensitive areas changes. However, for the parallel-connected system these characteristics also depend unambiguously on the value of f_H, as well as the system's structural parameters and the method used to process the output signals. The selection of the optimum parameters for this system requires a rigorous mathematical analysis of it, the realization of which within the limits of this article is not possible.

For the series-connected photoparametric system, several completely unambiguous sensitivity characteristics have been derived by the experimental method. For instance, in Figure 6 we present the characteristics of the change in contrast parameter K [8] as a function of the distance between the film with the seismogram recordings and the photoreceiver. The characteristics were read with the help of a high-sensitivity p-i-n photodiode and a GaAs light diode, with f_H = 4 MHz.

In Figure 7 we see, for different levels of illumination of the converter, the changes in the value of the series-connected photoparametric system's output signal as a function of the pumping voltage's amplitude. Experimental investigations of the proposed parametric systems made it possible to discover two special features of any families of similar characteristics: in all cases the indicated functions intersect the X-axis and in all cases the increase in the output signal, beginning with certain values of the pumping voltage, moves toward saturation. The latter fact means that in photoparametric systems it is possible to realize operating modes in which instability of the value of U_H will not have any substantial effect on the output signals' stability.

Finally, in Figure 8 we see the saturation curve for the series-connected photoparametric system in comparison with the analogous characteristics for photodiode and valve connection of the photoreceiver, which is the dependence of the change in the output signal's value on the distance r between a photodiode and a light diode by means of which light pulses with a power of 100 mW and a duration of 10 s were excited. Directly from Figure 8 it is obvious that for systems utilizing the photodiode and valve methods of connecting the converter, saturation sets in at considerably lower levels of illumination of the light-sensitive area than for the indicated photoparametric system

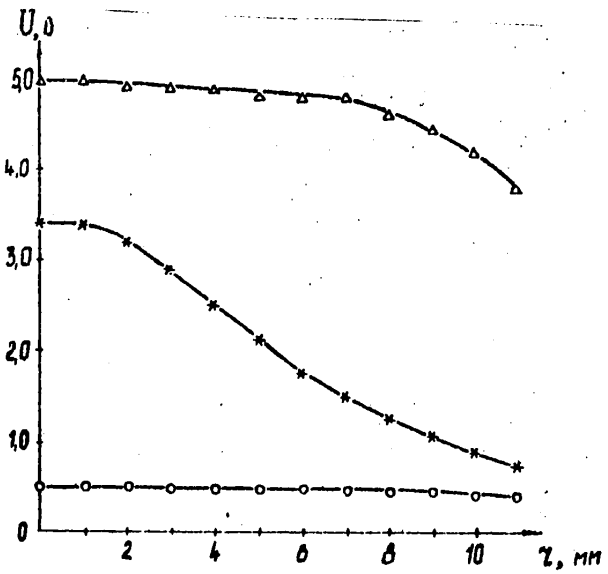

Figure 8. Saturation curves for FD-25K photodiode: * = for series-connected photoparametric system; Δ = for photodiode connection; o = for valve connection.

In conclusion we should mention that for a low load resistance value and pulsed pumping, the photoparametric mode in a series-connected system (Figure 3a) degenerates into the normal mode of photodiode connection with charge accumulation. In connection with this, the system's operating speed and sensitivity are determined by the relationship between the durations of the light signals and the pumping pulses.

BIBLIOGRAPHY

1. Potapov, O.A., "The Problem of Processing Large Masses of Geological and Geophysical Information and Ways of Solving It," in "Golografiya i opticheskaya obrabotka informatsii v geologii i geofizike" [Holography and Optical Information Processing in Geology and Geophysics], Leningrad, 1979, pp 5-18.

2. Kobayarsi, Ye., "Solid-State Image Sensors," DENSI DZAYRYO, Vol 17, No 8, 1978, pp 76-81.

3. Benedichuk, I.V., et al., "A Television Unit With Opticomechanical Scanning," TEKHNIKA KINO I TELEVIDENIYA, No 10, 1978.

4. Lawton, R.A., and Young, M., "Photodetectors Lose Dynamic Range With Modulated Signals," DIMENS/NBS, Vol 61, No 12, 1977, pp 16-19.

5. Voronin, V.G., Grebnev, A.K., Krivonosov, A.I., and Ruslanov, V.I., "Skhemy avtomatiki s fotochuvstvitel'nymi i izluchayushchimi poluprovodniknovymi priborami" [Automation Systems With Photosensitive and Emitting Semiconducting Instruments], Moscow, Izdatel'stvo "Energiya", 1972, p 80.

6. Elizbarashvili, O.A., "A Detector for Weak Light Signals Based on Photodiodes Operating in the Fetovarikap [translation unknown] Mode," TRUDY INSTITUTA KIBERNETIKI AN GRUZ. SSR, Vol 3, 1977, pp 133-142.

7. Gonorovskiy, I.S., "Radiotekhnicheskiye tsepi i signaly" [Radio Engineering Circuits and Signals], Moscow, Izdatel'stvo "Sovetskoye radio", 1971, p 672.

8. Dutov, A.V., "Investigation of the Noise Stability of Several Methods for the Optical Reading of Geophysical Information," in "Gologrāfiya i opticheskaya obrabotka informatsii v geologii i geofizike", Leningrad, 1979, pp 123-133.

UDC 550.834.05

ON THE QUESTION OF THE PHASE ENCODING OF SEISMIC SIGNALS IN OPTICODIGITAL INFORMATION PROCESSING SYSTEMS

Leningrad GOLOGRAFIYA I OPTICHESKAYA OBRABOTKA INFORMATSII V GEOLOGII in Russian 1980 (signed to press 19 Nov 80) pp 57-64

[Article by V.P. Ivanchenkov and A.I. Kochegurov from collection of works "Holography and Optical Information Processing in Geology", edited by Professor S.B. Gurevich and Candidate of Technical Sciences O.A. Potapov, Leningrad Physicotechnical Institute imeni A.F. Ioffe, USSR Academy of Sciences, 500 copies, 181 pages]

[Text] The authors discuss the possibility of using phase encoding of seismic signals when they are being entered in the optical processor of an opticodigital computer complex. They present the results of their statistical modeling and some evaluations of the effectiveness of the utilization of phase encoding in problems involving the correction of static correction factors.

Increasing the efficiency and productivity of the realization of hybrid computations in opticodigital information processing systems depends to a considerable degree on the choice of the method for encoding the seismic signals when the data are being entered in the optical processor. The correct choice of the signal encoding method makes it possible--depending on the realized processing algorithms--to reduce their statistical redundancy and to compress the data.

In a number of processing problems where information on the form of the seismic signals is not used directly, it is feasible to examine the possibility of using phase encoding methods. For instance, one of the basic procedures in the processing of seismic data is correction of the static correction factors. As is well known, the most widely used automatic correction algorithm, which is based on calculation of the cross-correlation function (FVK) of adjacent tracks, yields the required accuracy only for rather simple material. When there is a large degree of wave dispersion with respect to velocity in the interval being analyzed and a high noise level, the determination of the displacements with respect to the tracks' maximum cross-correlation can result in substantial errors in their evaluation. Therefore, the problem of improving the reliability of the evaluation of the mutual displacements remains one of the basic ones when correcting static correction factors. In view of this, in this article we discuss the question of improving the reliability of the determination of the mutual displacements of seismic tracks presented in the form of nulls of a clipped signal.

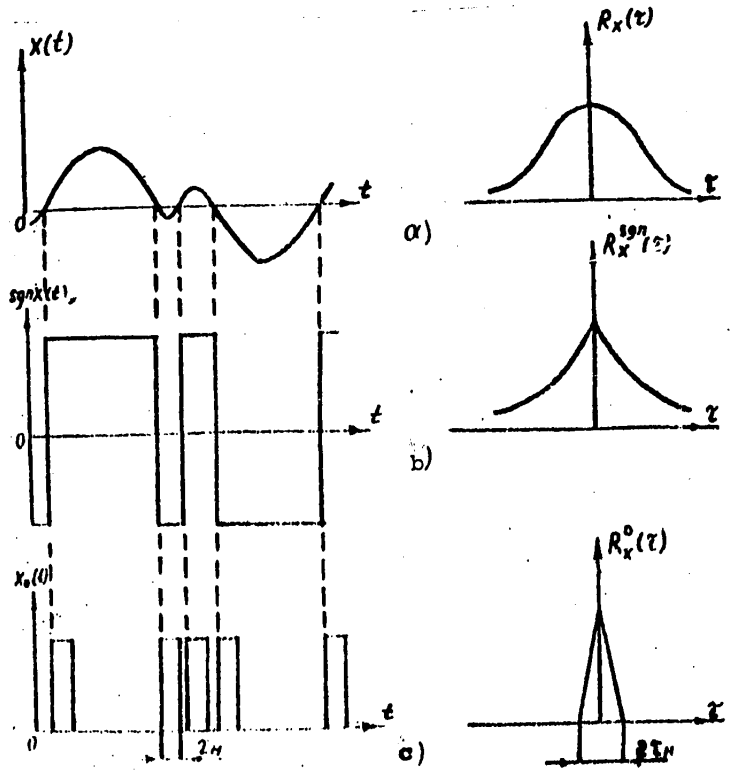

Figure 1.

Figure 1a depicts the realization of process x(t) and its corresponding correlation function $R_x(r)$. When the clipping is sufficiently thorough, this signal is converted into rectangular pulses (Figure 1b) and is frequently called a clipped signal. The use of character encoding is quite well known, particularly in the realization of various correlational processing algorithms. At the same time, the original information of phase encoding can be represented in a different form, as some sequence of nulls of the clipped signal $x_0(t)$ (Figure 1c):

$$\begin{cases} 1, & x(t)\cdot x(t+1)<0, \\ 0, & x(t)\cdot x(t+1)\geqslant 0. \end{cases} \tag{1}$$

The sequence of nulls contains all the necessary information about the clipped signal, as well as information about the initial phase of the original signal's first harmonic [1].

In order to evaluate the possibility of using phase encoding in the problem of correcting static correction factors at the stage of determining the mutual displacements of the tracks, we utilized statistical modeling on a computer to investigate the noise stability of the correction algorithm for such a recording.

The assumed given was two seismic tracks, representing an additive mixture of signal and noise, it being the case that the signal on the second track had a certain

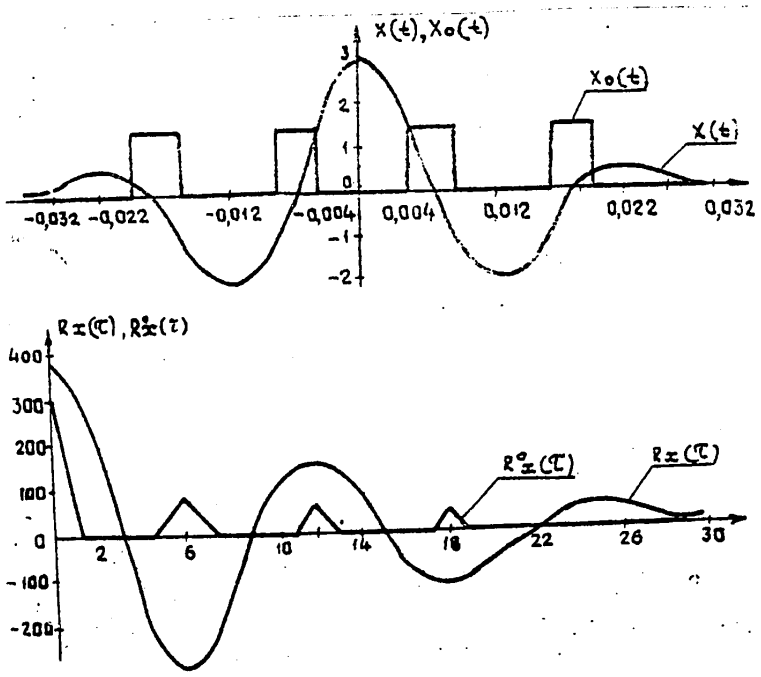

Figure 2.

displacement Δt:

$$y_1(t) = x(t) + N_1(t),$$
$$y_2(t) = x(t + \Delta t) + N_2(t). \qquad (2)$$

As the useful signal we chose a pulse with a bell-shaped envelope, which is widely used as the model of a singly reflected wave. Displacement Δt was determined beforehand and was chosen in accordance with practical recommendations. Noise N(t) was generated by a generator of random numbers having a normal distribution law $M[N(t)] = 0$ and $\sigma^2[N(t)] = 1$. As an example, in Figure 2 we show the original and transformed signals, as well as their corresponding correlation functions.

Between the tracks thus formulated, we determined the temporal displacement with respect to the FVK's maximum. The fact that the solution of any computational problem by constructing and realizing an artificial random process can, in the final result, give only approximate values of the unknown parameters, or so-called estimates of them, applies to a number of features of a method with statistical testing [2]. A solution obtained in this manner is of practical value only if it is possible to find an area of possible deviations of the obtained estimates from the corresponding unknown parameters; in other words, if the accuracy of the estimates is investigated. As the estimates in this problem, we chose the mathematical expectation m_τ and dispersion σ_τ^2 of the temporal displacement τ as a function of the signal-to-noise ratio. In order to evaluate the noise level, we used the ratio of the square of the signal's peak value to the dispersion of the noise, which is used very extensively in seismic surveying [3]:

$$\rho = \frac{A_\psi^2}{\sigma^2}, \qquad (3)$$

Analyses were conducted for ρ = 3, 1, 0.5, 0.2. It was assumed that the permissible measurement error was 2 ms. In order to achieve a confidence probability P of 0.95, the experiment encompassed 384 observations. The functions of the distribution of the temporal displacement between the tracks for the given values of ρ are shown in Figures 3 and 4 for the standard and converted forms of the recording, respectively.

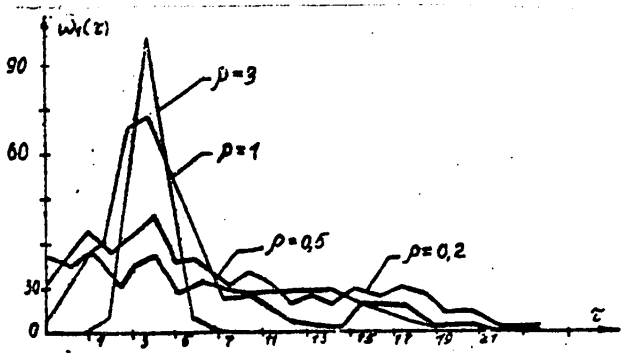

Figure 3.

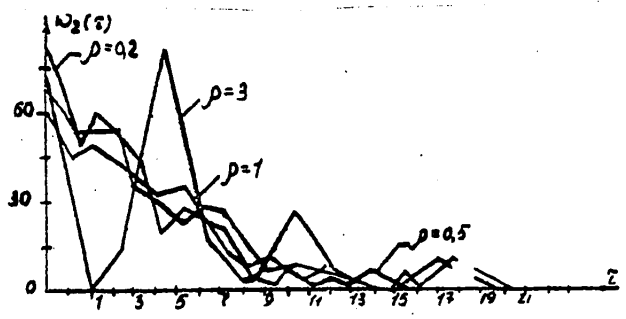

Figure 4.

The calculated statistical characteristics (mathematical expectation and dispersion) for the obtained distributions are presented in Table 1.

Figure 5 shows the dependence of the deviation in mathematical expectation m_τ on the true value for the given values of ρ, while Figure 6 shows the dependence of dispersion σ_τ^2 for the computed displacement τ.

Analysis of the results obtained with the help of the numerical experiment with the computer showed that for a sufficiently large signal-to-noise ratio ($\rho > 3$), phase encoding of the original information yields no gain in noise stability in comparison with the standard form of the recording, although for small signal-to-noise ratios ($\rho < 1$), the gain is obvious (Figures 5 and 6). This can apparently be explained by the fact that when there are severe distortions of the useful signal (a small signal-to-noise ratio), the cross-correlation function for the standard form of the recording is computed with more substantial errors than in the second case, where the form of the recording is not taken into consideration

Table 1.

ρ	Исходный сигнал (I) (1)		Преобразованный сигнал (2) (2)	
	m_τ	σ_τ^2	m_τ	σ_τ^2
3	4,92	0,46	5,06	I,8I
I	6,26	I8,3	4,27	I5,I6
0,5	7,43	28,25	3,76	II,36
0,2	7,83	30,24	3,42	I0,23

Key:
1. Original signal
2. Converted signal

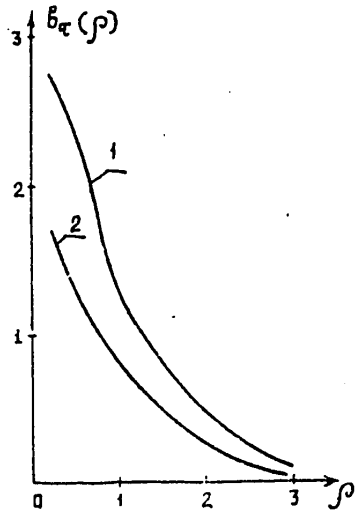

Figure 5.

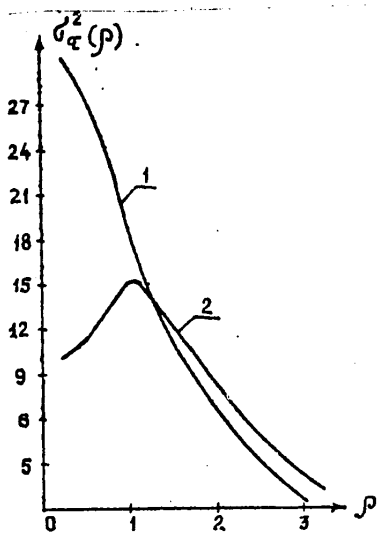

Figure 6.

Further, we carried out an experimental investigation of the possibility of using phase encoding when processing seismograms. For this purpose we developed an algorithm for computing the waves' mutual displacements for both the standard recording and the one converted into the form of nulls of a clipped signal; this investigation utilized materials from the Tomsk Geophysical Trust. The static correction factors computed with the algorithm were introduced into the appropriate tracks and the tracks were summed with the reference track with respect to which the correction factors had been computed. The summary recordings for the standard and converted forms of the recordings are presented in Figures 7 and 8, respectively.

A comparative analysis of the results showed that the location of the main maximum on the temporal axis of the summary recordings coincided and was 304 ms, while the values of the maximums themselves also differed very little. At the same time, on the second recording there is more nearly complete suppression of secondary waves and discrimination of the basic wave (three wave entries are quite visible in Figure 8).

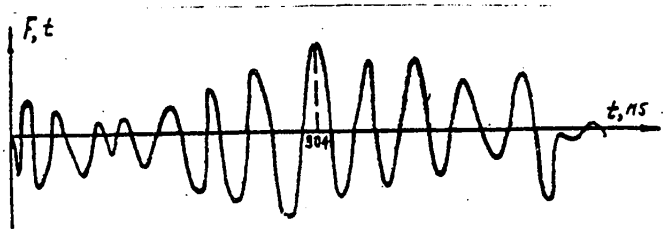

Figure 7.

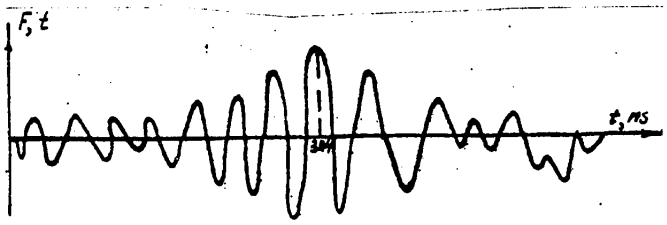

Figure 8.

Thus, our investigations indicate that the prospects are good for the utilization of phase encoding, in connection with which the volume of the original data can be reduced by a factor of 15-20 and the noise stability of the determination of the displacements for small signal-to-noise ratios can be improved.

BIBLIOGRAPHY

1. Komolov, V.P., and Trofimenko, I.T., "Kvantovaniye fazy pri obnaruzhenii radiosignalov" [Phase Quantization During the Detection of Radio Signals], Moscow, Izdatel'stvo "Sovetskoye radio", 1976.

2. Pustyl'nik, Ye.I., "Statisticheskiye metody analiza i obrabotki nablyudeniy" [Statistical Methods for Analyzing and Processing Observations], Moscow, Izdatel'stvo "Nauka", 1968.

3. Shestov, N.S., "Vydeleniye opticheskikh signalov na fone sluchaynykh pomekh" [Distinguishing Optical Signals Against a Background of Random Noise], Moscow, Izdatel'stvo "Sovetskoye radio", 1967.

UDC 550.834.05

MATHEMATICAL MODELING OF PROCESSES FOR RECORDING SEISMIC SIGNALS ON A THERMOPLASTIC CARRIER DURING THEIR INPUT INTO THE OPTICAL PROCESSOR OF AN OPTICODIGITAL COMPLEX

Leningrad GOLOGRAFIYA I OPTICHESKAYA OBRABOTKA INFORMATSII V GEOLOGII in Russian 1980 (signed to press 19 Nov 80) pp 65-73

[Article by V.P. Ivanchenkov and O.G. Dolmatova from collection of works "Holography and Optical Information Processing in Geology", edited by Professor S.B. Gurevich and Candidate of Technical Sciences O.A. Potapov, Leningrad Physicotechnical Institute imeni A.F. Ioffe, USSR Academy of Sciences, 500 copies, 181 pages]

[Text] The authors discuss questions concerning the mathematical modeling of the processes involved in the recording of seismic signals on a thermoplastic carrier, and investigate the effect of different parameters on the depth of the groove and the rate of relief development for the purpose of insuring the best matchup of temporal relationships during data input-output utilizing an optical processor.

During the development of an opticodigital computer complex (OEVK) for the processing of geophysical information as a somewhat complicated computer system, there arises the problem of choosing the most rational structure for the computer complex, allowing for the properties of the signals being analyzed and the processing algorithms being realized, the determination of the basic parameters of the systems' elements and assemblies, and the study of the effect of different factors on the entire process of the realization of hybrid computations.

The formulation of a mathematical model of the OEVK is of importance both for the synthesis and analysis of the hybrid opticoelectronic system.

The mathematical description of an OEVK can be determined in several stages. In the first stage, for example, on the basis of the required class of processing algorithms that must be realized in the OEVK, the general structure of the system is planned and several alternative formulations of it are examined.

During the next stage, a functional description of the separate units and assemblies is determined and the effect of their parameters on the system's characteristics and operating modes is investigated.

The basic functional elements of an OEVK include a spatiotemporal light modulator (PVMS) that makes it possible to carry out the operational input of data into an

optical processor. A comparative analysis of existing PVMS's showed that the use of light-valve tubes with a thermoplastic carrier shows promise for the processing of seismic data [1].

The processing of recording a signal on a TPH [thermoplastic carrier] with the help of an electron beam can be broken down into two stages: application of the charge to the TPN, which leads to the appearance of electrical forces capable of deforming the thermoplastic layer, and the recording appearance and erasure stage. Depending on the mode chosen for the recording of the seismic signals, these stages can be either carried out at the same time or realized separately.

In order to determine the mathematical description of the relief manifestation and erasure process, it is necessary to know the medium's equation of motion and the nature of the forces causing this motion.

In the literature there are several approaches to the description of the process of relief manifestation and appearance on a TPN [2,3].

For cases where the applied voltages and deformations are small, a TPN can be described in a linear approximation based on the relationships derived during the description of the mediums' motion with a (Fogt) model, which is the most common one and takes into consideration the properties of an elastic-viscous, as well as a viscous, medium.

Under these conditions, the problem of finding the mathematical description of the appearance and erasure of surface relief on a TPN can be reduced to the three-dimensional problem of determining the deformations of the surface of an incompressible, elastic-viscous layer of finite thickness d when it is acted upon by surface and volume forces with an initial disturbance F_{op}. In Cartesian coordinates x,y,z, the elastic-viscous medium's equations of motion have the following form [2]:

$$\begin{aligned}
\frac{\partial V_x}{\partial t} &= -\frac{1}{\rho}\frac{\partial P}{\partial x} + \nu\Delta V_x + \frac{G}{\rho}\Delta\int_0^t V_x\,dt + F_{ox};\\
\frac{\partial V_y}{\partial t} &= -\frac{1}{\rho}\frac{\partial P}{\partial y} + \nu\Delta V_y + \frac{G}{\rho}\Delta\int_0^t V_y\,dt + F_{oy};\\
\frac{\partial V_z}{\partial t} &= -\frac{1}{\rho}\frac{\partial P}{\partial z} + \nu\Delta V_z + \frac{G}{\rho}\Delta\int_0^t V_z\,dt + F_{oz};
\end{aligned} \tag{1}$$

where $P_0(x,y,z)$ = surface density of the forces, the value of which is assumed to be given at the initial moment; $P_0(x,y,z,t)$ = components of the initial volumetric density of the forces with respect to the axes; ρ = density of the medium; v = rate of motion of the medium's particles; Δ = a Laplace operator; G = equilibrium shear modulus; μ = coefficient of viscosity; $\nu = \mu/\rho$; V_x, V_y, V_z = velocity components, the initial values of which equal zero.

When recording with an electron beam on thermoplastic layers more than 10 μC thick, it is possible to allow for the effect of only the normal component of the surface forces $\zeta(x,y,z)$ on relief appearance and erasure.

When the layer is acted upon by a periodical normal force density of the type

$$P_{oz}(x,y,t) = \sum_{n=1}^{\infty}\sum_{k=1}^{\infty} P_{nk}\, e^{-\omega_p(n,k)t}\cos 2\pi f_{x_n}x\cdot\cos 2\pi f_{y_n}y \tag{2}$$

the equation for the deformation of the TPN's surface has the form

$$f_0(x, y, t) = \sum_{n=1}^{\infty} \sum_{k=1}^{\infty} A_{nk} \cos 2\pi f_{xn} x \cdot \cos 2\pi f_{yk} y, \quad (3)$$

where A_{nk} = the depth of the relief groove of the nk-th harmonic =

$$\frac{P_{nk} F_{nk} W_M(n,k)\left(e^{-w_p(n,k)t} - e^{-w_M(n,k)t}\right)}{\left(W_M(n,k) - W_p(n,k)\right)\left(4G\Omega_{nk} + \Omega_{nk}^2 F_{nk}\right)}, \quad (4)$$

where P_{nk} = amplitude of the density of the nk-th harmonic's forces; f_{xn}, f_{yk} = spatial frequencies with respect to the x- and y-axes, respectively; λ_{nk} = generalized spatial frequency;

$$\Omega_{nk} = 2\pi\sqrt{f_{xn}^2 + f_{yk}^2}, \quad W_M(n,k) = \frac{4G + \alpha\Omega_{nk}F_{nk}}{2\beta},$$

$\tau_\rho(n,k)$ = relaxation time constant of the nk-th harmonic's forces,

$$F_{nk} = \frac{ch\, r_{nk}\, sh\, r_{nk} - r_{nk}}{ch^2 r_{nk} + r_{nk}^2},$$

where r_{nk} = normalized generalized spatial frequency:

$$r_{nk} = d\Omega_{nk}$$

For each individual seismic track during the recording of the signals on a TPH, expression (4) can be discussed in a unidimensional approximation; that is, we assume that $\lambda_{nk} = 2\pi f_{xn}$ and

$$A_n = \frac{P_n F_n W_M\left(e^{-w_p t} - e^{-w_M t}\right)}{\left(W_M - w_p\right)\left[4G \cdot 2\pi f_{xn} + (2\pi f_{xn})^2 F_n\right]}, \quad (5)$$

For known charge motion time constants, the amplitude of the forces' density are determined by the relationship

$$P_n = \frac{\sigma_0 \sigma_1}{\varepsilon_0\left(\varepsilon_2\, th\, 2\pi f_{xn} d + \varepsilon_1\right)}, \quad (6)$$

where σ_0, σ_1 = surface density of the electrical charge (constant and sinusoidal components, respectively); ε_0 = electric constant; ε_1 = dielectric constant of a vacuum; ε_2 = dielectric constant of the thermoplastic.

By substituting expression (6) into (5), we can obtain an expression that makes it possible to investigate the dependence of the relief groove's depth on the charge density and the modulation factor.

In accordance with the model of the appearance and erasure of information recorded on a TPN that we have been discussing, we calculated and investigated (with the help of a computer) the temporal changes in the depth of the groove for several temperature modes and spatial frequencies of the signals for different charge density and modulation factor values.

The range of the change in temperature was selected so as to encompass the possible thermal operating conditions for a light-valve tube, ranging from the glass-transition temperature to the TPN's flow temperature (80-140°C).

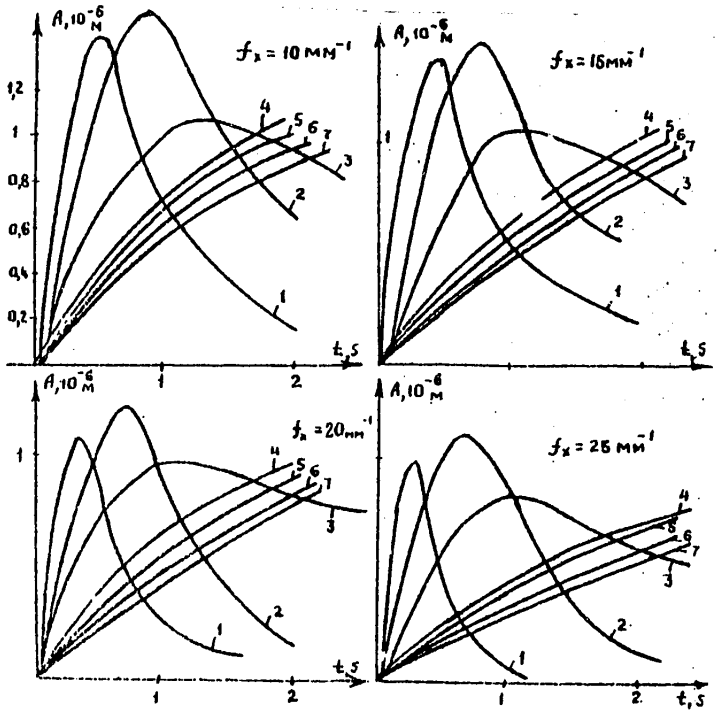

Figure 1. Curves 1-7 have been plotted for temperatures of 140, 130, 120, 110, 100, 90 and 80°C, respectively.

The choice of the spatial frequencies was made for a provisional band of seismic signal frequencies of 20-100 Hz, with due consideration for their recording on a TPN in amplitude-pulse modulation form [4]. The light-valve tubes's resolution with the TPN was assumed to be 20 lines/mm, which was preliminarily accepted as the signal quantification frequency during their recording with amplitude-pulse modulation. Starting from what has been said, during the numerical modeling we conducted our investigation for spatial frequencies ranging from 10 to 27 lines/mm. When calculating the depth of the relief groove on the TPN, in accordance with [5] it is necessary to allow for a number of parameters, the values of which depend on the temperature: viscosity factor μ, equilibrium shear modulus G, surface tension coefficient α. For our calculations, the values of these parameters were taken from sources in the literature [2].

Figure 1 contains graphs characterizing the temporal change in the depth of the relief groove for different temperatures and spatial signal frequences of 10, 15, 20 and 25 mm^{-1}.

Figure 2a depicts the dependence of the optimum appearance time t_{opt} on the temperature for different spatial frequency values. Here we understant t_{opt} to mean the appearance time obtained for the maximum value of the relief groove's depth.

An analysis of the results that were obtained showed that as the temperature increases to 130°C and the density of the applied charge remains the same, the relief groove's depth increases and its optimum appearance time decreases. In connection

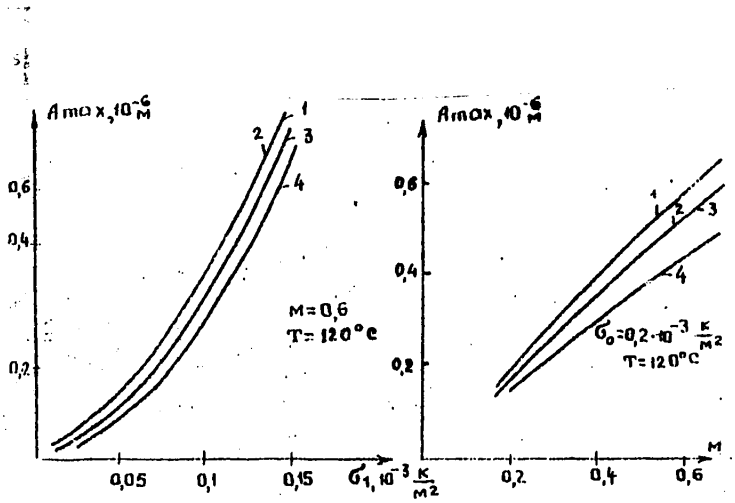

Figure 2. Curves 1-4 have been plotted for f_x = 10, 15, 20 and 25 mm^{-1}, respectively.

with this, however, there is also an increase in the relief erasure rate, it being the case that beginning with the temperature at which the thermoplastic changes from an elastic-viscous state to a viscous state (120°C), its properties change abruptly and the curves take on a resonance form.

Figure 2b shows the dependence of the relief groove's maximum depth on spatial frequency f_x for different appearance temperatures T.

At high temperatures the characteristics are of a resonance type, which makes it possible to lower the level of the high-frequency noise in the reproduced image. However, this property can result in signal distortion because of "butchering" of some part of its spatial frequencies. It is necessary to take all of this into consideration when selecting such parameters as the band of spatial frequencies of the signals being recorded and the temperature at which the information is recorded on and erased from the TPN.

Using the characteristics that have been obtained, it is possible to construct a dynamic manifestation surface $A = \phi(t,T)$ that describes most nearly completely the dynamics of the relief formation and erasure process on a TPN and makes it possible to select the best relief appearance and erasure mode as a function of the selected duration of a frame of the seismic signal recording.

The graphs that have been presented were calculated for charge density $\sigma_0 = 0.2 \cdot 10^{-3}$ C/m^2 and modulation factor M = 0.6.

A computer was also used to calculate the depth of the relief groove for different charge density and modulation factor M values.

The functions $A_{max} = (\sigma, M)$ are presented in Figure 3.

From the graphs it is obvious that A_{max} increases at the depth of the relief groove does, but--as is demonstrated in [5]--a decrease in the depth of modulation of the applied charge results in suppression of the nonlinear frequency distortions. Consequently, it is necessary to allow for both of these factors with selecting these parameters.

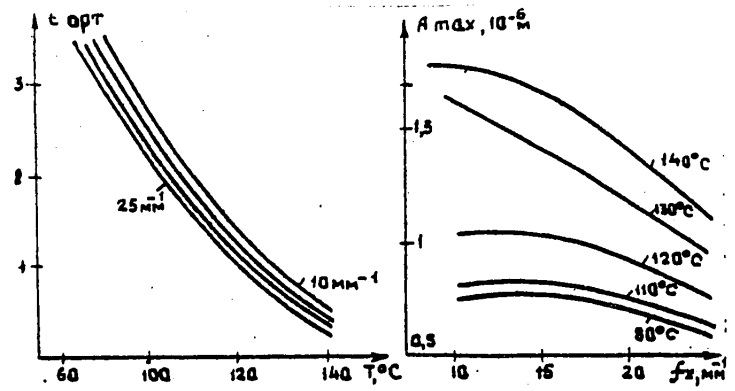

Figure 3.

At the present time, experimental investigations are being made of the processes involved in recording and erasing signals on TPN's, as well as the correction and refinement of modeling results, which in the future will make it possible to choose optimum conditions for recording, reading and erasing information, thereby insuring the best matchup of temporal relationships for data input-output utilizing an optical processor.

BIBLIOGRAPHY

1. Ivanchenkov, V.P., "Hybrid Opticoelectronic Systems for the Processing of Seismic Information," "Tezisy dokladov Vsesoyuznoy konferentsii po avtomatizatsii nauchnykh issledovaniy na osnove primeneniya EVM" [Summaries of Reports Given at the All-Union Conference on the Automation of Scientific Research Through the Use of Computers], Novosibirsk, 1979.

2. Gushcho, Yu.P., "Fazovaya rel'yefografiya" [Phase Reliefography], Moscow, Izdatel'stvo "Energiya", 1974.

3. Nakhodkin, N.G., and Novoselets, M.K., "Functional Description of a Thermoplastic Medium as a Complex Information System," in "III Vsesoyuznaya konferentsiya po golografii, tezisy dokladov" [Third All-Union Conference on Holography: Summaries of Reports], Leningrad, 1978.

4. Ivanchenkov, V.P., Poskonnyy, G.I., and Potapov, O.A., "Recording Seismic Signals on a Thermoplastic Carrier in a Real Time Scale," "EI VIEMS. Region. razved. i promysl. geofizika" [Express Information From the All-Union Scientific Research Institute of Economics of Mineral Raw Materials and Geological Exploration: Regional Prospecting and Industrial Geophysics], Moscow, No 22, 1979.

5. Preston, K., "Kogerentnyye opticheskiye vychislitel'nyye mashiny" [Coherent Optical Computers], Moscow, Izdatel'stvo "Mir", 1974.

UDC 550.834

ON THE POSSIBILITY OF OPTICAL MODELING OF SPATIALLY NONHOMOGENEOUS MEDIUMS

Leningrad GOLOGRAFIYA I OPTICHESKAYA OBRABOTKA INFORMATSII V GEOLOGII in Russian 1980 (signed to press 19 Nov 80) pp 74-83

[Article by V.B. Konstantinov and D.F. Chernykh from collection of works "Holography and Optical Information Processing in Geology", edited by Professor S.B. Gurevich and Candidate of Technical Sciences O.A. Potapov, Leningrad Physicotechnical Institute imeni A.F. Ioffe, USSR Academy of Sciences, 500 copies, 181 pages]

[Text] The authors analyze the use of holographic technology in the solution of seismic surveying problems. They determine the conditions under which an undistorted image of geological structures can be observed and present example of the use of holographic technology for the optical modeling of spatially nonhomogeneous phase and amplitude mediums.

The wave nature of the processes on which seismic surveying is based and the processes involved in the formation of an optical image make it tempting to use the achievements of modern optics for the solution of seismic and geophysical surveying problems. The present level of work being done on methods for the optical processing of information and in holography makes it possible to hope that it will be feasible and promising to use these methods both for processing and storing seismic surveying data and to interpret them. The discussion of the question of the feasibility of using optical methods instead of or together with modern computers is an extremely urgent one in view of the modern requirements for an increase in the efficiency and rapidity of methods for prospecting for useful minerals. In addition to the possibilities of their use in geophysics, optical methods may also prove to be useful in audiovisual and sound fixing and ranging systems. We will concern ourselves with the question of the use of holographic technology to solve seismic surveying problems.

In this area there exist several possibilities:
1. The visualization of a geometric structure's profile [1] or a three-dimensional image of this structure directly from seismic surveying data.
2. The visualization of a geometric structure's profile or a three-dimensional image from seismic surveying data after computer processing of the data.
3. The visualization of models of geological structures calculated by computers.
4. The synthesis of optical images of three-dimensional structures or elements of these structures with given parameters (optical modeling of spatially

nonhomogeneous mediums), both for the purpose of discovering methods for interpreting images of geological structures and directly, in order to interpret three-dimensional images of structures.

5. The use of analogy with optics, for the purpose of optimization of the number of seismic sensors used and the placement of seismic vibration sources and sensors, maximization of the signal-to-noise ratio and so on.

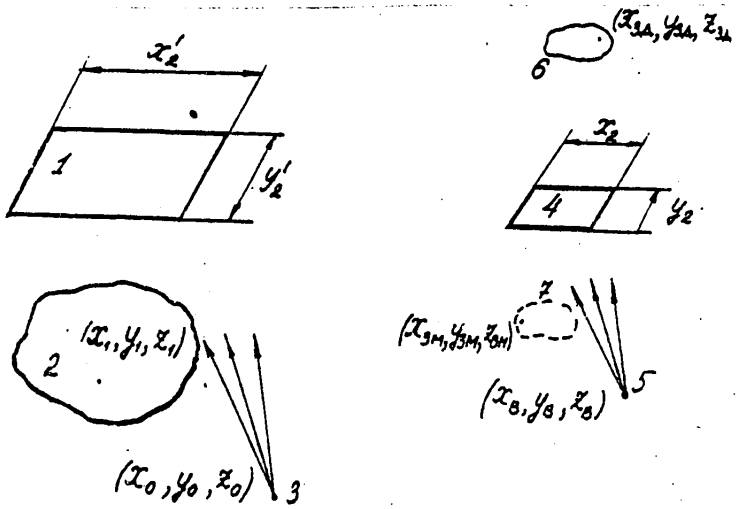

Figure 1. a. Diagram of hologram recording: 1. hologram; 2. object; 3. point reference source. b. Image reproduction diagram: 4. reduced hologram; 5. point reproducing source; 6. actual reproduced image; 7. imaginary reproduced image.

In order to answer questions about the feasibility of the practical realization of each of the listed possibilities, it is necessary to examine them carefully and, possibly, even conduct theoretical and experimental investigations. For instance, in order to obtain a three-dimensional image of a geological structure directly from seismic surveying data and from data processed by a computer, it is necessary to record the amplitudes and phases of the seismic waves and then transform the data obtained into (for example) a hologram, assuming that this can be done. There then immediately arises the question of what will be the nature of this hologram and whether or not the transformation will result in undesirable distortions. For this purpose, let us examine the relationships coupling the coordinates (x_1,y_1,z_1) (Figure 1) of a real geological structure with the coordinates (x_3,y_3,z_3) of the points in its optical image. Let the information about a seismic field be registered in area $x_2'y_2'$, while the length of the seismic wave is λ_1. In order to reproduce the optical image it is necessary to have a reduced hologram with area $x_2y_2 = m^2x_2'y_2'$ for the reproducing light on wavelength $\lambda_2 = \mu\lambda_1$, where m = coefficient of linear reduction of the hologram, while μ is the relationship between the registration and reproducing wavelengths. Then, in the general case, for arbitrary locations of the point reference source (x_0,y_0,z_0) and the point reproducing source (x_B,y_B,z_B), the relationship between the coordinates of the structure's points and those of its optical image is determined by the following relationships [2]:

$$z_{3A}^{M} = \left(\frac{1}{z_3} \pm \frac{\mu}{m^2 z_1} \mp \frac{\mu}{m z_0}\right)^{-1}, \quad (1)$$

$$x_{3A}^{M} = \frac{x_0 z_3}{z_0} \mp \frac{\mu x_1 z_3}{m z_1} \pm \frac{\mu x_0 z_3}{m z_0}, \quad (2)$$

$$y_{3A}^{M} = \frac{y_0 z_3}{z_0} \mp \frac{\mu y_1 z_3}{m z_1} \pm \frac{\mu y_0 z_3}{m z_0}, \quad (3)$$

$$M_{\text{попер}\,A}^{M} = \frac{dx_3}{dx_1} = \frac{dy_3}{dy_1} = \mp \frac{\mu z_3}{m z_1}, \quad (4)$$

$$M_{\text{прод}\,A}^{M} = \frac{dz_3}{dz_1} = \frac{\mu m^2}{\left(m \frac{z_1}{z_0} \mp \mu \pm \mu \frac{z_1}{z_0}\right)^2}, \quad (5)$$

where $M_{\text{попер}}$, $M_{\text{прод}}$ = scale coefficients for the transverse and longitudinal dimensions of the image. As is obvious from (4) and (5), these expressions are different and, in addition, depend on the geometric parameters of the holography and reproduction systems. This means that in the general case, the reproduced image will have geometric distortions that it is practically impossible to compensate for.

For the case of Fresnel's widely used holography system, where plane reference and reproducing waves are used (that is, $z_0 \to \infty$ and $z_B \to \infty$), expressions (1)-(5) take on the forms

$$z_{3A}^{M} = \left(\pm \frac{\mu}{m^2 z_1}\right)^{-1} = \pm \frac{m^2 z_1}{\mu}, \quad (6)$$

$$x_{3A}^{M} = \mp \frac{\mu x_1 z_3}{m z_1} = m x_1, \quad (7)$$

$$y_{3A}^{M} = \mp \frac{\mu y_1 z_3}{m z_1} = m y_1, \quad (8)$$

$$M_{\text{попер}\,A}^{M} = \mp \frac{\mu z_3}{m z_1} = m, \quad (9)$$

$$M_{\text{прод}\,A}^{M} = \mp \frac{m^2}{\mu}. \quad (10)$$

Although in this case the transverse and longitudinal scale coefficients differ from each other by the nature of their dependence on coefficients m and μ, as is shown in Figure 2 they do not depend on the geometric parameters of the holography system. This makes it possible to obtain a geometrically undistorted optical image of a geological structure when $m = \mu$.

However, calculation of the dimensions of the hologram and the reproduced image, as carried out for holography system parameters $x_2' = y_2' = x_1 = y_1 = z_1 = 2 \cdot 10^5$ cm, $\lambda_1 = 10\text{-}10^4$ cm^3 and reproduction system parameter $\lambda_2 = 0.63 \cdot 10^{-5}$ cm, shows that for $m = \mu = 6.3(10^{-8}\text{-}10^{-9})$, $x_2 = y_2 = x_3 = y_3 = z_3 = 1.2(10^{-2}\text{-}10^{-3})$ cm = 0.12-0.012 mm. The practical realization of a hologram of this size is possible, but in order to examine the details of the image it is necessary to use optics, which again leads to geometrical distortion of the image.

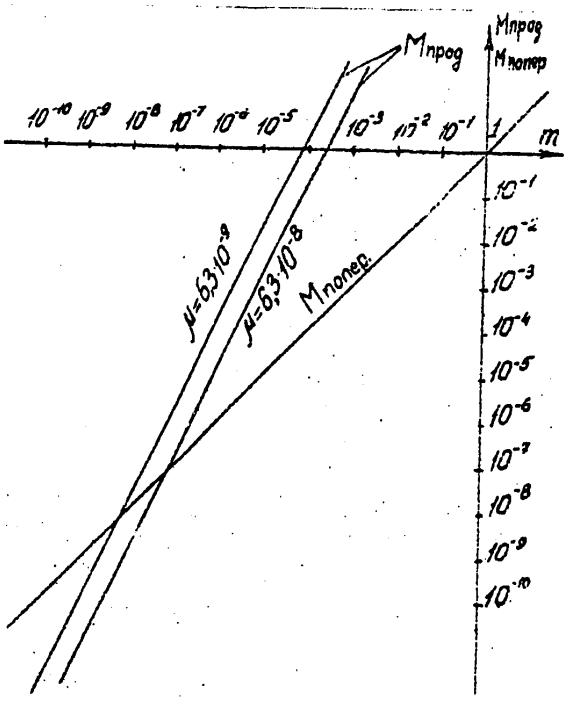

Figure 2. Dependence of transverse M_{nonep} and longitudinal M_{npog} scale coefficients on hologram's linear reduction factor m for $\mu_1 = 6.3 \cdot 10^{-8}$, $\mu_2 = 6.3 \cdot 10^{-9}$.

Therefore, it is necessary to look for an optimum solution to the problem of selecting coefficient m for a given μ that will make it easy to observe the three-dimensional image of a geological structure when there are moderate geometric distortions or to look for methods of compensating for those distortions.

In should be mentioned here that the calculation was made without allowing for the dispersion of the seismic waves, the nature of which differs from the dispersion of light.

Thus, even the question of depicting seismic data in the form of a three-dimensional image of a geological structure proves to be quite complex.

The problem of the formation of holograms with the help of a computer [3] can be solved successfully, although there also there are certain limitations caused, on the one hand, by the small equivalent aperture in which the seismic field is registered. On the other hand, a significant enlargement of the aperture--that is, an increase in the number of sensors and, therefore, the volume of information at the computer's input--can cause a sugstantial increase in the amount of time needed for the processing. For example, for the formation of a hologram that consists of 10^6 elements and makes it possible to reproduce the image of a plane object with no more than 10^5 elements, when a rapid Fourier transform is used the computer computation time will be 20 min [2]. It is obvious that in order to obtain even a stereo image the computation time will at least double, while the question of the

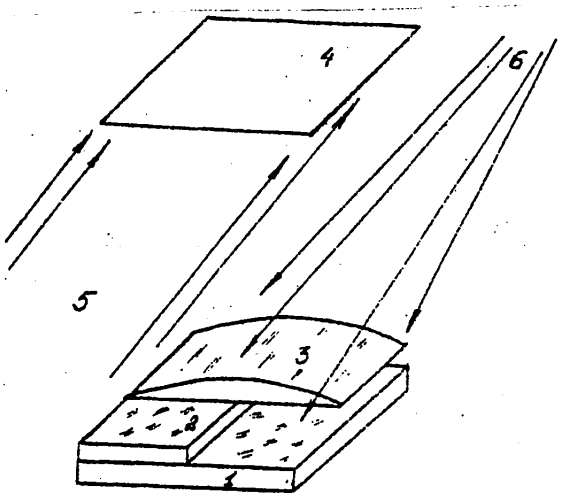

Figure 3. Holographic modeling of a layered structure: 1, 2, 3. glass plates with different refractive indices; 4. photographic plate; 5. parallel reference beam; 6. beam illuminating the object.

amount of information the hologram must contain in order to produce a three-dimensional image of satisfactory quality requires further investigation.

However, even assuming that the question of the formation of a hologram with given parameters can be solved successfully, it is necessary to be sure that the operator will be able to interpret the image of the geological structure. In connection with the holographic image of a geological object, it will be observed as if from above, from the direction of the diurnal surface. This observation position is not customary for geophysicists dealing with the profiles of geological structures. In addition to this, we should (using an optical analogy) regard the geological structure as a phase object; that is, an object in which the basic information is contained in phase, and not amplitudinal, relationships. Some layered structure with different refractive indices can be used as an optical model of such an object. Figure 3 is a representation of the simplest structure of this type and the layout for obtaining an optical hologram. In the reproduced image, the shape and location of the spots of reflected light on the layers' boundaries depends essentially on the depth of focus. Therefore, the question of the correct interpretation of the image by the operator requires special consideration. The creation by the holographic method of standard optical models of spatially nonhomogeneous structures may prove to be useful for educating operators. In connection with this, the holograms of these models can be formed by optical methods or can be designed on a computer.

In our opinion, the holographic method of synthesizing models of a complex three-dimensional structure is the most promising one. Figure 4 depicts a system for the holographic synthesis of a model of a three-dimensional, amplitudinal model. The point source, which in this case is the light guide's end face, is set, in turn, at given points in space. Because of the multiple exposure, the photographic plate sums up all the information about the all the positions of the point source. The

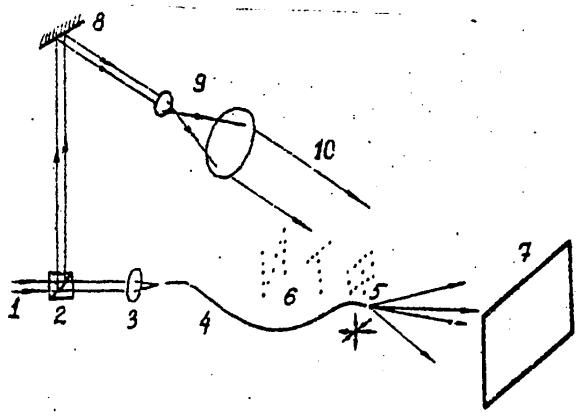

Figure 4. Diagram of holographic synthesis of model of amplitudinal, three-dimensional object: 1. laser beam; 2. splitter; 3. microlens; 4. light guide; 5. end face of light guide; 6. given positions of end face of light guide; 7. photographic plate; 8. mirror; 9. collimator; 10. reference beam.

set of the point source's simultaneously reproduced images also forms the three-dimensional image of a nonexisting object.

Conclusions

1. Thus, even when the discussion is only superficial, the use of optical methods for visualizing geological structures is extremely complicated.
2. In order to make a final judgment about the feasibility of the use of these methods, it is necessary that at least the following be done:
a. determine the feasibility of creating a three-dimensional image of geophysical structures;
b. determine the prospects for methods for the optical modeling of geophysical structures;
c. compare the possibilities of optical modeling methods with other methods for modeling geophysical structures.
3. The achievements that have been made in digital, acoustic and optical holography and the demonstrated capabilities for the synthesis of images of three-dimensional structures gives us a basis for hoping for a successful solution of these problems.

The authors are grateful to S.B. Gurevich and N.A. Karayev for the discussions that led to the appearance of this work.

BIBLIOGRAPHY

1. Timoshin, Yu.V., "Impul'snaya seysmicheskaya golografiya" [Pulsed Seismic Holography], Moscow, Izdatel'stvo "Nedra", 1978.

2. Kol'yer, R., Berkkhart, K., and Lin, L., "Opticheskaya golografiya" [Optical Holography], Moscow, Izdatel'stvo "Mir", 1973.

3. Yaroslavskiy, L.P., and Merzlyakov, N.S., "Metody tsifrovoy golografii" [Methods of Digital Holography], Moscow, Izdatel'stvo "Nauka", 1977.

UDC 550.834

DESIGNING OPTICAL BINARY FILTERS BY LOMAN'S AND LEE'S METHODS AND USING THEM FOR THE FILTRATION OF SEISMIC MATERIALS

Leningrad GOLOGRAFIYA I OPTICHESKAYA OBRABOTKA INFORMATSII V GEOLOGII in Russian 1980 (signed to press 19 Nov 80) pp 84-90

[Article by Ye.N. Vlasov, A.M. Kuvshinov and O.A. Potapov from collection of works "Holography and Optical Information Processing in Geology", edited by Professor S.B. Gurevich and Candidate of Technical Sciences O.A. Potapov, Leningrad Physico-technical Institute imeni A.F. Ioffe, USSR Academy of Sciences, 500 copies, 181 pages]

[Text] The authors explain the principles of the filtration of seismic materials with binary filters. They give the mathematical substantiation for this technique and present specific methods for its practical realization.

The production of an optical filter with a given transfer function is a rather complicated problem, so it is only natural to look for methods that can simplify its solution. In this article we discuss the possibility of applying Loman's and Lee's methods for calculating and forming binary digital hologram filters to the problem of designing different optical filters that can be used in the optical processing of seismic information.

Among the advantages of filters obtained with Loman's and Lee's methods over standard holographic filters synthesized by a computer, first place is occupied by their binary nature. This eliminates the need for halftone registration of the computer-synthesized filter and places less rigorous requirements on the modulator's linear band, since the filter's binary picture is less sensitive to the effects of modulator linearity. In addition to this, a binary picture can be depicted more easily and accurately with the help of standard devices for the output of information from a computer onto an optical carrier.

Let us discuss the process of the formation of an optical filter with a certain transfer function, using Loman's method [1].

Each element of such a filter can be either transparent or nontransparent; that is, it takes on one of two values that can be compared with zero or unity. Such a filter can even be developed on an alphabet printer and then copied onto a photographic carrier.

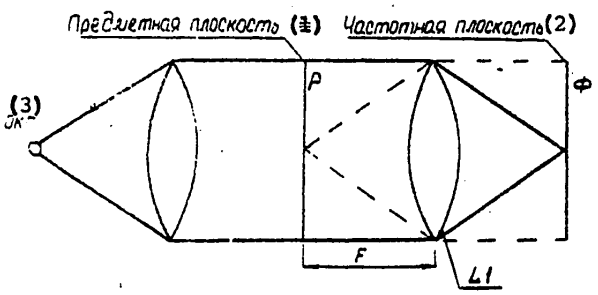

Figure 1. Diagram of KOP for Fourier transform operation.

Key: 1. Subject plane 2. Frequency plane 3. Laser

Figure 1 is a diagram of a coherent optical processor (KOP) that carries out a Fourier transform. Let coordinate system OXY be given in plane P, while system Ow_xw_y is given in plane Φ. We will designate the light field after it has passed the phototransparency in plane P as $h(x,y)$, while the field in plane Φ is $H(w_x,w_y)$. It is then the case that

$$H(w_x, w_y) = \frac{1}{\lambda f}\iint_{-\infty}^{\infty} h(x,y)\, e^{-\frac{2\pi i}{\lambda f}(x w_x + y w_y)}\, dx\, dy, \tag{1}$$

where λ = wavelength of the coherent light; f = focal length of lens L_i. Let function $H(w_x,w_y)$ be quantified in some allowable manner, whereupon

$$h(x,y) = \sum_m \sum_n H(w_x^m, w_y^n)\, e^{2\pi i (x w_x + y w_y)}, \quad m,n = 0,1,2,\ldots \tag{2}$$

Since integral (1) and series (2) converge uniformly, by substituting (2) into (1) we obtain

$$H(w_x, w_y) = \frac{1}{\lambda f}\iint_{-\infty}^{\infty} \sum_m \sum_n H(w_x, w_y)\, e^{-i\frac{2\pi}{\lambda f}[(w_x - w_x^m)x + (w_y - w_y^n)y]}\, dx\, dy. \tag{3}$$

Let us designate the amplitude spectrum as $|H_{mn}|$ and the phase spectrum of the quantified function $H(w_x^m, w_y^n)$ as ϕ_{mn}, whereupon

$$H(w_x^m, w_y^n) = |H_{mn}|\, e^{i\varphi_{mn}} \tag{4}$$

By changing the order of integration and summation in expression (3) and replacing $H(w_x^m, w_y^n)$ by its value from (4), we obtain

$$H(w_x, w_y) = \frac{1}{\lambda f}\sum_m \sum_n \iint_{-\infty}^{\infty} |H_{mn}|\, e^{-i\frac{2\pi}{\lambda f}[(w_x - w_x^m)x + (w_y - w_y^n)y - \varphi_{mn}]}\, dx\, dy. \tag{5}$$

When the variable $\Delta_{mn}x$ is added to and subtracted from the exponent in expression (5), it will take on the form

$$H(w_x, w_y) = \frac{1}{\lambda f}\sum_m \sum_n \iint_{-\infty}^{\infty} |H_{mn}|\, e^{-i\frac{2\pi}{\lambda f}[(w_x - w_x^m - \Delta_{mn})x + (w_y - w_y^n)y - \varphi_{mn} + \Delta_{mn}x]}\, dx\, dy. \tag{6}$$

Let us now select the value of Δ_{mn} so that $\Delta_{mn}x - \phi_{mn} = 0$; it is then the case that

$$H(w_x, w_y) = \frac{1}{\lambda f}\sum_m \sum_n |H_{mn}| \iint_{-\infty}^{\infty} e^{-i\frac{2\pi}{\lambda f}[(w_x - w_x^m - \Delta_{mn})x + (w_y - w_y^n)y}\, dx\, dy. \tag{7}$$

Making use of the relationship

$$\int_{-\infty}^{\infty} e^{-iKw_x}\,dx = \frac{2\pi}{K}\delta(w),$$

where δ is a Dirac delta function, we finally find

$$H(w_x, w_y) = \sum_m \sum_n |H_{mn}|\,\delta(w_x - w_x^m - \Delta_{mn})\,\delta(w_y - w_y^n). \tag{8}$$

For a fixed value of n, we will determine the value of Δ_{mn} from the expression

$$\Delta_{mn} = \frac{[1+(\varphi/m\pi)]}{d}, \tag{9}$$

while the main value of ϕ_{mn} is

$$\varphi = \frac{2\pi}{d}\Delta. \tag{10}$$

Here, ϕ = main value of ϕ_{mn}, d = distance between the apertures, m = number of the reading.

Relationship (8) is the expression for the Fourier spectrum of a binary optical filter. From this expression it is obvious that it is a set of transparent, rectangular apertures against a nontransparent background, it being the case that the width of the aperture is identical for a given filter, while its height is proportional to amplitude $|H_{mn}|$ at the point with coordinates (w_x^m, w_y^n) and its center is displaced along the w_x axis from the grid junction point with numbers (m,n) by distance Δ_{mn}.

Let us discuss the process of producing a binary optical filter according to Loman's method, using as an example a matched filter with the transfer function

$$L(w_x, w_y) = \frac{S^*(w_x, w_y)}{B_n(w_x, w_y)}, \tag{11}$$

where $S^*(w_x,w_y) = S(w_x,w_y)$ complexly conjugated to the useful signal's spectrum; $B_n(w_x,w_y)$ = energy spectrum of the interference.

Methods for evaluating the amplitude and phase spectrums of a seismic signal (assuming that the signal being processed is a minimal-phase one), as well as the interference's energy spectrum, are discussed in [3].

With due consideration for the evaluations given in [3], in order to construct a filter it is necessary to:
1. select distance d between the apertures;
2. select the size of the aperture;
3. calculate the value of $_{mn}$, starting from relationships (9) and (10);
4. determine the apertures' coordinates. (Since we need a value that is complexly conjugated to the useful signal's spectrum, we should use the relationship

$$\int_{-\infty}^{\infty} e^{-iK(-w)x}\,dx = \frac{2\pi}{K}\delta(-w).$$

We will then determine the apertures' coordinates from the equalities

$$\left.\begin{aligned}\Delta_{mn} + w_x^m - w_x = 0,\\ w_y^n - w_y = 0\end{aligned}\right);$$

5. calculate the apertures' heights, which must be proportional to $|H_{mn}|$;
6. compute the filter's transfer function according to formula (11);
7. transfer the picture obtained from the computer onto a photographic transparency.

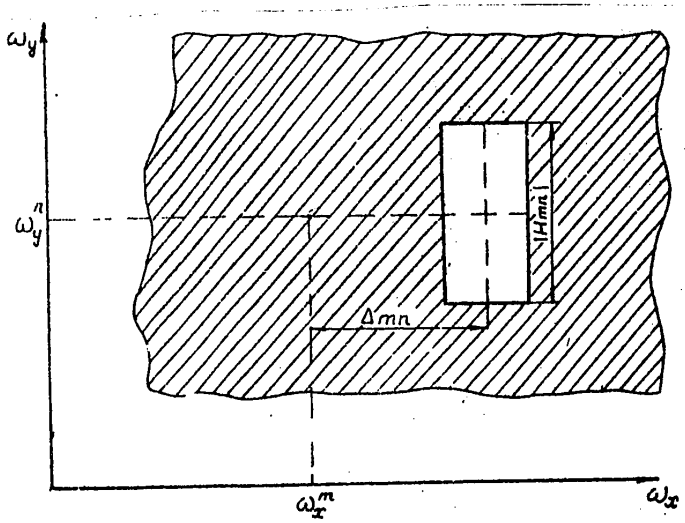

Figure 2. Element of an optical binary filter obtained by Loman's method.

In Figure 2 we seen an element of an optical binary filter obtained by Loman's method.

Here, (w_x^m, w_y^n) = the distance by which the aperture should be displaced along the w_x axis in order to preserve the phase relationships.

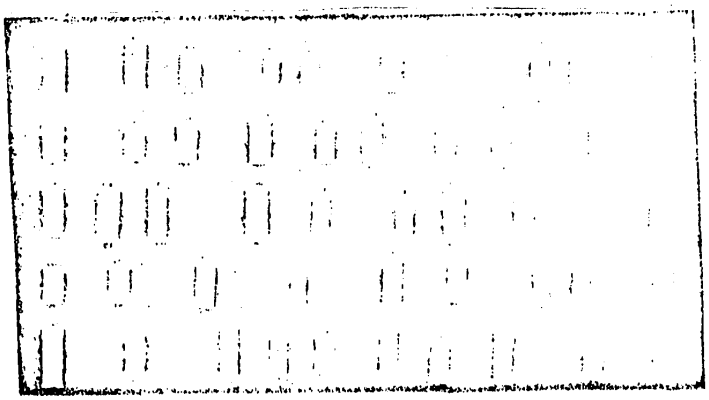

Figure 3. Fragment of a filter.
[Best reproduction available]

Figure 3 depicts a fragment of an optical filter designed on a computer by Loman's method and transferred from the computer onto a photographic transparency.

Filtration of seismic materials has been carried out with a "Kogerent" unit [4].

Another method for encoding the wave front is Lee's method [5], which also makes it possible to obtain binary filters.

The Fourier spectrum of a filter obtained by Lee's method can be written in the form

$$H(w_x, w_y) = \sum_m \sum_n [A_{mn}\,\delta(w_x - w_x^m)\,\delta(w_x - w_y^m) + B_{mn}\,\delta(w_x - w_x^m - \tfrac{\pi}{2})\,\delta(w_y - w_y^n) + D_{mn}\,\delta(w_x - w_x^m - \pi)\,\delta(w_y - w_y^n) + C_{mn}\,\delta(w_x - w_x^m - \tfrac{3}{2}\pi)\,\delta(w_y - w_y^n), \quad (13)$$

[sic--no (12)]

where $\delta(w)$ is a Dirac delta function.

Coefficients A_{mn}, B_{mn}, C_{mn} and D_{mn} in (13) have the following values:

$$A_{mn} = |H_{mn}| \cos\varphi_{mn},$$

$$B_{mn} = |H_{mn}| \sin\varphi_{mn},$$

$$C_{mn} = A_{mn} - |H_{mn}| \cos\varphi_{mn},$$

$$D_{mn} = B_{mn} - |H_{mn}| \sin\varphi_{mn}.$$

From (13) it is obvious that each complex reading of the filter's function, as made at point (w_x, w_y), is represented in four transparent apertures with coordinates

$$(w_x^m, w_y^n), (w_x^m + \tfrac{\pi}{2}, w_y^n), (w_x^m + \pi, w_y^n), (w_x^m + \tfrac{3}{2}\pi, w_y^n).$$

The aperture's width is identical for a given filter, while its height is proportional to A_{mn}, B_{mn}, C_{mn} and D_{mn}. Filters obtained by Lee's method can also be used to process seismic materials.

BIBLIOGRAPHY

1. Akayev, A.A., and Mayorov, S,A., "Kogerentnyye opticheskiye vychislitel'nyye mashiny" [Coherent Optical Computers], Leningrad, Izdatel'stvo "Mashinostroyeniye", 1977.

2. Fedorov, B.F., and El'man, R.N., "Tsifrovaya golografiya" [Digital Holography], Moscow, Izdatel'stvo "Nauka", 1976.

3. Kozlov, Ye.A., et al., "Tsifrovaya obrabotka seysmicheskikh dannykh" [Digital Processing of Seismic Data], Moscow, Izdatel'stvo "Nedra", 1973.

4. Potapov, O.A., "Opticheskaya obrabotka geofizicheskoy i geologicheskoy informatsii" [Optical Processing of Geophysical and Geological Information], Moscow, Izdatel'stvo "Nedra", 1977, p 184.

5. Lee, W.H., "Sampled Fourier-Transform Hologram Generated by Computer," APPL. OPT., No 9, 1970, p 639.

UDC 550.834

'MORGOL' MARINE SEISMOHOLOGRAPHIC SYSTEM

Leningrad GOLOGRAFIYA I OPTICHESKAYA OBRABOTKA INFORMATSII V GEOLOGII in Russian 1980 (signed to press 19 Nov 80) pp 91-99

[Article by O.A. Vorob'yev and A.D. Bezborod'ko from collection of works "Holography and Optical Information Processing in Geology", edited by Professor S.B. Gurevich and Candidate of Technical Sciences O.A. Potapov, Leningrad Physicotechnical Institute imeni A.F. Ioffe, USSR Academy of Sciences, 500 copies, 181 pages]

[Text] The authors discuss questions concerning the creation of a system for continuous marine investigations. They analyze the present state of the development of ship equipment and propose principles for the organization of a system for the collection, processing and visualization of geological and geophysical data.

Multichannel continuous profiling (MNP) entails the accumulation of large data flows. In connection with this, in order to evaluate the quality of the measurements it is necessary to carry out rapid processing and visualization of the data, in the form of a deep section, on board scientific research ships [1].

The on-board "Razrez" [Section] recorder, which was developed at the Gelendzhik branch of NIIMORgeofizika [probably Scientific Research Institute of Marine Geophysics], makes it possible to visualize a black-and-white temporal section on photographic film [2]. However, this instrument does not permit kinematic correction factors to be entered.

The ПУ rerecording device and the ГС-1 seismic holograph that were developed at UKRNIGRI [Ukrainian Scientific Research Institute of Geological Exploration] make it possible to obtain an image of a deep section with velocity and seismic deflection allowed for. However, the ГС-1 holograph does not make it possible to enter signals from a multichannel receiving unit ("tail") during the process of profiling with parallel visual monitoring of the results of the directed filtration of the image and scale transformations.

The construction of deep sections on the basis of the diffraction transformation proposed by Yu.V. Timoshin leads to regularization of the signals (as a result of low-frequency filtration), a change in the section's energy, and large expenditures of computer time for processing (in connection with the selection of the weighting factors) [3]. The equipment realization of the diffraction transformation method on the basis of a specialized computer is unjustifiably awkward and expensive. The

highest accuracy in the construction of deep sections for boundaries with an arbitrary shape is provided by the migration method that was developed by the American scientist (Klerbo). However, the realization of this method on the basis of analog equipment is difficult, while digital processing on a computer requires large amounts of time.

In order to insure operational control of marine research directly on board ships, the Laboratory of Marine Geophysical Holography (LMGG) of the Southern Branch (YuO) of the USSR Academy of Sciences' Institute of Oceanology is developing the "Morgol" system for the rapid processing and visualization of MNP data. The "Morgol" system is the first stage in the creation of a hybrid opticodigital complex for the processing of marine geophysical data on board scientific research ships [4]. It is being created on the basis of mathematical modeling and coupling of the measuring, recording and control instruments by a common main information line. The modular structure of the system and the use of the principle of program control makes it possible to do the following:
accelerate the planning and production of an experimental prototype of the system by using standard KAMAK modules that are produced in this country;
provide a capability for modernization and development of the system while in operation and when changing marine research techniques;
organize communication between the system and a computer-based on-board computational system.

The "Morgol" system receives signals from a seismic receiving unit (tail) that is towed behind a ship along with a source. In connection with this, both single-channel (single-channel continuous profiling (ONP)) and multichannel (MNP) tails are used.

On a real-time scale (in the on-line mode) the system provides for the visualization of:
incoming seismic signals (seismograms) from the tail, for the purpose of monitoring the quality of the data being recorded and controlling the operation of the emitting and receiving equipment;
temporal sections, for the purpose of determining the filtration modes, the angles of inclination of the reflecting boundaries, and the choice of the data processing parameters;
deep sections, for the purpose of geological interpretation, correcting the observation techniques, and changing the mode of the ship's motion.

A deep metric section is the final result of the processing of seismic data. This section, which is constructed with depth and distance scales on the profile and is tied in to the current coordinates, insures the visualization of geological structures while the ship is in motion. The interpretation of the deep section enables geologists on board the ship to institute operational measures at the place where the work is being done. In complicated situations, for the purpose of selecting the rule for the change in average velocity $\overline{V}(t)$ it is possible to turn repeatedly to the mass of data accumulated on magnetic tape by the on-board "Grad" [Degree] data collection system (in the on-line mode).

The initial stage in the creation of the "Morgol" system is the development of a single-channel deep section (holograph) plotting device, which is being done by Voronezh State University's Laboratory of Seismic Holography, under the direction of

V.I. Dubyanskiy, by agreement with LMGG YuO. The equipment is intended to operate by the central beam (TsL) method during ONP and provides for channel-by-channel input, amplification, filtration, compression, color division, light modulation and storage of seismic signals. When a carrier holding the light guide moves along the axis of a mirror semiconical converter (ZPP) (developed on the basis of V.D. Zav'yalov's method) according to the V(t) rule, holographic diffraction conversion (GDP) takes place; that is, the conversion of the seismic signals into an image of wave fronts. The use of the ZPP in the holograph results in signal scanning by circles, and during NSP [probably continuous seismic profiling] provides the following:
correct plotting of horizontal and inclined boundaries;
the possibility of visualization on a section of diffraction points, which is particularly fundamental for working in the ocean;
the possibility of preliminarily determining the rule governing the change of the waves' average velocity in the medium V(t) by focusing the diffracted waves on the diffraction points;
increasing the depth and the signal-to-noise ratio through the use of diffracted waves in the formation of the section image.

The basic difficulty in using the GDP methods and equipment developed by V.D. Zav'yalov, V.I. Dubyanskiy and A.I. Khvatov in marine research is the use of photographic film as the seismic signal storage medium. The use of photographic film requiring extensive processing makes it impossible to visualize sections on a real-time scale. The use of thermoplastic and photothermoplastic carriers in marine equipment is made difficult because of the complexity of the technology and the low sensitivity of these materials.

The holograph with channel-by-channel input that was developed at Voronezh State University by A.I. Khvatov has inadequate resolution, accuracy and operating speed, which makes its use during MNP not very effective.

The use of the semiconical converter in Voronezh State University's holographs when the MNP method is used results in significant distortions in the plotting of the images of inclined boundaries.

During MNP, the accurate plotting of the images of reflecting boundaries with large angles of inclination is possible if elliptical scanning of the signals is used to plot the sections. The realization of elliptical scanning is difficult when optico-mechanical holographs are used. For the on-board plotting of sections during MNP, it is most advisable to use the elliptical image scanning (ERO) principle proposed by V.V. Kondrashkov [5]. This principle has been realized in analogous form in an experimental model developed at the "Soyuzmorgeo" VNPO [probably All-Union Production Association] by Ye.Yu. Yakush and V.B. Gavryushin. The devices for spatial filtration and the input of the rule governing the change of velocity in the medium that are used in this model require further development. The ERO method presumes the plotting of temporal sections on the basis of the initial seismic traces, using a new system of coordinates and the input of correction factors. Theoretically this method is usable for the construction of holographs of boundaries with angles of inclination of up to 90°. The ERO method is the basis of the construction of temporal profiles in the "Morgol" system. In connection with this, the average velocity input unit makes it possible to select the V(t) rule on the basis of an analysis of the section's image by correlation of the holographs of the reflecting boundaries.

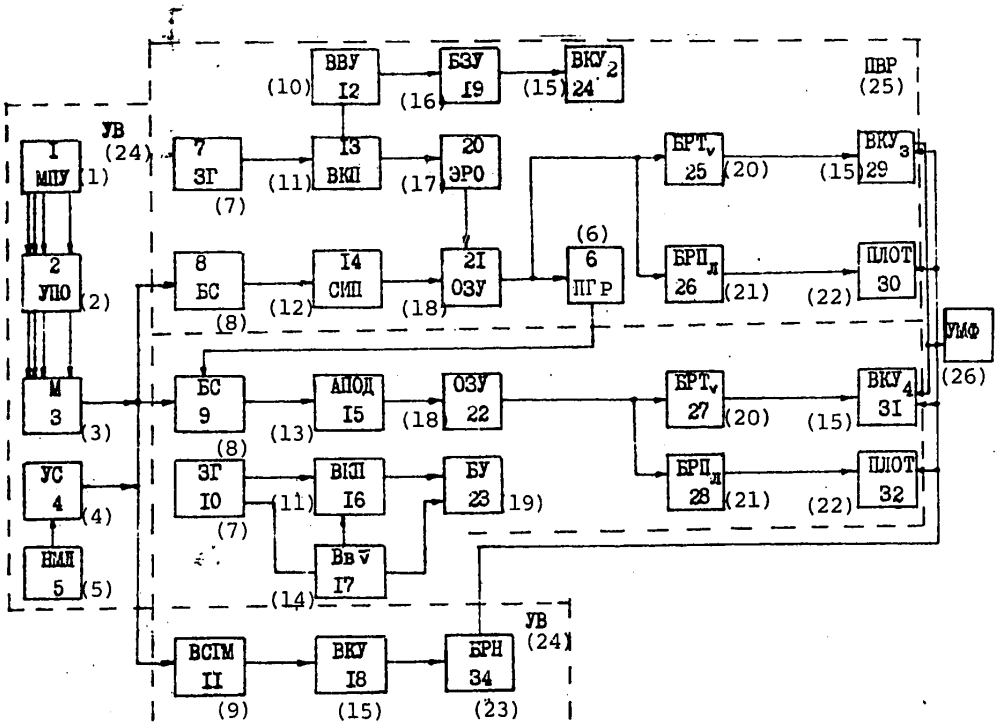

Figure 1. Block diagram of marine holographic seismic surveying system.

Key:

1. MPU	8. BS	15. VKU	21. BRP_{ℓ}
2. UPO	9. VSGM	16. BZU	22. PLOT
3. M	10. VVU	17. ERO	23. BRN
4. US	11. VKP	18. OZU	24. UV
5. NML	12. SIP	19. BU	25. PVR
6. PGR	13. APOD	20. BRT_{v}	26. UMF
7. ZG	14. Bbv		

Operating Principle of the System

The following units (Figure 1) make up the "Morgol" marine holographic seismic sensing system:
a) an input unit (UV);
b) a temporal section plotting device (PVR);
c) a deep section plotting device (PGR);
d) a microfilming unit (UMF).

The input unit makes it possible to enter seismic data from two sources:
a) a multichannel receiving unit (tail);
b) a digital magnetic tape storage unit (NML).

In preprocessing unit UPO (2), signals from multichannel receiving unit MPU (1) undergo amplification, filtration, compression and so on. From the output of UPO (2), the signals are sent to multiplexer M (3), where periodic interrogation of each

seismic track takes place; this makes it possible to enter seismic data in the system in real time.

Matching device US (4) is used to enter seismograms from magnetic tape storage unit NML (5).

Seismogram visualization unit VSGM (11) makes it possible to exercise operational monitoring of the primary seismograms on videomonitor unit VKU 1 (18).

Radio-navigation unit BRN (34) correlates the data being measured to the system of coordinates and real time.

Temporal section plotting device PVR operates in the following manner.

Signals from input unit UV pass through conjugation unit BS (8) into gating unit SIP (14) for the ERO isoclinals. The ERO isoclinals for boundaries with any angle of inclination are determined by the formula

$$t_0 = \left| \frac{4\ell_0(\ell_n - \ell_0)}{\bar{V}(2\ell_0 - \ell_n)} \right|, \tag{5.1}$$

where t_0 = recording time; ℓ_0 = current coordinate at the reception points, as read from the point of emission; ℓ_n = distance between the emission and reception points; $\bar{V}$ = average velocity.

Driving oscillator ZG (7) insures the recording of the information in operational memory OZU (21) and control the system's switching elements.

Velocity $\bar{V}$ input unit VVU (12) changes the amplitude of the sinusoidal control voltage. In kinematic correction factor computation unit VKP (13), recording time t_0 is calculated with due consideration for the following changing parameters: current time t_i, distance between the emission and reception points ℓ_n and average velocity $\bar{V}$. In order to determine the amplitude of the sinusoidal voltage, which is proportional to t_0 with respect to the known amplitudes of the cosinusoidal voltage that are proportional to $\ell_n/\bar{V}$ and t_i, it is necessary to make calculations with the formula

$$t_0 = \sqrt{(t_i)^2 - \left(\frac{\ell_n}{\bar{V}}\right)^2} \tag{5.2}$$

Recording of the data on the temporal section, which is obtained by the accumulation of the elliptical image scannings, takes place in operational memory OZU. The trajectories of these scannings are determined with the formula

$$\frac{t_0^2}{t_i^2 - \frac{\ell_n^2}{\bar{V}^2}} + \frac{\left(\ell_0 - \frac{\ell_n}{2}\right)^2}{\frac{\ell_n^2}{4}} = 1. \tag{5.3}$$

Operational visualization of the obtained temporal section is realized on the screen of videomonitor unit VKU 3 (29), with the help of television scanning unit BRT_V (25).

Plotter scanning unit BRP_ℓ is used to send the temporal section data accumulated in OZU (21) into plotter PLOT (30). The velocity curves are visualized on VKU 2 (24) with the help of buffer memory BZU (19).

With the help of the output unit in PGR (6), the data for a temporal section that has been obtained can be entered in deep section plotting device PGR.

Deep section plotting device PGR operates in two modes.

1) The plotting of deep sections from the primary material is done analogously to the plotting of the temporal section in the PVR, with the following differences:
a) directed fan filtration is carried out with the help of apodizatsiya [translation unknown] unit APOD (15);
b) kinematic correction factor computation unit VKP (16) makes calculations according to formula

$$H = \sqrt{\left(\frac{\overline{v}t_i}{2}\right) - \left(\frac{l_x}{2}\right)^2}, \qquad (5.4)$$

where H = radius of circular scanning corresponding to current time t_i.

2) Plotting of deep sections on the basis of the temporal sections obtained from the PVR is done with kinematic correction factor unit VKP (16) turned off.

The deep section that is obtained should be taken off through VKU 4 (31) or plotter PLOT (32).

With the help of microfilming unit UMF (26), images from the screens of VKU 2 (24), VKU 3 (29) and VKU 4 (31) can be recorded on photographic film.

The use of color division according to energy and frequency features in the "Morgol" system's plotting devices results in a significant increase in the geological information content of the sections visualized on board ships.

BIBLIOGRAPHY

1. Vorob'yev, O.A., "Evaluating the Effectiveness of Automated Systems for Collecting and Processing Oceanological Research Data," "Sb. trudov X shkoly po avtomatizatsii nauchnykh issledovaniy" [Collected Works of the 10th School for the Automation of Science Research], Leningrad, 1977, p 240.

2. Malvitskiy, Ya.P., editor, "Morskiye geofizicheskiye issledovaniya" [Marine Geophysical Research], Moscow, Izdatel'stvo "Nedra", 1977, pp 76-79.

3. Timoshin, Yu.V., "Impul'snaya seysmicheskiy golografiya" [Pulsed Seismic Holography], Moscow, Izdatel'stvo "Nedra", 1978, pp 125-138.

4. Potapov, O.A., Vorob'yev, O.A., and Dubyanskiy, V.I., "Holographic Opticodigital Processing of Seismic Surveying Data," in "Golografiya i opticheskaya obrabotka informatsii v geologii i geofizike" [Holography and Optical Information Processing in Geology and Geophysics], Leningrad, 1979, pp 95-101.

5. Kondrashkov, V.V., "Obtaining a Temporal Section by the Elliptical Image Scanning (ERO) Method," REGION. RAZVED. I PROMYSL. GEOFIZIKA, No 20, 1977.

UDC 550.834

ON THE POSSIBILITY OF CREATING A CLOSED CYCLE OF HOLOGRAPHIC TRANSFORMATIONS

Leningrad GOLOGRAFIYA I OPTICHESKAYA OBRABOTKA INFORMATSII V GEOLOGII in Russian 1980 (signed to press 19 Nov 80) pp 100-109

[Article by B.V. Pilipishin from collection of works "Holography and Optical Information Processing in Geology", edited by Professor S.B. Gurevich and Candidate of Technical Sciences O.A. Potapov, Leningrad Physicotechnical Institute imeni A.F. Ioffe, USSR Academy of Sciences, 500 copies, 181 pages]

[Text] The author demonstrates the possibility of creating a closed cycle of holographic transformations on the basis of modern algorithms and specialized equipment for the processing of geophysical information.

On the accumulative level, the basic purpose of seismic holography is the construction of a section of a depth scale. This problem is solved comparatively easily when the static correction factors and the laws governing the change in velocity with depth are known. Even in modern geophysical computer centers, static correction factors are sometimes determined without the use of a computer. Thus, a closed cycle of holographic transformations for the purpose of constructing a deep section without using a computer is possible if the relationship $V = V(H)$ (or any relationship that is unambiguously related to it, such as $V = V(tm)$, $\Delta T = \Delta T(tm)$, where tm = = time at the minimum of the wave's cophasal axis, ΔT = deflection of the cophasal axis, which determines its curvature, and so on) can be found by using a holograph.

The presently existing method of determining the relationship $V = V(H)$ (or any one that is unambiguously related to it) on the basis of a holograph, which consists of plotting a family of wavegrams on the basis of the same seismogram for different velocity values, has a number of disadvantages: the number of wavegrams is determined by the number of values taken on by parameter V; as a consequence of this, there arise complications in the identification of the waves (singly reflected, multiply reflected, regular interference waves and so on) when there is an extraordinarily large amount of output data. Free from these flaws, for example, is the method of determining the velocities by summing the instantaneous values of the signals with respect to the hyperbolic (parabolic) cophasal axes, with subsequent depiction of the resultant data (a signal function) in the system of coordinates (V,tm), which method has received the name of curvilinear summation (KS). One of the most powerful techniques for determining velocity--KS RNP [regulated directional reception]--requires the analysis of a set of signal functions (as in the case of wavegrams), although the rate of signal accumulation achieved is higher by an order of magnitude

or more than for the methods known at the present time, with all of the consequences emanating from this. Let us discuss the realization of the methods for determining wave propagation velocities using curvilinear summation--KS and KS RNP--on the basis of holographic transformations (having preliminarily described the realization of RNP, which is the classical method of seismic surveying) that are most widely used in computer centers at the present time. We will assume the most characteristic feature of holographic transformations to be the distribution of the signals' instantaneous values with respect to certain laws (such as circular scannings, but not them alone) on the accumulative plane, with natural further summation of the values falling on the same (or nearby) points on the plane.

Controlled Directional Reception and Its Realization by Holographic Techniques

We will assume that the observation system consists of sensors distributed uniformly along a straight line and having the numbers -N,...,0,...,N. Let us also assume that the waves picked up by a sensor have plane cophasal axes with the equation

$$t(n) = kn + \tau,$$

where τ = signal recording time for the central sensor in the base (n = 0); k = difference in times of arrival of signals forming the same cophasal axis at two adjacent sensors; that is, k = t(n) - t(n - 1) (angle of inclination of a wave, in milliseconds on a track). In accordance with RNP [1], standard processing consists of forming the signal function (RNP summation tape) $A_\Sigma(k,\tau)$ according to the rule

$$A_\Sigma(k,\tau) = \sum_n A(n, t = \tau_{RNP}(n)),$$

where A(n,t) = equation of the seismogram (n = number of the track, t = current time; $\tau_{RNP}(n)$ = kn + τ = equation of the summation lines; k, τ = variable parameters of the lines (angle of inclination of the wave on the seismogram (in milliseconds on the track) and time of its registration on the central track (n = 0) of the seismogram).

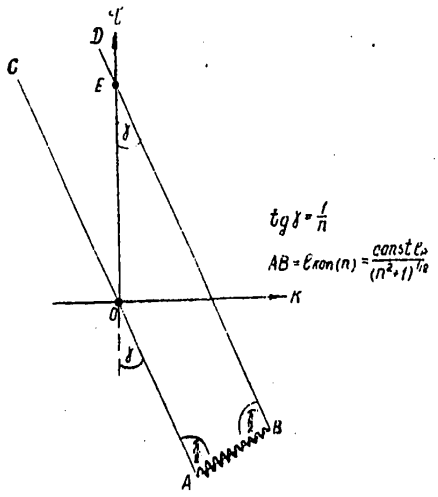

Figure 1. Formation of RNP signal function $A_\Sigma(k,\tau)$.

The holographic technique for forming the RNP signal function is as follows (Figure 1--we will not present the proofs). Let us identify the continuous, limited set of points that represents the plane of the signal function's arguments with the plane (for example) of the photographic layer and assign on the latter the rectangular system of coordinates (k,τ); $|k| \leqslant k_{max}$, $0 \leqslant \tau \leqslant \tau_{max}$. Using the method of variable density, we will rerecord the signals (tracks) previously registered by the sensors and recorded on magnetic tape, on photographic film. We will match the information recording and rerecording rates so that the linear dimensions of the n-th track on the magnetogram ℓ_p and the same on the photographic film ℓ_{kon} satisfy the relationship

$$\ell_{kon}(n) = \frac{const\, \ell_p}{(n^2+1)^{1/2}},$$

where "const" is the result of equalizing

the linear dimensions of the zero track on the magnetogram with those of the photographic layer along the τ axis. We will displace the track that has been rerecorded by the variable density method (Figure 1) parallel to the photographic layer's plane so that the projections of the directing motions AC and BD on it pass through points 0 and E with coordinates (0,0) and $(0,\tau_{max})$, respectively, and intersect the τ axis at angle γ ($tg\ \gamma = 1/n$). During the movement process we illuminate the track with a parallel beam of light, the source of which we position in such a fashion that the rays passing through the photographic film strike the photographic layer's surface perpendicularly. After this procedure has been carried out with all the tracks (but on the same photographic layer plane (k,τ)), on the photographic layer's plane there forms a distribution of densities corresponding to the RNP signal function $A_{\Sigma}(k,\tau)$, where a point of maximum signal accumulation corresponds to each cophasal axis. This setup can also be realized with the help of other equipment (a cathode-ray tube, a potentialscope and so on), although all its characteristic features (track compression, depending on its number, and the angle of inclination between the directing tracks and the τ axis) must be observed.

Curvilinear Summation and Its Realization by Holographic Techniques

We will assume, as before, that the observation system consists of sensors distributed uniformly in a straight line and having numbers $-N,\ldots,0,\ldots,N$. Let us also assume that the waves received by the sensors have curvilinear--parabolic--cophasal axes with the equation

$$t(n) = k'n^2 + \tau'$$

where τ' = signal recording time by the central sensor in the base ($n = 0$); k' = difference in arrival times of signals belonging to the same cophasal axis at the end and central sensors in the base, divided by N^2; that is, $k' = [t(N) - t(0)]/N^2 = \Delta T/N^2$ (ΔT is the deflection of the cophasal axis). Curvilinear summation of seismic signals (in one of its modifications--the velocity sorting method) is a well-known procedure that is used for the purpose of determining wave propagation velocities as a function of their registration time. The origins of KS are explained in [2-4], while further developments of it are described in [5-9].

Standard processing in accordance with KS consists of the formation of a signal function (KS summation tape) $A_{\Sigma}(k',\tau')$ according to the rule

$$A_{\Sigma}(k',\tau') = \sum_{n} A(n, t = \tau_{Kc}(n)),$$

where $A(n,t)$ = equation of the seismogram (n = number of the track, t = current time); $\tau_{KS}(n) = k'n^2 + \tau'$ = equation of the summation lines; k', τ' = the lines' variable parameters; $k' = \Delta T/n^2$; T = deflection of the cophasal axis; τ = signal recording time on the central track ($n = 0$) of the seismogram.

Let us identify the continuous, limited set of points that represents the plane of the signal function's arguments with the plane (for example) of the photographic layer and assign on the latter the rectangular system of coordinates (k',τ'); $0 < k' \leqslant k_{max}$, $0 \leqslant \tau' \leqslant \tau_{max}$.

The holographic method for forming the KS signal function $A_{\Sigma}(k',\tau')$ coincides with the method for forming the RNP signal function by the same technique that was described above. The necessary changes in the method are as follows (Figure 2): the information registration and rerecording rates should be matched in such a

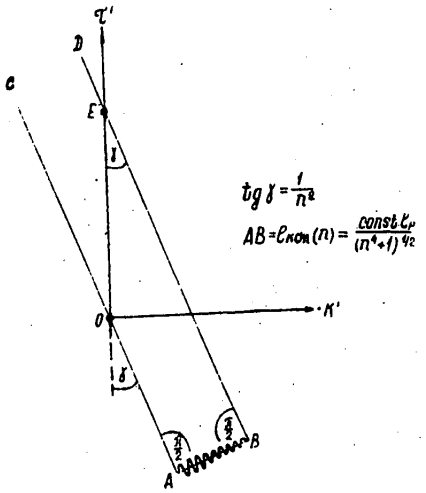

Figure 2. Formation of KS signal function $A_\Sigma(k',\tau')$.

fashion that the linear dimensions of the n-th track on the magnetogram ℓ_p and the photographic film ℓ_{kon} satisfy the relationship

$$\ell_{kon}(n) = \frac{const\,\ell_p}{(n^4+1)^{1/2}},$$

the projections of the directors of the photographic film's motion onto the plane of the photographic layer AC and BD must intersect the τ' axis at angle γ ($tg\,\gamma = 1/n^2$).

The remarks previously made are also correct with respect to the possible equipment realization of the system.

The KS RNP algorithm consists of three basic parts: curvilinear summation (KS), a former and controlled directional reception, and involves the sequential, joint processing of a group of seismograms by the KS and RNP methods. The rational integration of these methods is described in [7] and is realized by the former. An investigation of the properties of the KS RNP complex and its realization in programs for a "Sigma-5" computer are described in [8]; several applied aspects that are related to the use of the complex and its realization in programs for a "Minsk-32" computer are discussed in [9].

Into the system's input are fed an odd number (2S + 1) of OGT [common deep point] seismograms $A^S(n,t)$ ($S = 0,\pm1,\ldots,\pm S$) formed from a series (2S + 1) of side-by-side common deep points. Let us carry out the curvilinear summation of these points (the definitions are the same as before):

$$A^S_\Sigma(k',t) = \sum_n A^S(n, t = \tau_{ke}(n))$$

At the output of the KS unit we obtain (2S + 1) KS summation tapes $A^S_\Sigma(k', ')$ that are quantified by the independent variable k'. From the KS summation tapes, we form group KS tapes (by analogy with directed RNP group tapes [1, pp 17-19], the only difference being that instead of the angle of wave arrival we use curvature of the cophasal axis k') $A^{k'}_\Sigma(S,\tau)$ in the following manner: the first KS group tape is put together from all of the first tracks of the KS summation tapes by arranging them (the tracks) in the order of arrangement of the KS summation tapes and is labeled with the indicator "k'" of the first tracks of the KS summation tapes and so on; the last KS group tape consists of all the last KS summation tape tracks, arranged in the order of arrangement of the KS summation tapes and labeled with the indicator "k'" of the last tracks of the KS summation tapes. The KS group tapes $A^{k'}_\Sigma(S,\tau')$ are formed from the KS summation tapes $A^S_\Sigma(k',\tau')$ by the former. The meaning of the transformation $A^S_\Sigma(k',\tau') \rightarrow A^{k'}_\Sigma(S,\tau')$ is as follows: if for any of the reflecting horizons the cophasal axis curvature $k' = k'_0$ that corresponds to it was selected during the curvilinear summation process, on the group tape formed from these tracks (and labeled with the indicator k'_0) is depicted a fragment of the temporal section: a plane, reflecting area with an unknown angle of inclination. This fact makes it possible to subject each KS group tape to repeated summation according to RNP; that is,

$$A^{k'}_{\Sigma\Sigma}(k,\tau) = \sum_{S} A^{k'}_{\Sigma}(S, \tau' = \tau_{RNP}(S)),$$

where $\tau_{RNP}(S) = kS + \tau$ = equation of the summation lines; k, τ = variable parameters of the lines (the angle of inclination of the reflecting area (in milliseconds on a track) and time of registration of the area on the central track S = 0 of the KS group tape); $A^{k'}_{\Sigma\Sigma}(k,\tau)$ = summation tapes--signal functions of the KS RNP algorithm, the number of which equals the number of values taken on by parameter "k." From the description of the complex that has been presented it follows that the number of accumulated signals equals the product of the number of accumulations during KS and the number of accumulations during RNP. Thus, the summary signal is frequently the result of the accumulation of 80 or more original seismic signals (for example, 9 accumulations according to KS and 9 according to RNP results in 81 accumulations (9 x 9)). The large number of accumulations provides the KS RNP algorithm with a whole series of advantages over other well-known algorithms.

Let us mention here that the realization of the KS RNP algorithm in accordance with the setup that has been described (and which is unique at the present time), using any devices (optical, electro-optical), is possible but extremely awkward. During its realization we have two intermediate masses of information (KS summation tapes and group tapes) that have to be recorded, stored and read.

Let us assume that the planes on which the formation of the KS RNP algorithm's signal functions $A^{k'}_{\Sigma\Sigma}(k,\tau)$ takes place are formed of a continuous, limited set of points (such as the plane of the photographic layer). On each of these planes we will assign a rectangular system of coordinates (k,τ), where $|k| \leqslant k_{max}$, $0 \leqslant \tau \leqslant \tau_{max}$; we will assume the parameter of each plane to be the corresponding value of k' from its search interval.

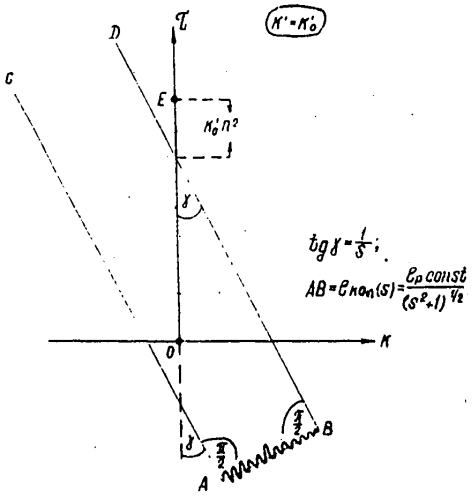

Figure 3. Formation of one of the KS RNP signal functions ($k' = k'_0$) $A^{k'=k'_0}_{\Sigma\Sigma}(k,\tau)$.

The holographic technique for the formation of the KS RNP algorithm's signal functions (we will describe it in an example of the formation of $A^{k'=k_0}_{\Sigma\Sigma}(k,\tau)$) coincides with the technique for the formation of the RNP signal function that has been described. The necessary changes are as follows (Figure 3):

the information registration and rerecording rates should be matched in such a manner that the linear dimensions of all tracks of the S-th seismogram on the magnetogram ℓ_p and the photographic film ℓ_{kon} satisfy the relationship

$$\ell_{kon}(S) = \frac{\ell_p \, const}{(S^2+1)^{1/2}};$$

after the dimensions of the n-th track of the S-th seismogram are reduced to the value $\ell_{kon}(S)$, the track must be shifted downward relative to the τ axis by the distance k'_0n^2, which has also been preliminarily transformed according to the formula presented above;

the projections of the directors of the photographic film's motion onto the plane

of the photographic accumulator AC, BD must intersect the τ axis at angle γ, for which $\text{tg}\ \gamma = 1/3$ is correct.

The remarks previously made relative to the possible equipment realization of this system are also correct.

The results obtained indicate the possibility of creating a closed cycle of holographic transformations on the basis of contemporary algorithms. In order to do this, it is sufficient to "furnish" the holograph with curvilinear scanning with respect to a number of directions and possible displacement of the scans along the τ axis, while the original information is "compressed," using a certain compression factor, during rerecording on the photographic carrier.

BIBLIOGRAPHY

1. Ryabinkin, L.A. (editor), Napalkov, Yu.V., Znamenskiy, V.V., Voskresenskiy, Yu.N., and Rapoport, M.B., "Theory and Practice of the RNP Seismic Method," TRUDY, MINKh i GP [Moscow Institute of the Petrochemical and Gas Industry imeni Academician I.M. Gubkin], Moscow, Izdatel'stvo "Gostoptekhizdat", No 39, 1962.

2. Garotta, R., and Michon, D., "Continuous Analysis of the Velocity Function and of the Move Out Corrections," GEOPHYS. PROSP., Vol 15, No 4, 1967, pp 584-597.

3. Chervonskiy, M.I., Pilipishin, B.V., and Mikhaylik, Z.M., "A Method for Transforming Seismic Information," Patent No 271820, 28 May 1968, BYULL. IZOBR., No 18, 1970.

4. Taner, T., and Kochler, F., "Velocity Spectra Digital Computer Derivation and Application of Velocity Functions," GEOPHYS., Vol 34, No 6, 1969, pp 853-871.

5. Pilipishin, B.V., and Chervonskiy, M.I., "Krivolineynoye summirovaniye seysmicheskikh signalov" [Curvilinear Summation of Seismic Signals], Moscow, Izdatel'stvo "Nedra", 1974, p 79.

6. Matusevich, Yu.F., Mironov, V.Ya., Binkin, I.G., and Klochkov, G.D., "Controlled Summation in the Common Deep Point Method," SER. REGION., RAZVED. I PROMYSL. GEOGIZIKA, Moscow, VIEMS [All-Union Scientific Research Institute of Economics of Mineral Raw Materials and Geological Exploration], 1974, p 53.

7. Mezhbey, V.I., Vaks, Z.M., and Daderko, Yu.R., "A Method for Determining the Propagation Rate of Seismic Waves in a Medium," Patent No 343235, applied for 14 July 1971, published 5 September 1972.

8. Tsatsko, Ye.L., "Sistema obrabotki dannykh MOGT na baze raznovremennogo summirovaniya" [A System for Processing Data Gathered by the Common Deep Point Method on the Basis of Summation at Different Times], author's abstract from dissertation for degree of candidate of technical sciences, Kiev, IG AN USSR [Institute of Geology, Ukrainian SSR Academy of Sciences], 1977.

9. Chervonskiy, M.I., Pilipishin, B.V., Sigalova, Ye.I., and Frankovich, M.P., "Sovershenstvovaniye metodicheskogo kompleksa izucheniya fizicheskikh parametrov

real'nykh sred primenitel'no k konkretnym seysmogeologicheskim usloviyam neftegazonosnykh regionov USSR" [An Improvement in the Complex of Methods Used to Study the Physical Parameters of Real Mediums, as Applied to the Specific Seismo-geological Conditions Encountered in the Gas- and Oil-Bearing Regions of the Ukrainian SSR], UkrNIGRI [Ukrainian Scientific Research Institute of Geological Exploration] funds, 1979.

UDC 550.834

ON THE QUESTION OF USING HOLOGRAPHIC SYSTEMS IN MARINE GEOLOGY AND GEOPHYSICS

Leningrad GOLOGRAFIYA I OPTICHESKAYA OBRABOTKA INFORMATSII V GEOLOGII in Russian 1980 (signed to press 19 Nov 80) pp 110-121

[Article by A.V. Zuyevich, V.B. Gavryushin, V.V. Alekseyenko and V.M. Sugak from collection of works "Holography and Optical Information Processing in Geology", edited by Professor S.B. Gurevich and Candidate of Technical Sciences O.A. Potapov, Leningrad Physicotechnical Institute imeni A.F. Ioffe, USSR Academy of Sciences, 500 copies, 181 pages]

[Text] The authors discuss the applicability of the holographic method in the sonic band to the solution of exploratory geological and geophysical problems under the conditions encountered in the region of the continental shelf. They describe a multichannel, sonic-band holographic device and experiments conducted under conditions that were as close to natural as possible. They present the results of these experiments, which involved obtaining images of objects embedded in the ground. Finally, they analyze the problems involved in realizing marine holographic systems and give a list of prospective geological and geophysical problems that can be solved with the help of holographic systems under the conditions encountered in the area of the continental shelf.

Long-wave holography is already an effective method for various types of investigations in nontransparent mediums. A number of authors have attempted to use the holographic method in the seismic and sonic bands in both land [1-4] and sea [5-8] research. The interest in holography is explained primarily by its well-known advantages, such as the three-dimensional nature of the image of objects being investigated, the high level of noise stability, the possibility of obtaining images of objects with any configuration, and the possibility of processing multidimensional information rapidly. Although these advantages are realized only partially in the long-wave band, the use of holography in the seismic and sonic bands is promising, according to many evaluations. One cannot think, however, that in most cases marine holographic systems are regarded as a means of solving certain problems in the aqueous layer. In only one work [6] is there a report of experiments involving the obtaining of images of objects located in the nontransparent ocean bottom. For a number of reasons, however, the techniques used in these investigations are not widely used in the practice of exploratory work at sea. Despite this, the article cited is valuable in the sense that it turns a new page in the search for ways and

means of investigating the ocean. The need for this search, particularly in view of the importance of developing the continental shelf, is extremely urgent at the present time. In confirmation of this we have the opinion of the well-known French researcher K. (Riffo) [9], who writes: "...marine prospecting for useful mineral deposits is an expensive proposition. One of the reasons for this is of a technical nature--we still have an almost complete lack of knowledge of how to work under water. Modern geophysical investigative methods still do not enable us to determine accurately the presence of deposits of useful minerals under the ocean bottom, and the technology of deep-water geological mapping is still far from perfect."

At NIIMorgeofizika [probably Scientific Research Institute of Marine Geophysics], the "Soyuzmorgeo" VMNPO [possibly Naval Scientific Production Association] is investigating the applicability of sonic-band holography to the solution of geological and geophysical exploratory work under the conditions encountered on the continental shelf. In this article we describe several experimental results of this research and evaluate the prospects for the use of this method in the future.

1. Multichannel Holographic Systems

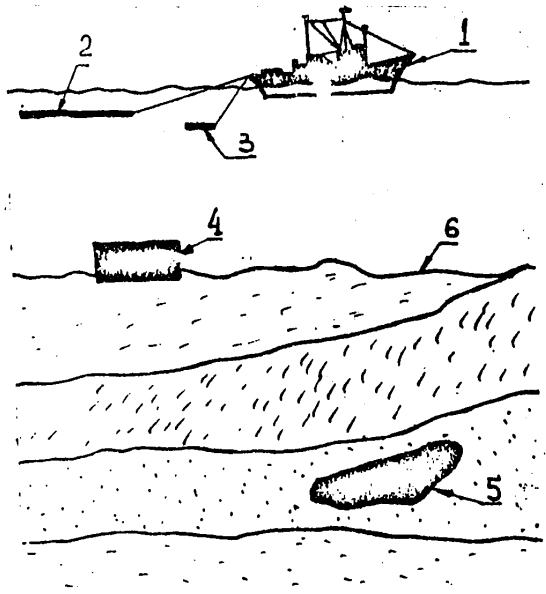

Figure 1. Diagram of a holographic system for investigating the continental shelf.

Figure 1 is a conventional diagram of a holographic system for investigating the shelf. The special feature of this system is the necessity of obtaining information while ship (1) is in motion. The receiving (2) and emitting (3) systems are connected to the ship. The investigated objects are located both on the bottom (4) and in the rocks (5) of which the sea bottom (6) is composed. The thickness of the water layer over the continental shelf ranges from 20 to 500 m. The rocks that form the sea bottom are distinguished by the considerable range of their physical parameters such as (for example) wave resistance, attenuation, porosity and characteristic size of the particles. The nonuniformity of the medium, the broad range of physical

parameters, the presence of a layer of water, the specific nature of marine observations--all of these determine the considerable complexity involved in obtaining and processing holographic information. This facts results in the necessity of a careful investigation of the capabilities of holographic systems under conditions that are as close to real as possible.

Investigations of multichannel holographic systems in the ultrasonic band were conducted with a modeling unit. The model was tank containing water, into which various objects were placed. In the work we used the aperture synthesis method, which was realized by scanning with a linear receiving antenna. The techniques used in the work, the equipment and the basic results of the experiments are described in [10]. In experiments related to the testing of the resolving power of a holographic system with a limited aperture under near-field conditions, the plane resolution was $2\lambda_{ak}$[1], while the vertical resolution was $6\lambda_{ak}$. During the experiments, we obtained reproduced images of the model objects with no worse than $2\lambda_{ak}$ resolution.

1.1. Plan of the Experiment

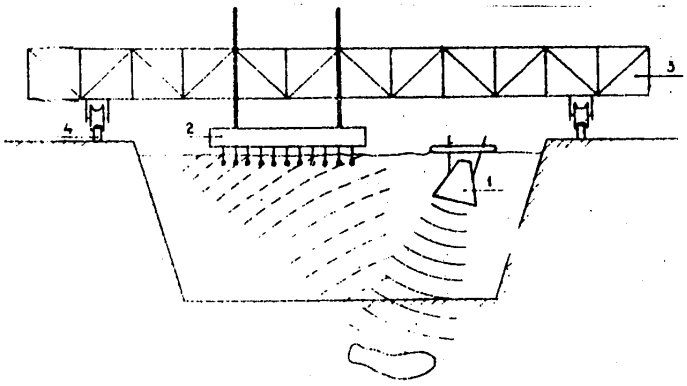

Figure 2. Diagram of conduct of experiments in a range holographic complex: 1. emitter; 2. receiving antenna; 3. load-bearing truss; 4. rails.

Experiments that were conducted in the ultrasonic band made it possible to evaluate several parameters of the holographic system. However, the model simulated a homogeneous medium, whereas in practice the medium being investigated is essentially heterogeneous. In view of this, the results of the experiments cannot be used as a basis for the development of a holographic system that is suitable for the solution of exploratory problems on the continental shelf. For the purpose of testing the method under conditions that essentially approximate real ones, a multichannel sonic-band holographic system was developed and experiments involving the obtaining of images of objects in the ground were performed. Figure 2 is a diagram of the conduct of the experiments. The work was done in a basin measuring 50 m x 20 m x 5 m. Carrier truss (3), along with receiving antenna (2) and the equipment complex, moved on rollers along rails (4). The receiving antenna contained 127 hydrophones mounted at 5-cm intervals. When the carrying truss was moved mechanically with the

[1]Here and henceforth, λ_{ak} is the wavelength of the sounding emissions.

help of a motor and a system of cables, synthesis of a two-dimensional aperture measuring 6.35 m x 6.35 m was provided. Objects located on or under the bottom of the basin were irradiated by emitter (1). The emitter was mounted on a raft and could be placed at any point in the basin. The information registered during scanning by the receiving antenna was transmitted over cables into the processing system. The holograms obtained were photographed and reproduced in He-Ne laser beams.

1.2. Recording and Processing System and Basic Parameters

The holographic information recording and processing system consisted of a single stand that contained several functional units: a control unit, a memory unit, a television unit and a power unit. Part of the units were removable and were placed on the truss (the blocks of amplifiers and phase detectors and the decoding unit), which made it possible to lower the noise level and simplify the information recording process.

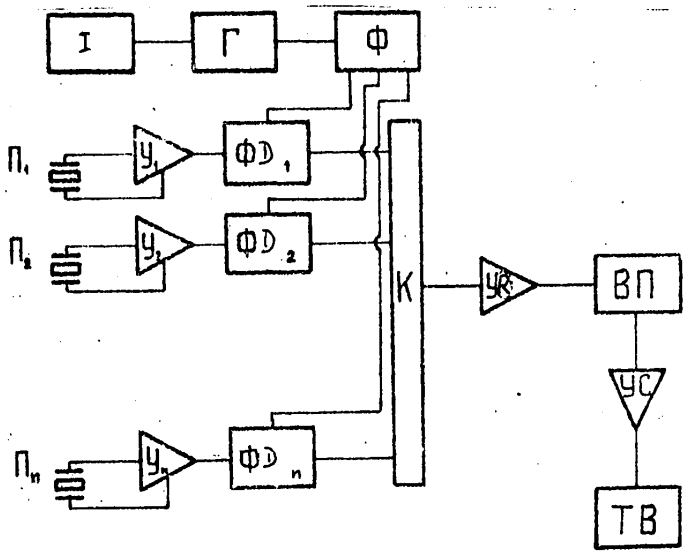

Figure 3. Block diagram of processing equipment of range holographic complex: $П_1,\ldots,П_n$ = receiving hydrophones; $Y_1,\ldots,Y_n$ = = amplifiers; $ФD_1,\ldots,ФD_n$ = phase detectors; I = emitter; Г = = generator; Ф = phase shifter; K = electronic switchboard; UR = = recording amplifier; ВП = memory unit; YC = reading amplifier; ТВ = television unit.

Figure 3 is a diagram of the information recording and processing setup. Generator Г excites emitter I with rectangular pulses with filling of the working frequency. Signals reflected by the objects are picked up by receiving hydrophones $П_1,\ldots,П_n$. The received signals are then amplified on a channel-by-channel basis by amplifiers $Y_1,\ldots,Y_n$ and sent to the signal inputs of phase detectors $ФD_1,\ldots,ФD_n$. A signal from the same generator that has passed through phase shifter Ф is sent into the phase detectors' reference inputs. The phase detectors' outputs are interrogated by electronic interrogation commutator K and the signals are sent into the input of recording amplifier YR. They are then recorded in memory unit ВП, for which a

cathode-ray tube with a memory (of the LN-17 type) is used. Upon completion of the aperture synthesis cycle, a holograph is formed on the cathode-ray tube's target. It is taken off through recording amplifier YC and sent into television unit TB for visualization. The working frequency selected for the system was 10 kHz (λ_{ak} = 15 cm in water). The choice of the frequency was determined by determined by the need for operation in soil, where attenuation is quite high even for this frequency and ranges (according to different data) from 1 dB/m to 5 dB/m for the clays making up the bottom of the basin. The operation of all the system's working assemblies is tied together by a crystal driving oscillator on a frequency of 10 kHz. The parameters of the emitted pulses were assigned on the control panel board and were varied within wide limits. The duration of the pulses could be changed in 1 ms increments in the 1-10 ms band and 10 ms increments in the 10-100 ms band. The pulse repetition rate could be set at either 10 or 50 Hz, while the filling frequency was 10 kHz. In addition to this, the control unit could exercise continuous control over the lag time of the signal being read with respect to the emitted pulse within limits of 1-100 ms. Continuous regulation of the time lag insures tuning on the objects being investigated.

1.3. Results of the Experiments

Using the system described above, we conducted experiments involving the obtaining of images of objects located on and under the bottom of the basin. Objects in the shape of the letter "T" and in the shape of two parallel segments were placed on the bottom of the basin. The "T"-shaped object's dimensions were $8\lambda_{ak}$ by $10\lambda_{ak}$, while those of the two parallel segments were $8\lambda_{ak}$ by $6\lambda_{ak}$, with the distance between the inner edges of the segments being $4\lambda_{ak}$. The objects were irradiated from above by the emitter on the raft. The holograms were recorded in accordance with the description given above. The quality of the images and the resolution achieved make it possible to identify the objects quite confidently.

The next series of experiments involved obtaining images of objects beneath the floor of the basin. When the basin was being built, objects in the form of the letters "H" and "S" were buried in its bottom. They were made of sheet steel 1 cm thick and measured 1.5 x 2 m^2 ($10 \times 13\lambda_{ak}^2$), while the width of the individual elements was 0.45 m ($3\lambda_{ak}$). The objects were placed one above the other, with the "H"-shaped one being 3 m below the bottom and the "S"-shaped one 1 m below the bottom. An object in the shape of a pyramid was made from marble cubes. It measured 0.4 x 0.4 x 0.4 m^3 [sic] and was located under the bottom so that the distance from the pyramid's upper edge to the bottom was 1 m. A stationary source mounted on a raft at some distance from the synthesized aperture irradiated the objects from above. The reading time lag was changed by selection of the useful signal during tuning on an object being investigated. The results that were obtain prove the possibility, in principle, of using holographic systems for searching for and detecting objects in nontransparent mediums.

2. Difficulties in the Realization of Marine Holographic Systems

At the present time, many examples of the realization of holographic systems in the sonic and ultrasonic bands are known. However, they are all laboratory models. The practical investigation of these systems under marine conditions is hindered by a number of difficulties that must be overcome. In the first place, the use of holographic systems under marine conditions is held back by the lack of experience in

realizing large receiving apertures at sea. For example, on the frequency of 10 kHz, a $100\lambda_{ak}$ aperture will be 15 m in size. It is necessary to tow antennas of such size behind a ship, perpendicular to the direction of the ship's motion, which is still a complicated technical problem. In connection with this, it is necessary to take into consideration the fact that the problem of stabilizing a towed system still has not been solved. Holographic requirements for stabilization are quite rigorous, which leads to a need for looking for and realizing the appropriate stabilization methods.

Another important question is the lack of reliable knowledge about velocity and attenuation in the soil that makes up the sea bottom. Measurement data in the literature are scarce and are distinguished by considerable variance. The realization of on-the-spot measurements of these parameters in the search mode is practically impossible, even for the layers near the bottom. The lack of such data is still hindering the accurate interpretation and correlation of the results that have been obtained.

The problem of the rapid and reliable interpretation of reproduced images remains unsolved at the present time. It is necessary to make this interpretation in real time, under marine surveying conditions, which is still a difficult problem. To this problem, also, is related the question of creating memory units with considerable capacity that are suitable for recording and reading information at the rate at which it arrives. The solution of this special problem must insure the recording of information and the reproduction of the image directly in the area being investigated and without interruption or omissions.

One of the problems of marine holography is the depth at which the investigation takes place. As is known, increasing the depth means lowering the frequency, which is unacceptable in holographic work, since this results in an increase in the size of the aperture, the difficulties involved in the realization of which were mentioned above. The difficulties that have been enumerated are delaying the practical utilization of holographic systems for surveying the continental shelf.

3. Prospects for the Use of Holographic Systems in Marine Geology and Geophysics

The world ocean is regarded as a promising area for prospecting for useful minerals. Until now, vast expanses of the ocean have not been studied thoroughly in the geological sense. Acoustic methods have recently begun to be used extensively to look for useful minerals on continental shelves. This is no accident, since these methods are quite effective in the solution of problems of detailing the upper part of layer covering the ocean bottom. Providing that the difficulties listed above are overcome, acoustic holography systems can supplement the instrumentation and methodology used in investigations at sea. Under the conditions encountered on the continental shelf, with their help it might be possible to solve a whole series of problems related to the study of the ocean bottom and the sedimentary layer covering it to depths of several dozen meters. Let us point out some of them:

1. Mapping the sea bottom for the purpose of determining microstages in bottom relief and steeply dipping outcroppings of bedrock, as well as exploring and preparing areas for drilling under conditions of considerable silting of the bottom or the presence of a sedimentary layer.

2. Searching for buried river beds, with which the presence of placer deposits of useful minerals is very frequently related.

3. Searching for dislocations with a break in continuity, which are also related to the presence of useful mineral deposits.

4. Searching for deposits of phosphate and polymetal concretions.

5. Searching for ore deposits, the nature of which in the shelf zone corresponds to deposits on land as far as their basic features are concerned.

The special feature of the problems outlined above is that most of them cannot be solved by well-known traditional methods.

It should be taken into consideration that the problem of developing the shelf includes an entire complex of problems. Along with the problems involved in prospecting for useful minerals, there will soon arise those related to their intensive extraction, which will require the construction of various types of structures, such as (for example) oil and gas lines, drilling platforms, oil storage tanks and so on. This will make it necessary to solve a whole series of problems of a "service" type: the preparation of areas for construction (including looking for outcroppings of bedrock), monitoring the safety of structures (such as the integrity of oil and gas pipelines) and so forth. Such problems can be solved by holographic methods. In connection with this, we should turn out attention to [7], in which the author reports on the development by the "Holosonics" Company of holographic equipment intended, in particular, for monitoring the state of oil pipelines under marine conditions. It is obvious that the solution of even part of these problems with the help of holographic systems will be of considerable practical and scientific use.

Conclusions

1. Tests of multichannel holographic systems that have been developed for the purpose of conducting laboratory and range model investigations demonstrated their suitability for the solution of the problems involved in searching for and identifying objects in transparent and nontransparent mediums.

2. The tests of the multichannel holographic systems showed that with their help and a limited aperture (no larger than 45 x $45\lambda_{ak}^2$), under near-field conditions no worse than $2\lambda ak$ resolution is achieved, while the reproduced images' quality is adequate for confident identification of objects.

3. According to its fundamental capabilities, long-wave holography can be an extremely promising method for detecting, under marine conditions, diffusely scattering geological and geophysical objects lying on the bottom and in the bottom sediments at shallow depths.

BIBLIOGRAPHY

1. Karla, A.K., and Rodgers, P.W., "Detection of Buried Geological Ore Bodies by Reconstruction Wave Fronts," ACOUSTICAL HOLOGRAPHY, Vol 4, 1973, p 686.

2. Fitzpatrick, G.L., "First Arrival Seismic Holograms," ACOUSTICAL HOLOGRAPHY, Vol 4, 1973, p 381.

3. Fitzpatrick, G.L., and Price, T.O., "Acoustical Holography Goes Underground," OPTICAL SPECTRA, Vol 11, No 9, 1977, p 57.

4. Fitzpatrick, G.L., Nichells, H.R., and Munson, R.D., "An Experiment in Seismic Holography," BUREAU OF MINES REPORTS OF INVESTIGATION, No 7607, 1972.

5. Booth, N., and Saltzer, B., "An Experimental Holographic Acoustic Imaging System," ACOUSTICAL HOLOGRAPHY, Vol 4, 1973, p 371.

6. Farer, John B., "Earth Holography as a Method to Delineate Buried Structures," ACOUSTICAL HOLOGRAPHY, Vol 6, 1975, p 435.

7. Peterson, R.C., "3-D Acoustical Holography System Detects Corrosion, Stress, Cracking," PIPELINE AND GAS JOURNAL, March 1978, p 31.

8. Wollman, M., and Wade, G., "Experimental Results From an Underwater Acoustical Holographic System," ACOUSTICAL HOLOGRAPHY, Vol 5, 1974, p 153.

9. Riffo, K., "Budushcheye--okean" [The Future--the Ocean], Izdatel'stvo "Gidrometeoizdat", 1978 (translated from French).

10. Zuyevich, A.V., Alekseyenko, V.V., and Sugak, V.M., "Recording and Reproduction of Long-Wave Holograms, Using Small Apertures," PIS'MA V ZhTF, Vol 4, No 6, 1978, p 333.

UDC 550.834

SOME RESULTS OF THE OPTICAL PROCESSING OF GEOLOGICAL DATA

Leningrad GOLOGRAFIYA I OPTICHESKAYA OBRABOTKA INFORMATSII V GEOLOGII in Russian 1980 (signed to press 19 Nov 80) pp 122-131

[Article by V.V. Alekseyenko, A.A. Bobin, A.V. Zuyevich, V.I. Kara and B.V. Senin from collection of works "Holography and Optical Information Processing in Geology", edited by Professor S.B. Gurevich and Candidate of Technical Sciences O.A. Potapov, Leningrad Physicotechnical Institute imeni A.F. Ioffe, USSR Academy of Sciences, 500 copies, 181 pages]

[Text] The authors describe a coherent optical system for the processing of geological and geophysical information that realizes the semiautomatic plotting of the radiation patterns of two-dimensional graphic information. They describe the technique in detail and present some processing results.

The study of the possibilities of using optical methods to process geophysical and geological information is being conducted intensively both in our country and abroad. A review of the basic achievements in this field is given in [1], where, however, the basic attention is devoted to the processing of seismic surveying data.

At the same time, geological material in the form of different kinds of maps, which is practically not suitable for processing by a computer, turns out to be almost ideal input information for optical systems.

Most methods for the statistical processing of graphic geological information feature the plotting of rose diagrams. When done by hand, this operation is extremely laborious, even when special reference grids ((Shmidt), (Vul'f) and so on) are available. In connection with this, a changeover from manual methods of processing such materials to processing by high-speed optical systems is extraordinarily effective.

The first results of the processing of lineament maps by optical methods were obtained by A. Fontanel and G. Graw [2] in 1968. In the USSR, analogous work is being done by several organizations, such as VNIIGRI [possibly All-Union Petroleum Scientific Research Institute of Geological Exploration], TsGT [Central Geophysical Trust], NPO [Scientific Production Association] "Aerogeologiya," FMI AN USSR [Institute of Physics and Mathematics, Ukrainian SSR Academy of Sciences]. The results of this work confirm the prospects of optical processing methods, although the possibilities of these methods are far from being fully used.

Since 1978, the authors of this article have been working on the optical processing of geological materials at the VNPO [probably All-Union Scientific Production Association] "Soyuzmorgeo." The goals of this work were:
the development and introduction into production of an optical system for plotting both radiation patterns of lineaments (DNL) and radiation patterns of the isolines (DNI) of any parameters, including those found on topographic, bathymetric, magnetic, gravimetric and structural maps, hydrological network maps and other materials;
automation of the production of DNL's and DNI's with a significant increase in operating speed, which is particularly necessary in view of the large volumes of information gathered during regional investigations;
the optical summation and sorting of the lineaments that are obtained.

The authors have built and operated in a production mode an optical device that plots DNL's and DNI's automatically, with a productivity rate of about 100 diagrams per hour. At the present time, various algorithms have been used with this device to process materials covering more than 50 million square kilometers of the Soviet Union's territory and adjacent waters (several thousand diagrams).

The theory and principles of the construction of analogous systems are explained quite thoroughly in the specialized literature [3,4], so here we will present only a brief technical description of the system and the basic stages of the processing operation.

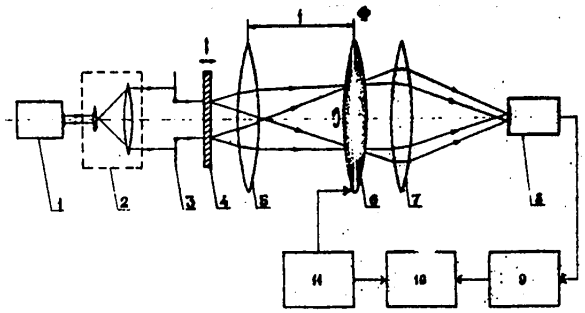

Figure 1. Diagram of optical device.

A diagram of the device is presented in Figure 1. The light source is He-Ne laser (1). The laser beam is broadened in beam expander (2) and directed onto optical transparency (4), which is a microphotocopy of a map. The transparency can be moved both horizontally and vertically, with the help of micrometric screws. In front of the transparency there is framing window (3), which consists of two pairs of mutually perpendicular shutters set up so that the length of the rectangular window's sides can be changed within limits of 1 to 20 mm. In our work we basically used a square window 1-3 mm on a side. The light diffracted by the transparency strikes lens (5), which has a focal length f = 600 mm. In its focal plane the lens creates a two-dimensional Fourier spectrum from the two-dimensional function of the transparency's transmission coefficient. Binary sector filter (6), which is a non-transparent disk with symmetrical sector cutouts, the angle of opening of which can be changed within broad limits, is located in the spectral plane. When the filter is turned, sequential isolation of sections of the spectrum being analyzed takes place. The light passing through the filter is concentrated by converging lens (7) on the photocathode of FEU [photomultiplier] (8). From the FEU, the signal is fed

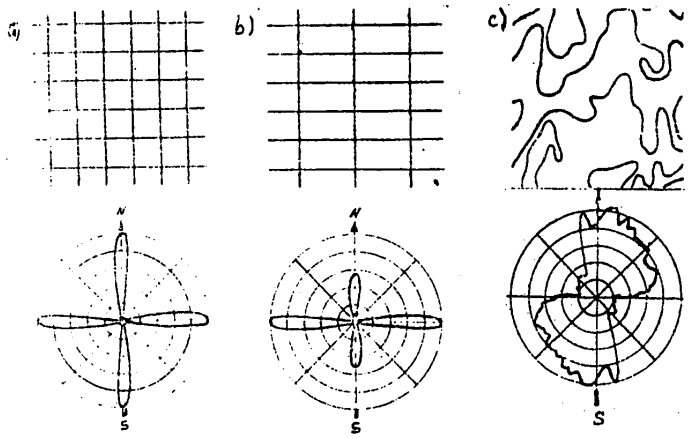

Figure 2. Tests (a, b), map section (c) and the diagrams corresponding to them.

into amplifier (9) and then into recording unit (10). The filter's rotation is synchronized with the recording unit by means of synchronization unit (11). The diagram is recorded on blanks with a polar coordinate grid. Figure 2 illustrates the operation of the system.

It should be mentioned here that there are two basic variable parameters in the system: the size of input window (3) and the angle of opening of filter (6). The size of the window is selected on the basis of the original material. It is usually chosen so that it corresponds to a map square with sides ranging from 30 to 100 km in length. In connection with this, one transparency measuring 20 x 20 mm^2 [sic] contains up to 100 sections. The filter opening angle is determined by the necessary directional resolution. The choice of an opening angle of less than 5° is not advisable, since the plotting accuracy of the original material itself is usually on the order of several degrees. Moreover, in order to distinguish the prevailing directions it is sometimes convenient to increase the angle to 15-20°. Basically, we used a 5° angle.

In order to obtain good results, a map is laid out in lines of equal thickness and anything not participating in the processing (including isoline numbers, elements of geographic correlation, the coordinate grid) is removed. The map is then divided into sections (usually squares) by fine pencil lines. The area of a square depends on the scale of the investigation; that is, the degree of generalization of the structures. It has been established experimentally that for a map scale of 1:1,000,000, a grid in which the sides of the square are 3-5 cm long is optimal. The map is then photographed with a reduction factor of 20-40. When doing the photography, it is desirable to use a lens with good resolution and a photographic film of the "Mikrat" type. The film is developed in a high-contrast developer and the negative is placed in a slideholder before being introduced into the optical system.

Geological interpretation of DNL's and DNI's is aimed at the solution of the following problems:
the detection of systems of lineaments and the study of the laws governing their

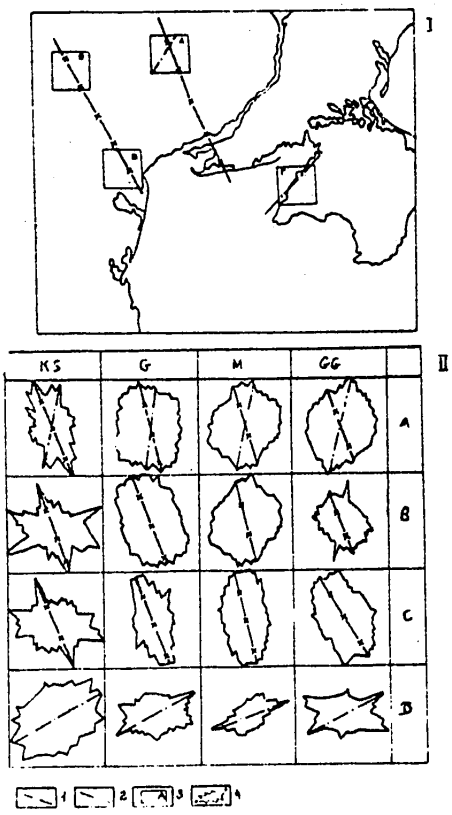

Figure 3. The southern Ukraine: results of testing the technique.

distribution (in plan);
the division of lineaments according to the degree of expression in profile in geophysical fields and structural maps on different levels.

On the basis of the regularities governing the distribution of lineaments in plan and profile that were determined, the solution of these two problems by a single method makes it possible to discover those lineaments that are related to deep fault zones and follow their temporal evolution.

As an experimental region for testing the technique, we chose the southern part of the Ukraine. Inside this region we selected sections located in known deep fault zones: Nikolayev (A), Odessa (B, C) and the relatively rarely delineated Tarkhankut (D) zones in Figure 3. These faults--particularly the first two--are described quite thoroughly in the literature, are clearly distinguished on the basis of various geophysical (GZS [expansion unknown], gravimetry and magnetometry) and geological data, and are an integral part of the present tectonic structures in this region [5,6]. In Figure 3 we present the DNL's and DNI's obtained for the selected areas and the faults named above on the basis of data obtained by interpreting space photographs (KS), gravimetry (G), magnetometry (M) and hydrography (GG). It is clearly obvious that all of these data unambiguously establish the direction of the faults that corresponds to their active distribution. As far as the Tarkhankut fault is described, on the basis of the results obtained it can, with complete substantiation, be removed from the category of presumed faults to the category of established ones.

In order to study the structure of the Sea of Okhotsk with this technique, the following maps were compiled: anomalous magnetic fields, distribution of thicknesses of sedimentary and sedimentary-volcanic formations and hypsometric with respect to the foundation. All the maps had a scale of 1:5,000,000 and were divided by a grid into squares with sides 3 cm long. From each map, 158 DNI's were obtained. As an example of the original material, in Figure 4 we show the map of the magnetic field anomalies in the Sea of Okhotsk. The small grid in the lower lefthand corner, which has a cross-shaped spectrum, is used to place the transparency in the optical system correctly.

The plan for the analysis of the results of the optical processing of this map is presented in Figure 5. On each DNI, lineaments in four basic directions--submeridional, north-east, sublatitudinal and north-west--were isolated separately.

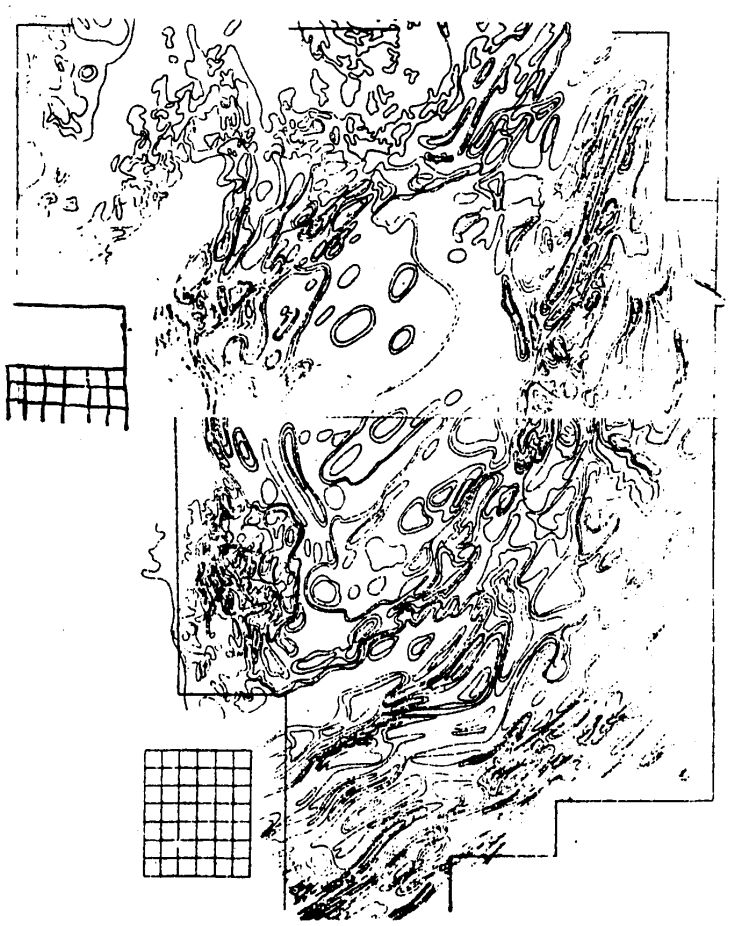

Figure 4. Map of magnetic field anomalies in the Sea of Okhotsk.

As a result, the diagram shown in Figure 5.1 was obtained. The lineaments were then broken down into the four basic types. Figure 5.2 depicts the zoning of the lineaments running in the submeridional direction, which is characterized by the presence of areas of Alpine folding and the distribution of the structure-forming faults for these areas. Figure 5.3 shows the same thing for lineaments running in the northeast direction and characterizes the process of the formation of the Sea of Okhotsk's basin. Figure 5.4 does the same for the sublatitudinal strike and shows that faults running in this direction do not play a structure-determining role in this region. Figure 5.5 depicts the north-west lineaments, which area is characterized by intensive, extremely recent tectonic movements. Figure 5.6 shows the layout of the faults discovered as the result of optical processing. It was obtained by correlating to the magnetic field the systems of lineaments depicted in Figures 5.2-5.5.

These results, as well as the results of an analysis of the maps of the Sea of Okhotsk mentioned above, enabled us to draw a number of conclusions of substantial importance and to carry out tectonic zoning of the Sea of Okhotsk region.

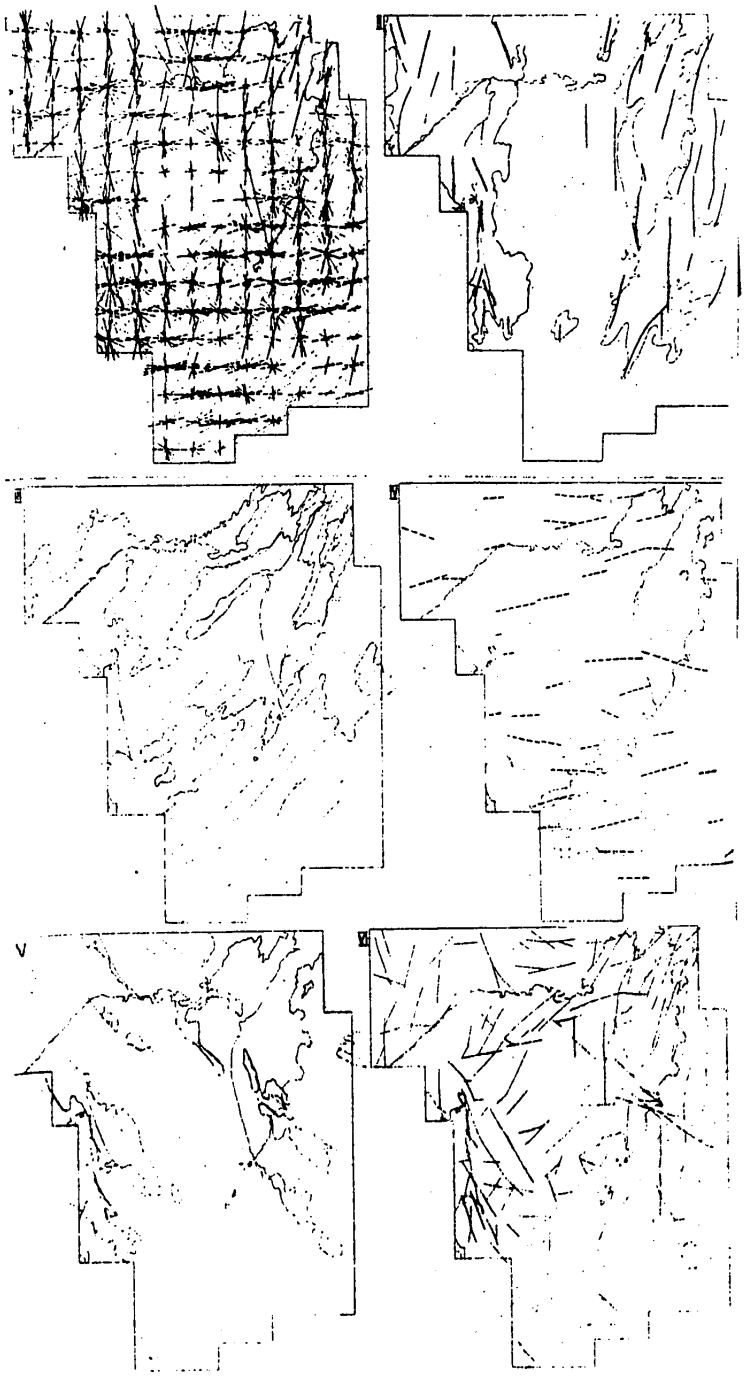

Figure 5. Results of optical processing of the map presented in Figure 4.

The examples presented of the processing of geological and geophysical materials again proves convincingly that the use of optical systems makes it possible to increase the yield of information from these materials substantially and to formulate and solve fundamentally new and important problems while achieving a significant increase in the productivity of labor at the same time.

In conclusion the authors wish to express their gratitude to I.A. Garkalenko, A.V. Semenov and V.B. Gavryushin for their useful discussion and valuable remarks, and N.I. Yefimova and S.V. Mamontov for their assistance in the work.

BIBLIOGRAPHY

1. Potapov, O.A., "Opticheskaya obrabotka geofizicheskoy i geologicheskoy informatsii" [Optical Processing of Geophysical and Geological Information], Moscow, Izdatel'stvo "Nauka", 1977.

2. Fontanel, A., and Graw, G., "Fraitement optique de l'information en geophysique et dans le domaine de la photographie alrienne," L'ONDE ELECTRIQUE, Vol 48, 1968.

3. Gudmen, Dzh., "Vvedeniye v fur'ye-optiku" [Introduction to Fourier Optics], Moscow, Izdatel'stvo "Mir", 1970.

4. Soroko, L.M., "Osnovy golografii i kogerentnoy optiki" [Principles of Holography and Coherent Optics], Moscow, Izdatel'stvo "Nauka", 1971.

5. Garkalenko, I.A., "Horizontal Movements of Blocks of the Earth's Crust in the Southern Ukraine and the Basins of the Black Sea and the Sea of Azov," DOKLADY AN USSR, Series B, No 2, 1977, pp 99-101.

6. Chekunov, A.V., "Struktura zemnoy kori i tektonika yuga Yevropeyskaya chasti SSSR" [Structure of the Earth's Crust and Tectonics of the Southern Section of the European Part of the USSR], Kiev, Izdatel'stvo "Naukova dumka", 1972.

UDC 550.834

USING CATHODE-RAY MEMORY TUBES IN SEISMIC INFORMATION PROCESSING DEVICES

Leningrad GOLOGRAFIYA I OPTICHESKAYA OBRABOTKA INFORMATSII V GEOLOGII in Russian 1980 (signed to press 19 Nov 80) pp 132-142

[Article by Ye.Yu. Yakush from collection of works "Holography and Optical Information Processing in Geology", edited by Professor S.B. Gurevich and Candidate of Technical Sciences O.A. Potapov, Leningrad Physicotechnical Institute imeni A.F. Ioffe, USSR Academy of Sciences, 500 copies, 181 pages]

[Text] The author analyzes the basic parameters of Soviet-made potentialscopes from the viewpoint of their utility for recording seismic signals. He shows that the parameters of potentialscopes with grid control make it possible to use them in devices for the processing of seismic information.

Success in solving problems related to the seismic surveying of the Earth's crust for the purpose of discovering gas and oil deposits is directly dependent on the correctness of the formulation of the geophysical work, allowing for the specific seismogeological conditions. The solution of this problem is facilitated to a considerable extent by the use of the analysis of materials obtained in a profile in order to make appropriate corrections in the work. Such analysis must, naturally, be conducted at a rate that matches the rate of the performance of the seismic surveying work.

Scientists at the VMNPO [probably All-Union Marine Scientific Production Association] "Soyuzmorgeo" (in Krasnodar), have developed devices that make it possible to carry out a rapid analysis of seismic data on board a ship, construct temporal seismic profiles on a real time scale [1], construct deep seismic sections [2] and monitor the quality of seismic material at different stages in its processing [3]. Cathode-ray memory tubes (ZELT) were used as the operational memories (OZU) in these instruments. During the development process there was a study of the parameters of ZELT's produced by Soviet industry for the purpose of determining the possibility of using them in devices for the processing of seismic information [4].

In this article we present some of the results of these studies.

At the present time, ZELT's with a dielectric target (potentialscopes) are the most widely used ones. In these devices, the recording process consists of the application of electrical charges on the surface of the target, as a result of which there forms on the target a potential relief that is retained for a certain period of

time; that is, information storage takes place. Existing ZELT's can be subdivided into groups according to the nature of the conversion of input information to output information that they perform [9]:
ZELT's for converting an electrical signal into another electrical one;
ZELT's for converting an electrical signal into a visible image;
ZELT's for converting a visible image into an electrical signal;
ZELT's for converting an image into another image.

Of these groups, the most suitable ZELT's for creating memory devices are those that convert one electrical signal into another one, since this makes it possible to use an electronic method and the appropriate algorithm to gain access to the information recorded on their targets. In Table 1 we present the basic parameters of several types of potentialscopes produced by Soviet industry [8,9].

Table 1.

Тип ЭЗЛТ (1)	Число лучей (2)	Разрешающая способность, лин/мм (3)	Число воспроизводимых градаций изображения (4)	Время считывания, с (5)	Число считываний (6)	Число накапливаемых сигналов (7)
ЛН8(8)	I	200	I0	-	32	I28
ЛНI02	2	700	4	30	-	-
ЛНI04	2	500	4	60	-	-
ЛНI7	I	600	5	I80	-	-
ЛНI8	I	800	5	300	-	-
ЛНI9	2	800	7	720	-	35

Key:
1. Type of ZELT
2. Number of beams
3. Resolution, lines/mm
4. Number of reproducible image gradations
5. Access time, s
6. Readout number
7. Number of accumulated signals
8. LN...

Let us dwell briefly on the characteristics of the ZELT's under discussion. In the LN8 potentialscope, recording and reading are accomplished because of overcharge processes on the target that are based on secondary electron emission; that is, the recorded information is destroyed during the reading process. This limits the number of readouts or, in the case of digital recording, requires regeneration of the recorded information. The advantage of the LN8 potentialscope is its ability to accumulate (integrate) signals (up to 128), which makes it possible to use it to isolate useful information against a background of interference. The LN8 potentialscope's integrating properties make it possible to use it in digital-analog complexes for the processing of seismic information [10,11], although the small capacity of its memory (up to 40,000 bits on the target during digital recording [9]) limits its utility.

The LN102 and LN104 potentialscopes are two-beam grafekony [translation unknown] based on the recording of high energy (10-12 kV) excited by conductivity with the help of a beam and overcharge reading. The recording method makes it possible to obtain high resolution, although their read time is limited. Grafekony make it possible to obtain a half-tone image with four or five gradations. The presence of two

beams makes it possible to have different types of scanning, functioning simultaneously, for each beam. This makes it possible, in particular, to review the recorded information on the kinescope's screen, the scanning of which is coupled with the scanning of the reading beam, it being the case that the scale of the image being read can, within certain limits, be changed by varying the reading beam's scanning voltages. This makes it possible to review individual fragments of the image on a larger scale, which reduces to a certain degree the effect of the line structure of the kinescope's raster on the ZELT-kinescope's resolution.

In recent years, Soviet industry has mastered the production of potentialscopes with recording because of secondary electrons on a penetrable dielectric target and reading by grid control; these are the LN17, LN19 and LN19 potentialscopes. In them is realized a mode in which there is no contact between the target's charged elements and the reading electrons. As with electron tubes, this is achieved by negative displacement of the potential of the target's dielectric with respect to the reading projector's cathode. Overcharge processes do not appear in this mode, for all practical purposes, while the nondestructive access time is determined by the target's conductivity and ion seeding. As far as resolution and number of gradations are concerned, ZELT's with grid control are better than grafekony. The LN17 and LN18 potentialscopes are single-beam devices and are used to record single signals or television pictures, with subsequent reproduction of the information on the desired time scale and with the desired beam-scanning rule. They have the capability to accumulate signals on the target by repeated recording without erasing, although this parameter is not presented in the certification information. The LN19 potentialscope is a double-beam one. Information recording and reading are done on different sides of the target, in connection with which there is no seeding of the target with reading electrons, which provides an extended reading time: the best examples of this potentialscope permit reading for up to 100 minutes. An important feature of the LN19 potentialscope is its ability to accumulate incoming signals. The number of linear accumulation cycles is at least 35 (this parameter actually varies between 45 and 60). As is the case with a grafekon, the LN19 potentialscope provides the possibility of reading the information as it is being recorded, which makes it possible to create different electronic information processing systems that are coupled with a device for depicting the information on the screen of a cathode-ray tube (kinescope), thereby providing visual observation of the processing operations.

Having discussed the parameters of these ZELT's, we can draw the following conclusions:
the best accumulative properties of the potentialscopes we have discussed belong to the LN8 integrating instrument (see Table 1).

However, the low resolution results in the necessity of placing the information from even a single seismogram on several ZELT's [11], which makes it impossible to create sufficiently simple devices for the visual depiction of the information being processed. A substantial shortcoming of the LN8 potentialscope is the destruction of the information during the reading process, which limits the number of readings from each element to no more than 32. This means that during raster readout according to the television standard for the purpose of reviewing on the kinescope's screen, the recorded information is destroyed in less than 2 seconds, since there are 25 readouts per second from each element.

Potentialscopes with grid control can be used to create devices for depicting seismic information. They have the highest resolution, a nondestructive readout method

and a sufficient number of transferable image half-tones (gradations). Of this series of potentialscopes, the best parameters belong to the two-beam LN19 instrument. Its great advantage is the possibility of observing the information on the screen of a cathode-ray display during the recording process.

Let us evaluate the frequency properties of the LN19 potentialscope. It is convenient to relate the temporal frequency at the ZELT's input and output to the spatial frequency ν, which characterizes the ZELT's resolution and is numerically equal to the number of lines recorded per unit of target length:

$$\nu = \frac{f_r}{v_r} = \frac{f_c}{v_c},$$

where f_r, f_c = temporal frequencies of the recording and reading signals, respectively; v_r, v_c = rates of movement of the beam along the target during recording and reading.

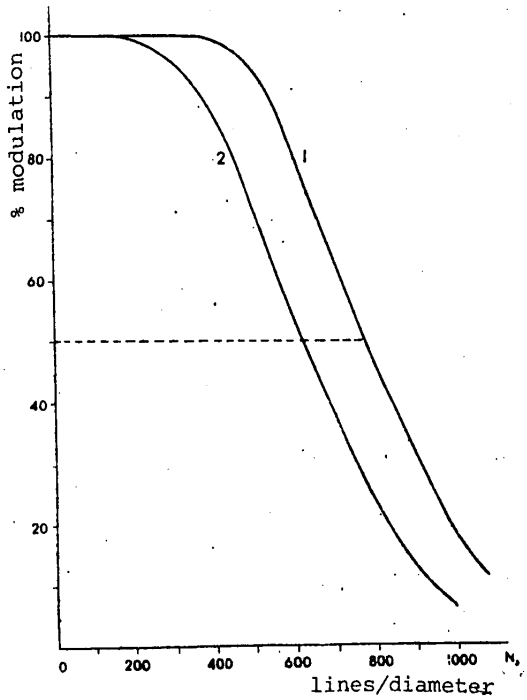

Figure 1. Spatial frequency characteristic of the LN19 potentialscope.

The spatial frequency characteristic of the LN19 potentialscope is shown in Figure 1, where the spatial frequency, expressed as the number of lines on the target's diameter, is plotted on the x axis, while the percent of modulation of the signal that has been read is plotted on the y axis. The zone bounded by curves 1 and 2 is the field of permissible technological variation in the resolution of individual examples of the potentialscope. As is obvious from the figure, when ν increases the signal at the ZELT's output is reduced because of the finite dimensions of the electronic spot during recording and reading.

The recording speed is

$$V_r = \frac{d}{t_r},$$

where d = diameter of the target; t_r = time required for the passage of the beam along the diameter during recording. Taking into consideration the fact that $\nu = N/d$, where N is the number of recorded lines on the target's diameter, let us find the expression for the frequency of the signals being recorded:

$$f_r = V_r \cdot \nu = \frac{d}{t_r} \cdot \frac{N}{d} = \frac{N}{t_r}.$$

When recording sinusoidal signals, each period of the sinusoid is recorded by two lines, so that

$$f_r = \frac{N}{2t_r}. \quad (1)$$

Let us evaluate the LN19 potentialscope's capabilities for recording seismic signals. In order to do this, we will find the upper recording frequencies f_u for different recording times. When plotting seismic sections, we will obviously not use the entire area of the target, but only a square with sides $\ell = d/\sqrt{2}$, so that for this case equality (1) takes on the form

$$f_r = \frac{N}{2\sqrt{2}\, t_r}, \qquad (2)$$

where N = number of lines on the diameter, as determined by the curves in Figure 1. According to the producer plant's specifications, N is selected at the level of 50-percent modulation.

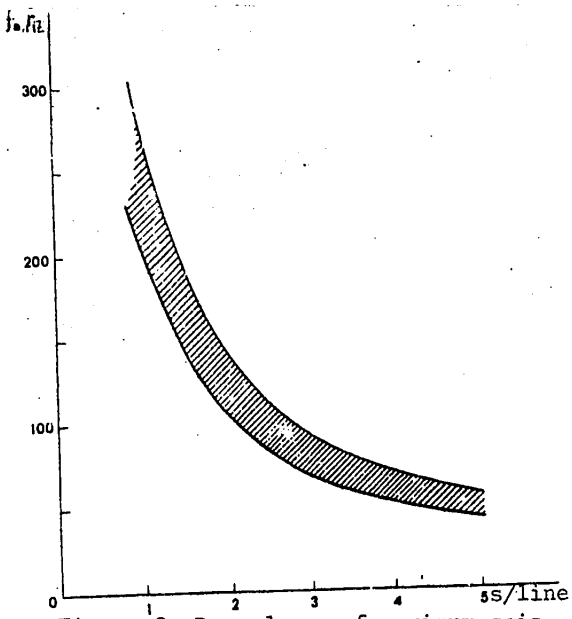

Figure 2. Dependence of maximum seismic signal frequency on recording time on the LN19's target.

Figure 2 shows the results of the calculation of the maximum seismic signal frequency that makes it possible to record with a potentialscope, as a function of the recording time. The calculations were made in accordance with equality (2) for the cases of maximum and minimum resolution of the potentialscope (curves 1 and 2 in Figure 1).

When recording seismic information, one must deal with seismic waves that have arrived from different depths and, consequently, through different number of layers of different thickness in a real medium that has filtering properties and affects the spectral composition of the oscillations being registered [12,14]. It is a well-known fact that as the depth of the layer increases, for reflected waves there occurs a lowering of the predominant frequency of the spectrum of seismic oscillations being recorded. For recording times of 3,...,5 seconds, the predominant frequency of the seismic signal spectrum lies in the 20,...,30 Hz range, and increases to approximately 100,...,150 Hz for recording times of 0.3,...,0.5 seconds [12]. Comparing the data on the frequency spectrum of a seismic signal with the frequency characteristic of the LN19 potentialscope (Figure 2), we see that the potentialscope's resolution makes it possible to record seismic information both in the standard recording interval t_r = 5 s and when the recording period is shortened (to 1-2 s, for example) for the purpose of studying the upper part of a section in more detail. Increasing the maximum possible recording frequency on the potentialscope while shortening the duration of the recording period makes it possible to record seismic vibrations that increase in frequency as the depth decreases. The modern technique of multiple observations provides a different overlap multiplicity factor, depending on the specific seismological conditions. The maximum multiplicity factor equals the number of reception points in the receiving system. For example, for a 24-channel receiving system the number of overlaps is usually chosen as 3, 6, 12 or 24. A higher overlap multiplicity factor is used for complex processing algorithms, a high level of interference and when a

48-channel receiving and recording device is used. For the sake of achieving operational and rapid processing, in most cases it is possible to restrict oneself to an overlap multiplicity factor of no more than 24 or, as a rule, 6 or 12, which makes it possible to obtain a resultant signal within the limits of potentialscope's dynamic range when the signal level is chosen appropriately. In connection with this, naturally, it is necessary to compensate for the nonlinearity of the potentialscope's modulation characteristic and use the appropriate controls in the seismic signal channel.

On the basis of what has been said, the following conclusions may be drawn.

1. High-speed operational memories with an adequate capacity, which are needed for the creation of seismic section plotting devices, can be built on the basis of cathode-ray memory tubes (potentialscopes).

2. The storage of information recorded in a ZELT's memory in the form of an image makes it possible to use ZELT's as a basis for building simple and efficient devices for depicting graphic information.

3. In order to create devices for the depiction of graphic (seismic) information, it is advisable to use two-beam potentialscopes with grid control that have high resolution and a nondestructive information readout method.

4. An investigation of ZELT's has shown that the following basic parameters are provided for seismic section plotting devices based on them:
a dynamic range of at least 30 dB (see Table 1);
a frequency range of up to 50 Hz for a recording length of 5 s, and up to 200 Hz for a recording length of 1 s;
high operating speed, which insures the plotting of sections on a real time scale.

5. The use of two-beam ZELT's having separate scanning devices for each beam makes it possible to build devices providing:
visualization of the information being recorded during the profile plotting process, which makes it possible to actively influence the plotting process by making the appropriate adjustments;
evaluate the obtained seismic section and eliminate the recording of intermediate results during the selection of the parameters;
change the scale of an image by varying the scanning voltages of the ZELT's reading beam, which makes it possible to reduce the effect of the line structure of the raster of the display cathode-ray tube on the device's resolution.

BIBLIOGRAPHY

1. Yakush, Ye.Yu., and Gavryushin, V.B., "Device for Plotting Temporal Seismic Sections," GEOFIZICHESKAYA APPARATURA, Leningrad, Izdatel'stvo "Nedra", No 66, 1979, pp 102-105.

2. Yakush, Ye.Yu., and Gavryushin, V.B., "Electronic Plotting Device for Deep Seismic Sections," GEOFIZICHESKAYA APPARATURA, Leningrad, Izdatel'stvo "Nedra", No 65, 1978, pp 70-74.

3. Yakush, Ye.Yu., "Seismic Videomonitoring Device," GEOFIZICHESKAYA APPARATURA, Leningrad, Izdatel'stvo "Nedra", No 66, 1978, pp 99-102.

4. Yakubovskiy, S.V. (editor), "Analogovyye i tsifrovyye integral'nyye skhemy" [Analog and Digital Integrated Circuits], Moscow, Izdatel'stvo "Sovetskoye radio", 1979, 336 pp.

5. Anisimov, B.V., and Chetverikov, V.N., "Osnovy teorii i proyektirovaniya ETsVM" [Principles of the Theory and Design of Digital Computers], Moscow, Izdatel'stvo "Vysshaya shkola", 1970, 575 pp.

6. Arkhipov, V.K., "Masshtabno-vremennoye preobrazovaniye korotkikh signalov pri pomoshchi elektronno-luchevykh trubok pamyati" [Scaled-Time Conversion of Brief Signals With the Help of Cathode-Ray Memory Tubes], Moscow, Izdatel'stvo "Energiya", 1968.

7. Arkhipov, V.K., and Stepanov, B.M., "Operation of a Cathode-Ray Tube in the Charge Accumulation Mode With Forced Takeoff of Secondary Electrons During Recording," AVTOMATIKA I TELEMEKHANIKA, MIFI [Moscow Engineering Physics Institute], Izdatel'stvo "Gosatomizdat", No 3, 1962.

8. Denbnovetskiy, S.V., and Semenov, G.F., "Zapominayushchiye elektronno-luchevyye trubki v ustroystvakh obrabotki informatsii" [Cathode-Ray Memory Tubes in Information Processing Devices], Moscow, Izdate'stvo "Sovetskoye radio", 1973, p 472.

9. Kantsel'son, B.V., et al., "Elektrovakuumnyye elektronnyye i ionnyye pribory" [Electrovacuum Electron and Ion Instruments], A.S. Larionov, editor, Moscow, Izdatel'stvo "Energiya", Vol 1, 1970.

10. Borochin, A.S., "The Possibility of Using a Potentialscope for Discrete-Analog Systems for the Accelerated Processing of Seismic Information," PRIKLADNAYA GEOGIZIKA, Moscow, Izdatel'stvo "Nedra", No 63, 1971.

11. Borochin A.S., and Shestakov, V.I., "High-Speed Device for Processing and Storing Seismic Information," PRIKLADNAYA GEOFIZIKA, Moscow, Izdatel'stvo "Nedra", No 66, 1972.

12. Berzon, I.S., et al., "Dinamicheskiye kharakteristiki seysmicheskikh voln v real'nykh sredakh" [Dynamic Characteristics of Seismic Waves in Real Mediums], Moscow, Izdatel'stvo AN SSSR [USSR Academy of Sciences], 1962, 490 pp.

13. Berzon, I.S., "On the Change in the Predominant Frequencies of Seismic Waves as the Distance From the Source of Oscillations Increases," IZV. AN SSSR, SER. GEOFIZICHESKAYA, No 1, 1956.

14. Polak, A.S., "Attenuation and Absorption of Reflected Waves in Sedimentary Rocks," PRIKLADNAYA GEOFIZIKA, Izdatel'stvo "Gostoptekhizdat", No 17, 1975.

UDC 550.834

PRINCIPLES OF THE COLOR VISUALIZATION OF SEISMIC DATA

Leningrad GOLOGRAFIYA I OPTICHESKAYA OBRABOTKA INFORMATSII V GEOLOGII in Russian 1980 (signed to press 19 Nov 80) pp 143-153

[Article by V.I. Dubyanskiy and V.A. Starodubtsev from collection of works "Holography and Optical Information Processing in Geology", edited by Professor S.B. Gurevich and Candidate of Technical Sciences O.A. Potapov, Leningrad Physicotechnical Institute imeni A.F. Ioffe, USSR Academy of Sciences, 500 copies, 181 pages]

[Text] The authors discuss the importance of color as an additional parameter that facilitates the interpretation of seismic recordings. They propose methods for the color depiction of seismic sections and specific ways of realizing them.

The use of color in seismic surveying and, in particular, seismic holography offers the prospect of increasing the information content of seismic images through the depiction of a set of additional data and parameters embedded in the processing algorithm. There are two ways to obtain a color image of an object: additive (supplementary) and subtractive (deductive) mixing of three colors. Additive mixing of colors takes place when the retina of the eye is struck simultaneously or in rapid succession by several emissions of different colors that, in the general case, come from different spontaneously emitting sources (Figure 1). An analogous effect appears when one observes a white surface with colored spots, the angular size of which is less than the minimum size resolvable by the eye. In connection with this, the eye transmits the impression of a single color. The summary color depends only on the color of the emissions being mixed, which makes it possible to calculate it by calorimetric methods. By mixing three colors it is possible to obtain any color in the color spectrum inside the triangle with apices that lie at points cprresponding to the color index of the emissions being mixed.

Subtractive mixing of colors occurs when emissions from a single source pass through successive filters or pigments are mixed on a carrier (Figure 2). The color of the mixture depends on the absorption of the illuminating light in the separate filters or pigments and is determined by the spectral characteristics of the source and the spectral transmission or reflection curves of the mediums absorbing the light. Subtractive mixing takes place in color cinematography, color photography, printing and so on.

Let us discuss the possible principles of the color depiction of the dynamic and kinematic characteristics of seismograms and sections. The general principles of

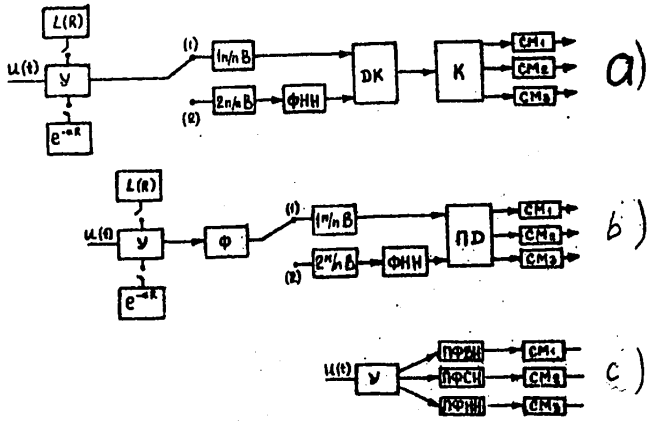

Figure 1. Diagram of color division of a signal u(t): a. with respect to amplitude (1) and energy, with commutation on three levels; b. with respect to amplitude (1) and energy (2); c. with respect to frequency. Definitions: L(R) = divergence function registration unit; Y = amplifier; $e^{-\alpha R}$ = absorption function registration unit; 1 n/n B, 2 n/n B = half-wave and full-wave rectifiers; ФНН = low-frequency filter; DK = discriminator; K = commutator; $CM_{1,2,3}$ = light modulators; Ф = filter; D = threshold divider; ПФ ВН, СН, НН = high-, medium- and low-frequency bandpass filters; $П\Phi_{1,2,3}$ = color filters for basic colors of the spectrum; YC = combining unit; CI = color image; O = illuminator; H/B ФР = black-and-white photographic recorder.

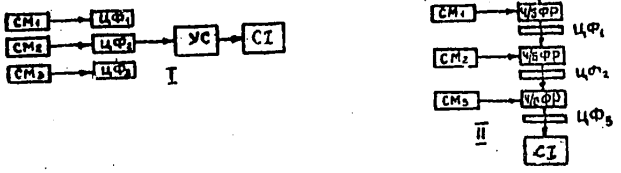

Figure 2. Diagram for obtaining color images by the additive (1) and contractive (2) methods.

obtaining a color image are: 1. color separation of the original image's parameters into three components--F_1, F_2 and F_3; 2. coloration of the color-separated functions by the basic colors of the spectrum of white light--C_1, C_2 and C_3; $F_1 = f(C_1)$, $F_2 = f(C_2)$, $F_3 = f(C_3)$; 3. additive or contractive mixing of the colored color-separated functions in order to produce a summary color image:

$$f(C_I + C_2 + C_3) = F_{\Sigma}(C).$$

In seismic surveying, the color spectrum can depict the following basic parameters, the choice of which depends on the formulation of the surveying assignments: 1. dynamic characteristics of seismic signals in the spatiotemporal plane of a seismogram or a temporal section (for example: amplitude, energy, spectral characteristics); 2. dynamic characteristics of a holographic image of a section obtained as the result of the diffraction conversion [2,3] of seismic signals (the values of the reflection or absorption factors); 3. kinematic characteristics of temporal or holographic sections (distribution of bed velocities, angles of inclination of

reflecting boundaries, diffraction areas); 4. local and integral distribution of relative values of kinematic and dynamic characteristics and so forth.

The transformation of seismic frequencies into visible spectrum frequencies makes obvious physical sense. This transformation must be done with due consideration for some similarity factor (K) that allows for the relationship of the optical (λ_o) and seismic (λ_c) wavelengths in the scale of the final image. In this case the seismic image that is obtained will be colored in "natural" light. Let us make our choice of the similarity factor for the low-frequency components of the spectrum of seismic and light (red) waves, which are the most stable in an absorbing medium. Let us assume that the length of the low-frequency seismic wave in the medium is λ_c = 100 m. On the scale of the seismogram's image (M = 1:10,000, for example), the length of the reference seismic wave will be $\lambda_c' = M\lambda_c$ = 10 mm. We will determine the color similarity factor for the low frequencies from the relationship

$$K = \frac{\lambda_o^{kp}}{\lambda_c'},$$

where $\lambda_o^{kp} = 71 \cdot 10^{-5}$ mm = the wavelength of red light. The similarity factor turns out to be

$$K = 71 \cdot 10^{-6}.$$

The value of the frequencies of the narrow-band filtration of the seismogram for isolating the reference wave with length λ_c = 100 m in sections with different average elastic wave propagation rates (v_i) is established from the relationship

$$f_i(t) = \frac{\bar{V}_i}{\lambda_c}.$$

We are interested in the values of the basic band filtration frequencies for a color-separated seismogram, which correspond (for example) to the yellow and violet basic colors of the visible spectrum. Taking the previous relationships into consideration, it is possible to write (in general form)

$$f_{fsg} = K \frac{\bar{V}}{\lambda_o^{fv}} M$$

where f_{fsg} = necessary frequency of color separation of the seismogram; λ_o^{fv} = wavelength of visible light. The formula that has been obtained makes it possible to determine the band frequency filtration parameters for seismic signals for the purpose of color separation for mediums characterized by different average velocities (Figure 3). For example, for a medium with $\bar{v}$ = 3.0 km/s, the color red should correspond to seismic frequency f_1 = 30 Hz, green to f_2 = 40.6 Hz and violet to f_3 = = 51.9 Hz. Additive mixing of the color-separated signals that have passed through the bandpass filters with frequency characteristic maximums f_1, f_2 and f_3 and have been colored red, green and violet, respectively, will make it possible to obtain a color image of a seismogram where the color range corresponds to the distribution of the seismic frequencies in the medium. The application of the basic colors in different combinations gives a full spectrum of additional colors, which in turn depict certain frequency characteristics of the seismogram being visualized.

Inasmuch as the relationships depicted in Figure 3 are of a linear type, let us apply the principle of superposition to the application of the colors. From here it turns out to be possible to calibrate the additional colors in the image that is obtained according to the seismic frequencies that correspond to them or, according to the color in the image, to determine to which signal frequency it corresponds. For example, for $\bar{v}$ = 3.0 km/s, orange in the image corresponds to a signal on frequency

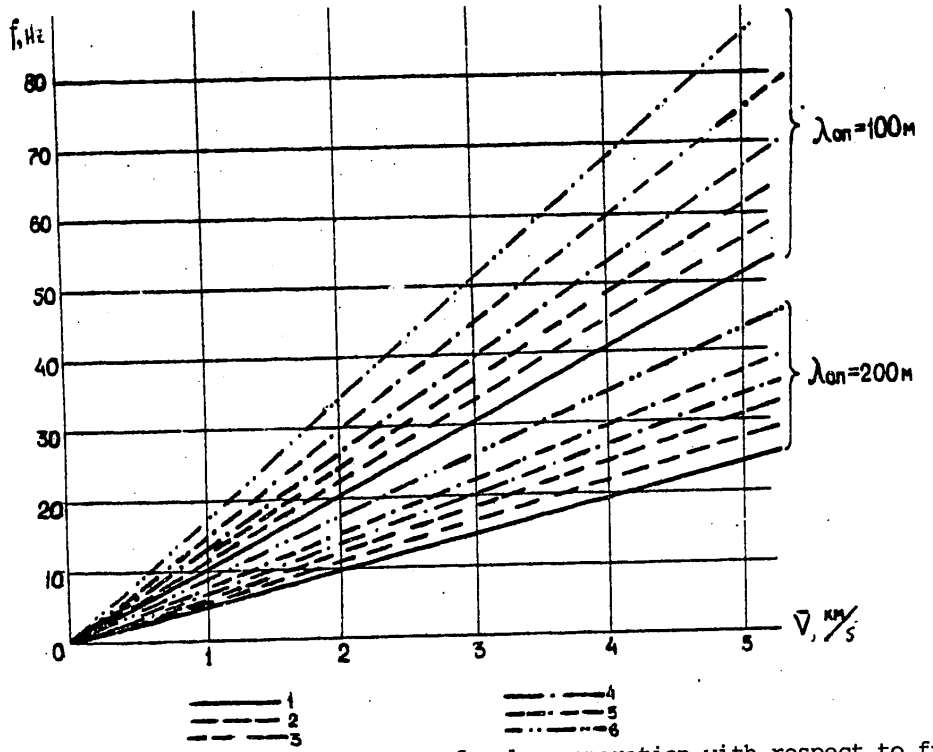

Figure 3. Nomogram of parameters of color separation with respect to frequency: 1. red; 2. orange; 3. yellow; 4. green; 5. blue; 6. violet.

f = 34.2 Hz, while for light blue it is 45.3 Hz (Figure 3). It is a well-known fact that green is a combination of yellow and blue. If the principle of superposition is implemented, the arithmetical mean of the color-separated seismic frequencies corresponding to these colors must equal the seismic frequency of green:

$$f_{зел.} = \frac{f_{жс} + f_{гол}}{2} = \frac{37\ Гц + 45\ Гц}{2} = 41\ Гц.$$

Using the graph (Figure 3) to determine the frequency of green, we obtain the value

$$f_{зел} = 40{,}6 \sim 41\ Гц.$$

Color separation of seismic signals can also be done with respect to amplitude-energy characteristics. In this case the summary color image will depict the distribution of the dynamic parameters in the plane of the seismogram. The choice of the basic tones of the seismic data's color separation will be determined not by the medium's parameters, but by the interpretation algorithm.

Color separation with respect to an amplitudinal feature must allow for the factors affecting the amplitudes of reflected waves. In a homogeneously stratified structure characterized by absorption factor α, the amplitudes of the reflected waves also depend on the source's directivity I(w), the divergence factors L(R), and reflection from the boundary K(w) and the diurnal surface (conversion) [4,5]:

$$A(w) = \frac{\mathcal{Y}(w)\, K(w)}{L(R)}\, e^{-\alpha R}$$

where w = frequency of the oscillation, R = path of the wave in the medium.

The reflection and absorption factors K(w) and α are immediate characteristics of the medium's properties. The goal of color visualization is to depict the medium's dynamic characteristics for the purpose of enlarging the information content of seismic surveying work, as well as (in some cases) to search directly for deposits of useful minerals.

In order to solve this problem, it is necessary to distinguish and isolate the factors characterizing the medium from the overall group of functions affecting the reflected wave's amplitude and then subject them to color separation. For constant values of the source's directivity function, the reflected waves' intensity depends to a considerable extent on the reflection factor and the divergence function [3,4]. Permanence of the source's directivity function is best maintained during seismic observations at sea, while under land conditions--particularly when the upper part of a section has a complicated structure (in ore regions, the trappean provinces of Siberia), it is practically impossible to take the source's directivity into consideration. In a rough approximation, therefore, we must assume it to be constant for standard sources of the explosive type. Exceptions are nonexplosive sources and explosive sources having assigned and controllable directivity characteristics [5,6], which must be taken into consideration during color separation of a function of a medium's dynamic characteristic.

The formula for A(w) is rigorously accurate for any stable frequency and a single harmonic $w = w_i$ (i = 1,2,3,...). If absorption in the medium is ignored, this formula expresses the wave's amplitude, since there is no dependence on frequency. If the wave's shape changes, this formula expresses the amplitude spectrum of the components. During the standard reproduction of a seismic recording without expansion of the signals into their spectral components, the formula expresses the amplitude of a reflected wave on a visible frequency.

The strongest effect on the amplitude is exerted by the divergence function L(R) in the medium, which in homogeneous and gradient mediums is described by the principles of geometric seismic surveying [4,5]. In order to obtain a medium's dynamic characteristics in "pure" form, the divergence function must be compensated for by (for example) using programmed regulation of the amplification. The divergence and absorption functions in a medium change a signal smoothly in time toward diminution. Therefore, they can be allowed for simultaneously and compensated for by programmed amplification of the reflected signals. In this case the reflected waves' amplitudes will depend oly on the reflection factors for I(w) = const. The color image of the seismogram obtained by color separation of the function

$$A(w) = DF[K(w)]$$

will depict the medium's reflecting properties. Here,

$$D = D(w,R) = \frac{\mathcal{Y}(w)}{L(R)}\, e^{-\alpha R}$$

The energy characteristics of seismic signals can be obtained by full-wave rectification and smoothing by low-frequency filters. In this case the modulating function corresponds to the total area of the signal being reproduced.

Depending on the method used to synthesize the color image, absolute or relative values of the parameter being reproduced will be depicted in it.

The use of the method of color separation with discrimination with respect to given levels and subsequent commutation of the parameter with respect to three color channels makes it possible to depict the absolute values of the parameter being reproduced in color (Figure 1). Each of the color-separated transparencies will contain parameters only on its own discrimination level. This method, for example, can be used to obtain three color-separated masses of seismograms, on each of which are waves with dynamic characteristics given beforehand. On the summary color image, signals obtained from seismic boundaries with different reflection factors will appear in different colors. In this case, intermediate reflection factor values (lying between the three given during color separation) will be depicted by intermediate colors, according to the principle of superposition of the basic colors of the visible spectrum. The reflection factors' values can be calculated by determining the color's coordinates by calorimetric methods (quantitatively) or qualitatively, according to a standard scale that allows for the original levels of color separation of the parameter being reproduced.

The use of controllable levels of color separation for seismic data makes it possible to realize the "bright spot" method; that is, discrimination on the image of objects with dynamic parameters that are given in advance or expected. The "bright spot" method is used for direct searches for useful mineral deposits.

The method of color separation with respect to dynamics and separate commutation makes it possible to solve the problem of separating a wave field into its components: regular waves and the wave background. If the regular waves, for example, are reflected as if from a mirror and have clearly expressed dynamic and correlation properties, the wave background has a diffraction character in the form of separate, short cophasal axes with different orientations.

The nature of the wave background has not yet been studied sufficiently well, although there are all grounds for assuming that it is related to local irregularities scattered throughout the medium. The depiction in color of the wave background's properties will make it possible to supplement our ideas about a medium that is being investigated because we will obtain the dynamic characteristics of the diffracting objects as well as those of the smooth, mirror-reflecting boundaries.

On the whole, color separation with commutation on three color channels makes it possible to depict, on a summary color image, any interrelated and unrelated parameters of an object, divided into three independent groups according to the operator's judgment. For example, this could be the results of directional filtration of the cophasal axes with respect to three apparent velocity values; the results of extensive profiling, the distribution of the parameters of the average velocities in a section, the amplitudes of the reflected signals of the visible periods of longitudinal and transverse waves and so on, rising and falling vertical seismic profiling waves. For example, the additive combination of the color-separated results of extensive profiling with respect to three parallel profiles makes it possible to obtain a three-dimensional illusory image.

The use of the method of color separation of seismic information by levels, without commutation, for three color channels makes it possible to depict on a summary color

image the relative values of the parameter being reproduced, such as amplitude. In order to do this, the scale of the amplitudes of the registered signals within the limits of the recorder's dynamic range are divided into three color-separated levels, while the color signals that have passed through these levels are summed up in a single channel, as the output of which the following pattern is seen:

$F(A_1) \sim \Delta C_1 = f(C_1)$ = low signal level;
$F(A_2) \sim \Delta C_2 + C_1 = f(C_2)$ = medium signal level;
$F(A_3) \sim \Delta C_2 + C_1 + C_2 = f(C_3)$ = high signal level.

Low-level signals are depicted by variations in the color $f(C_1)$; medium-level ones by the same for $f(C_2)$, in which light C_1 is a constant component; high-level ones by variations in $f(C_3)$, in which C_2 and C_3 [sic] are constant components. Thus, on the summary color image, the color range depicts the relative values of the seismic signals' amplitudes.

The use of this method makes it easy to reproduce in color the smoothly changing functions of a medium such as the average velocity of the elastic waves in the plane of a section, the absorption function, the average amplitude levels, wavelengths and other integral characteristics.

The principles of the color depiction of seismic data that were explained above have been partially realized in the "Geospektr-1" equipment complex, which was developed in Voronezh State University's Seismic Holography Laboratory.

BIBLIOGRAPHY

1. Elliot, L., and Uilkoks, U., "Fizika" [Physics], Moscow, Izdatel'stvo "Nauka", 1975.

2. Zav'yalov, V.D., et al., "Holographic Transformations of Seismograms on a Plane," SER. "RAZVED., PROMYSL. I REGION. GEOFIZIKA", ONTI VIEMS [Department of Scientific and Technical Information, All-Union Scientific Research Institute of Economics of Mineral Raw Materials and Geological Exploration], No 32, 1970.

3. Timoshin, Yu.V., "Impul'snaya seysmicheskaya golografiya" [Pulsed Seismic Holography], Moscow, Izdatel'stvo "Nedra", 1978.

4. Berzon, I.S., et al., "Dinamicheskiye kharakteristiki seysmicheskikh voln v real'nykh sredakh" [Dynamic Characteristics of Seismic Waves in Real Mediums], Moscow, Izdatel'stvo AN SSSR [USSR Academy of Sciences], 1962.

5. Petrashen', G.I. (editor), "Voprosy dinamicheskoy teorii rasprostraneniya seysmicheskikh voln" [Questions in the Dynamic Theory of Seismic Wave Propagation], Moscow, 1961.

6. Benderskiy, V.Ya., Raykher, L.D., and Kharaz, I.I., "Metod upravleniya frontami voln v seysmorazvedke" [A Method for Controlling Wave Fronts During Seismic Suring], Moscow, Izdatel'stvo "Nedra", 1973.

UDC 550.834.05

INFORMATION CHARACTERISTICS OF A FIELD OF SEISMOHOLOGRAPHIC IMAGES

Leningrad GOLOGRAFIYA I OPTICHESKAYA OBRABOTKA INFORMATSII V GEOLOGII in Russian 1980 (signed to press 19 Nov 80) pp 154-158

[Article by O.T. Oleynik from collection of works "Holography and Optical Information Processing in Geology", edited by Professor S.B. Gurevich and Candidate of Technical Sciences O.A. Potapov, Leningrad Physicotechnical Institute imeni A.F. Ioffe, USSR Academy of Sciences, 500 copies, 181 pages]

[Text] Since the basic intermediate carrier of seismic information at the present time is a photographic layer, the author studies its information characteristics and shows that it is possible to obtain a dynamic range of seismoholographic images of up to 65 dB and more.

The method of seismoholographic transformations on a plane makes it possible to plot a field of imaginary emission sources and permits scale transformation of this field. Scale transformation makes it possible to transfer each imaginary source to the point of intersection of a reflecting boundary with a central beam [1]. The transformed field of imaginary points describes geometrically the field of mirror-reflecting boundaries at the points where they intersect with the central beam.

In view of the fact that the imaginary emission points are formed by broad seismic pulses, each imaginary point has the form of superimposed rhombs formed by the intersection of a pair of cross bearings [2]. The rhombs' long diagonals coincide with the normals to the central beams. One rhomb corresponds to one observation base and one detonation point. The sequence of normal rhombs interpolates the reflecting boundary in the same manner as when graphic plotting by the method of imaginary points is used [3].

In contrast to the graphic realization of the method of imaginary points, in seismoholographic transformations the essential role is played by the width of the seismic pulse and its amplitude. They determine the degree of overlap of adjacent normal rhombs and the continuity of the correlation of the reflecting boundaries.

In most cases the parameters of the seismoholographic transformations can be chosen in such a manner that each point of a seismic boundary is accumulated by n signals, where n is the number of observation points of a single installation [2]. This creates conditions for improving the signal-to-noise ratio by a factor of $\sqrt{n}$.

It is a well-known fact that with magnetic tape it is possible to reproduce an analog electrical signal in a dynamic range on the order of 50 dB. Such a dynamic range is sufficient to transmit, without amplitude distortion, all the information obtained during recording times that are longer than 1 s [4].

The realization of 24-fold holographic accumulation expands the dynamic range of the resulting materials by a factor of 24 and extends it up to 54 dB.

When processing the materials of S-fold overlaps by the seismic holography method within the limits of a profile length equal to the observation base line, S rhombs that are normal to the central beam are formed, with the number of accumulations within the limits of the normal being n. For all practical purposes, these normals overlap completely (the overlap factor is $1 - 1/S$) and form in the field of the seismoholographic image a resulting normal with $nS(1 - 1/S)$ accumulations. In the case of an S-fold observation system, this improves the signal-to-noise ratio by a factor of $\sqrt{nS(1 - 1/S)}$ and causes an enlargement of the same magnitude of the dynamic range. In particular, for $S = 12$ the signal-to-noise ratio is improved by a factor of 16, while the dynamic range of the seismoholographic images can reach 65 dB.

An improvement in the signal-to-noise ratio that appears after summation makes it possible to distinguish weak signals that remain outside the field of vision during analysis of the primary materials. This is the basic advantage of summing systems.

As experience has shown, the high efficiency of summation operations is the basis for their use in the primary stage of the analysis of seismic information [5]. At the present time, the method of field observations and the processing of materials with respect to a common deep point [MOGT] is widely used under production conditions.

The effectiveness of summation of the seismoholographic transformation method is greater than the effectiveness of MOGT summation. This follows from the fact that during the realization of S-fold MOGT in the plane of an image, on a profile length equal to one observation base line, n common deep points are formed with a number of accumulations (for example, 24 points with 12 accumulations); that is, the gain in the signal-to-noise ratio is only $\sqrt{S}$. For a 12-fold system it will be 3.5, which corresponds to an extension of the dynamic range to 51 dB [6].

There arises the question of which accumulation technique is preferable: 24 points with 12 accumulations each (MOGT) or one normal with 264 accumulations? The unambiguous choice of the transformation technique is determined by the nature of the seismic material and the purpose of the field investigations.

Under conditions where high resolution along the profile is necessary--that is, when the work is aimed at finding small structural elements--preference should be given to differential summation with respect to individual points, as is done in MOGT. If homogeneous strata with poorly contrasting transitions are being investigated, then in order to detect weak reflections it is necessary to increase the statistical accumulation effect and here the capabilities of the seismic holography method should doubtlessly be used.

The processing of field seismic materials by the seismic holography method demonstrated the validity of the premises explained above [7].

There exists yet another fact that demonstrates the advisability of increasing the number of summed signals: the statistical effect of reducing the summary signal's dispersion with respect to a single measured signal.

This effect is described by the method of least squares as

$$\sigma_m = \frac{\sigma_o}{\sqrt{m-1}},$$

where σ_m, σ_o = dispersion of the sum and a single signal; m = number of summed signals.

Thus, for a 12-fold observation system, seismoholographic transformations on a plane reduce the root-mean-square deviations of the original signals' phases and amplitudes by a factor of 16, while for MOGT the reduction factor is 3.5. From this follows the conclusion that as far as noise stability and accuracy of the obtained images are concerned, the method of seismoholographic transformations on a plane is better than MOGT by a factor of 5, given the same original information.

On the other hand, in order to achieve the same results with respect to the indicated parameters, the seismoholographic transformation method can use original information about phase and amplitude dispersions that exceed the allowable dispersions for MOGT by a factor of 5.

If we take as an example an allowable phase dispersion on an image of 0.1 period (5-10 m in depth), original MOGT materials must be prepared with an accuracy of no worse than 0.35 period (17-35 m), while for the seismoholographic method the permissible error in the original data input is 1.7 periods, or 85-170 m.

This fact makes it possible to use the seismoholographic plotting technique to process seismic materials with a low level of orderliness and under conditions of limited knowledge of prior data about the section.

BIBLIOGRAPHY

1. Zav'yalov, V.D., "Introduction to Seismic Holography on a Plane: Review," SER. REGION., RAZVED. I PROMYSL. GEOFIZIKA, Moscow, VIEMS [All-Union Scientific Research Institute of Economics of Mineral Raw Materials and Geological Exploration], No 27, 1969, p 20.

2. Oleynik, O.T., "Holographic Transformations of Seismograms on a Plane," DEPON. RUKOP., No 3 (77), 1978, p 149.

3. Zav'yalov, V.D., and Timoshin, Yu.V., "Holographs of Reflected Waves for Curvilinear Interfaces and Their Interpretation," IZV. AN SSSR, SER. GEOFIZICH., No 2, 1955.

4. Kauzov, K.M., Krylov, I.B., Kuznetsov, V.V., et al., "Using Nonexplosive Excitation Sources in Structural Seismic Surveying," in "Problemy vibratsionnogo prosvechivaniya Zemli" [Problems in the Vibration Transillumination of the Earth], Moscow, Izdatel'stvo "Nauka", 1977, pp 162-185.

5. Turchanenko, N.T., and Dyadyura, V.A., "Digital Seismic Surveying in the Oil and Gas Provinces of the Ukrainian SSR," GEOFIZICH. ZHURNAL, Kiev, Izdatel'stvo "Naukova dumka", No 1, 1979, pp 81-90.

6. Perel'man, S.A., "Experimental Data on the Non-Gaussian Distribution of Random Components of Geophysical Observations," IZV. AN SSSR, SER. GEOFIZICH. FIZIKA ZEMLI, No 9, 1969.

7. Rakova, N.S., Oleynik, O.T., and Kmitsikevich, I.Ye., "Some Results of the Holographic Transformation of Seismograms on a Photoaccumulative Plane," DEPON. RUKOP., No 5 (91), 1979, p 111.

UDC 550.834

THE ISOCHRONE METH D IN SEISMIC HOLOGRAPHY

Leningrad GOLOGRAFIYA I OPTICHESKAYA OBRABOTKA INFORMATSII V GEOLOGII in Russian
1980 (signed to press 19 Nov 80) pp 159-166

[Article by V.N. Moskalenko and O.A. Vorob'yev from collection of works "Holography and Optical Information Processing in Geology", edited by Professor S.B. Gurevich and Candidate of Technical Sciences O.A. Potapov, Leningrad Physicotechnical Institute imeni A.F. Ioffe, USSR Academy of Sciences, 500 copies, 181 pages]

[Text] The authors explain the results of modeling that they carried out and that indicate the area of applicability of methods for transforming a wave field T_0 when plotting deep sections, depending on the velocity model of the medium being studied.

A new field has appeared in seismic methodology: seismic holography [1,2], the basic assignment of which is to reproduce a deep section by transformation of the wave field. In a number of organizations in this country that are involved in the processing of seismic data, analog equipment has been developed for the processing of continuous seismic profiling materials by the method of isochrones (by V.D. Zav'yalov [3] in L'vov, by V.I. Dubyanskiy in Voronezh, by Ye.Yu. Yakush [4] in Krasnodar and in other places). In the Southern Branch of the USSR Academy of Sciences' Institute of Oceanology, computers have been used for the mathematical modeling of the method of isochrones realized in these instruments, which are devices for plotting deep seismic sections.

The technique used in seismic profiling work determines the form of the observed wave field. In single-channel seismic profiling, where the seismic signal source and receiver are collocated (this profiling technique is sometimes called the central beam (TsL) method), the wave field is recorded normally to the reflected rays. In seismic surveying it is called field T_0. In multichannel profiling, the receiving system consists of 24 or more receivers arranged in a straight line. As a rule, the source is placed at one of the ends of this line. In this case, a spatial wave field with multiple overlapping (6-, 12-, 24-fold or more) is registered.

In this article we discuss methods for transforming wave field T_0 obtained by single-channel seismic profiling. The special feature of field T_0 is that the isochrones for the two classes of waves--reflected and diffracted--are described by the same equations. The registration time of a reflected and a diffracted wave at a reception point is always twice the time of propagation of the wave from the source to the reflecting boundary or the diffracting point. Wave field $T_0/2$ should be used

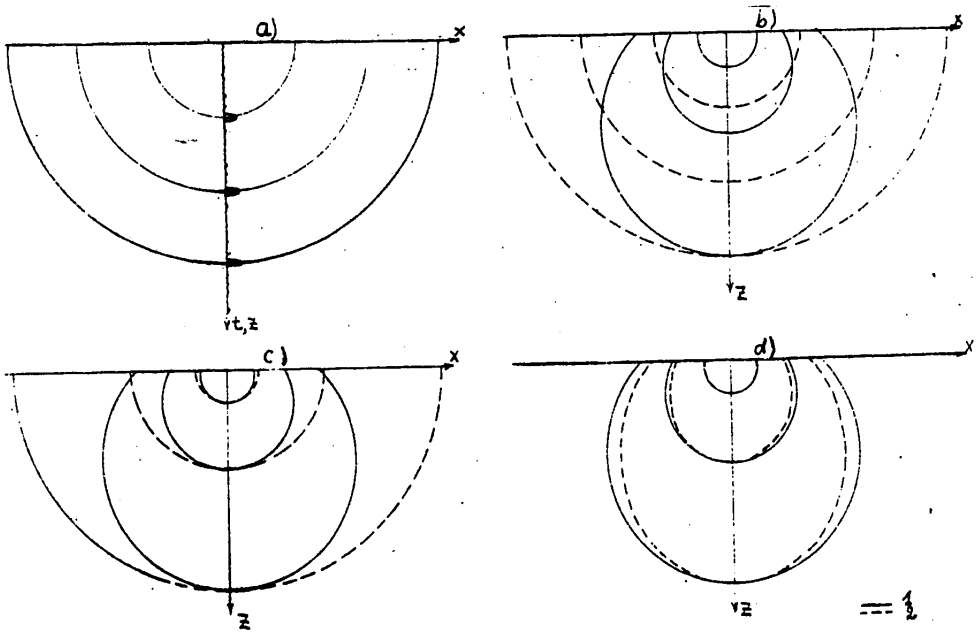

Figure 1. Methods of transforming wave field $T_0/2$ into a deep section: a. circular scanning of the seismic track; b. first method, V = const.; c. second method, $V_{cp} = \Phi (Z_{max})$; d. third method, $V_{cp} = \Phi (Z)$; 1 = true isochrone; 2 = isochrone calculated by an approximate method.

to obtain an image of a reflecting boundary or a diffracting point. Otherwise, if the T_0 field is used we will obtain an image of the trajectory of an imaginary source in the case of reflected waves or a cloud of points corresponding to a diffracting element.

The essence of the isochrone method is well known. On a seismogram, each seismic wave pulse corresponds (in the ideal case) to a reflecting area or diffracting point that can be located (generally speaking) at any point on an isochrone (Figure 1a). If there is preliminary information on the structure of the section and the probable angles of inclination of the reflecting boundaries, the area of existence of the isochrone is reduced. Isochrones are constructed for all the seismic pulses. The brightness (intensity) of the isochrone is determined by the seismic signal's amplitude. Thus, an isochrone that has reached a reflecting boundary or a diffracting point is depicted by a brighter line. For adjacent points on a profile, isochrones corresponding to the same reflecting element will be arranged side by side, while their envelope will depict the location of the reflecting element. The envelope is not found in any of the deep section plotting devices, which use the points of intersection of adjacent isochrones. At the point of intersection, the image's brightness increases. The set of bright points forms the image of a line that corresponds to the reflecting boundary with adequate accuracy. The method of isochrones transforms a field of diffracted waves into a image of the diffraction points.

The accuracy of the isochrone method is determined by the accuracy with which the shape of the wave front is calculated. The degree of distortion of the real

geological section reproduced by the isochrone method depends on the accuracy with which the wave front is plotted. In order to calculate the shape of the wave front, several approximate methods are used that differ in the velocity models used for the medium.

In an example of a very simple model of a medium--a gradient half-space in which the velocity increases with depth according to a linear law--we will demonstrate the differing nature and magnitude of the distortions resulting from the use of approximate methods of transforming wave fields into deep sections.

First Method. Let us replace the gradient medium by a medium with a constant average velocity in such a manner that the depth of occurrence of the reflecting element corresponding to the maximum registration time, as calculated by by approximate and accurate methods, coincides. For a medium with a constant wave front velocity there exist neighborhoods

$$X^2 + Z^2 = (V_{cp} \cdot T)^2, \tag{1}$$

the radius of which changes proportionally to the wave's arrival time. All isochrones differing in time by the constant value ΔT are equally remote from each other within the limits of the entire section (Figure 1b). The true isochrones are also presented in this figure. The equation of the isochrone for the gradient half-space is expressed in analytical form:

$$X^2 + \left[Z - \frac{1}{\beta}(ch(V_0 \beta t) - 1)\right]^2 = \frac{1}{\beta^2} sh^2(V_0 \beta t). \tag{2}$$

From the figure it is obvious that the first method for transforming a wave field into an image of the medium is the most approximate one and is characterized by the maximum distortions.

Second Method. This transformation method allows for a change in velocity in the medium with depth, but the wave front is constructed on the assumption that up to a given isochrone (that is, to the depth of the ray's maximum vertical penetration), the medium is characterized by the constant average velocity

$$X^2 + Z^2 = (V_{cp}(Z_{max}) \cdot T)^2. \tag{3}$$

This method is realized in the holographs developed in L'vov and Voronezh (by Zav'yalov and Dubyanskiy). In this second method the seismic track is preliminarily transformed and the temporal axis is transformed into a depth axis with respect to the change in the average velocity with depth. Circular scanning is then carried out on a mirror cone and the isochrones are obtained.

The second method's accuracy varies sharply, depending on the reflecting boundary's angle of inclination (Figure 1c). The larger the reflecting boundary's angle of inclination, the higher with respect to the isochrone (the section) the reflecting element must be located, the greater the error admitted in the velocity, and the more significant the discrepancy between the true and approximate wave fronts. From the figure it is obvious that even for a boundary angle of inclination of more than 10°, an isochrone calculated according to the second method moves quickly away from the real one. At a depth of about 9 km the difference is about 1.0 km, while the inclination of the boundary at that point does not exceed 20°.

Considering the large distortions contributed by the second method to the transformation of wave fields into a deep seismic section, its area of applicability is

extremely limited. It is suitable for mediums characterized by boundary surfaces with small angles of inclination amounting to only a few degrees. For almost horizontal mediums, however, it is possible to confine oneself to stretching the temporal section with respect to depth proportionally to the propagation rate of the seismic waves. Consequently, if the wave field is represented by reflected waves, the necessity of transformation by circular scanning is absent. If there are diffracted waves in the wave field, the second transformation method makes it possible to "purify" the section of these waves (so-called "whiskers"), but in connection with this a general transformation background will appear. It should again be emphasized that even in the case of diffracted waves the second method is suitable for mediums in which the diffraction points are located close to the vertical axis.

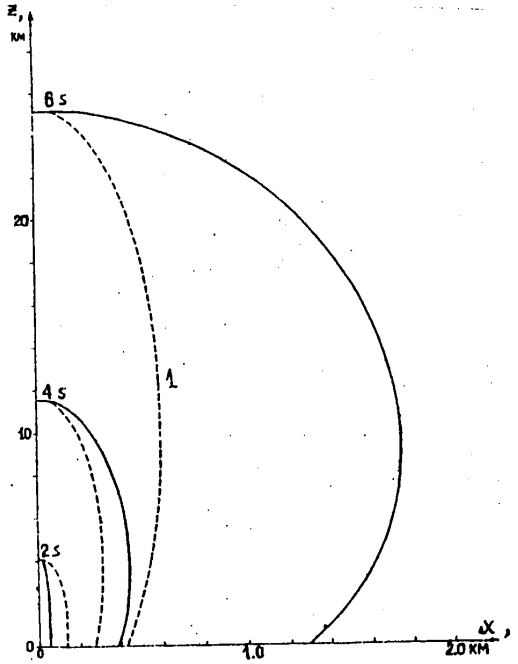

Figure 2. Absolute error in calculating an isochrone according to the third method: 1. area of distortions of no more than 4 percent.

Third Method. As does the second, this method for transforming a wave field into a deep section allows for a change in the average velocity with depth, but differs in that the isochrone is calculated with a variable velocity

$$X^2 + Z^2 = (V_{cp}(Z) \cdot T)^2, \qquad (4)$$

The wave front's curvature changes continuously, depending on the velocity at the given depth (Figure 1d). The third transformation method is more accurate than the two outlined above. A wave front calculated by the third method has a form that is close to the real one. For example, the maximum difference in the position of isochrone $T_0/2 = 4$ is 0.43 km (in the second method it is more than 5 km).

The third method for transforming a wave field into a deep section also contributes distortions, with their value basically increasing as the wave front propagation time does and (to a lesser extent) as the velocity gradient does. If we set the permissible isochrone distortion at no more than 0.04X, where X is the isochrone's x axis, then all isochrones with time $T_0/2$ of less than 3.4 s are located in the area of permissible distortions (Figure 2). To a depth of about 9 km, the section will be distorted within allowable limits.

A curvilinear vertical cone is no longer suitable for the equipment realization of the third method. In the third method it is necessary to have a preliminary calculation of the isochrone for each moment of time and to derive it on an accumulating device, such as a cathode-ray memory tube [4], or a computer's memory, or on a photographic layer.

The third method for transforming a wave field into a deep section was tested on a six-layer model that is close to a real section of the Black Sea basin. The

velocity curve was given in the form of a broken line: at depths of 0, 2, 4, 6, 10 and 20 km, the following velocity values were assumed: 1.5, 2, 3, 6 and 8 km/s. In each layer the velocity changes according to a linear law, with no discontinuities at the boundaries. This velocity curve was used to calculate the curve of the average velocities, after which the third method was used to calculate the approximate isochrones. For isochrone $T_0/2$ = 3 s, five points were checked by an accurate solution according to the "Check of the Direct Problem" program formulated by M.Ye. Romanov, a worker at the Novosirbirsk Computer Center, Siberian Department, USSR Academy of Sciences. The results of the check with the precise solution are presented in the table.

Distance with respect to X, km	4.387	4.031	3.508	2.709
Depth Z, km	1.0	2.0	3.0	4.0
Error ΔT, s	-0.0081	0.0181	0.0754	0.0826
Error ΔX, km	-0.0122	0.0272	0.1319	0.1652

From the results of the calculations it is obvious that the absolute error increases with depth. At a depth of 4 km, the temporal error is 83 ms and the distance error is 165 m. The relative accuracy or degree of distortion of the section is about 3 percent. It is noteworthy that the accuracy of the construction of a deep section by the third method does not depend on the reflecting boundaries' angle of inclination. This is quite obvious from the figures and the table. The greater the boundary's angle of inclination, the shallower the depth at which the boundary must lie, while when the depth decreases there is a decrease (!) in the magnitude of the absolute error.

The mathematical modeling that has been carried out shows that the third method for transforming a wave field into a seismic deep section can be used when processing continuous seismic profiling data.

The programs for computing the isochrones were written in FORTRAN, for a BESM-4m high-speed computer.

BIBLIOGRAPHY

1. Vasil'yev, S.A., Savarenskiy, V.Ye., and Urupov, A.K., "Results of the Transformation of Seismic Recordings of Profile Observations Into Deep Sections on the Basis of the Principles of Seismoholography," PRIKLADNAYA GEOFIZIKA, Moscow, Izdatel'stvo "Nedra", No 71, 1973, pp 3-14.

2. Timoshin, Yu.V., "Impul'snaya seysmicheskaya golografiya" [Pulsed Seismic Holography], Moscow, Izdatel'stvo "Nedra", 1978, 286 pp.

3. Zav'yalov, V.D., and Tsimbrovskaya, L.I., "Methods for the Holographic Transformation of Seismic Information," in "Metod, vopr. seysmorazvedki" [Methods and Questions in Seismic Surveying], L'vov, 1972, pp 28-36.

4. Yakush, Ye.Yu., and Gavryushin, V.B., "An Electronic Plotting Device for Deep Seismic Sections," GEOFIZICHESKAYA APPARATURA, Leningrad, No 65, 1978, pp 70-74.

UDC 621.391.2:535.241

ON THE REALIZATION OF COMPLEX FILTERS IN POLARIZED LIGHT

Leningrad GOLOGRAFIYA I OPTICHESKAYA OBRABOTKA INFORMATSII V GEOLOGII in Russian 1980 (signed to press 19 Nov 80) pp 167-173

[Article by V.P. Ivanchenkov and P.V. Mineyev from collection of works "Holography and Optical Information Processing in Geology", edited by Professor S.B. Gurevich and Candidate of Technical Sciences O.A. Potapov, Leningrad Physicotechnical Institute imeni A.F. Ioffe, USSR Academy of Sciences, 500 copies, 181 pages]

[Text] The authors discuss a method of synthesizing complex spatial filters on the basis of the properties of polarized light. In an example of a concrete system, they demonstrate the possibility of obtaining a filter with a real alternating transfer function. In order to synthesize the complex filter, the function describing it is presented in the form of the sum of real and imaginary parts, the signs of both of which can change. The authors show that when the system's elements are arranged in a certain way and an additional phase shift between the components of the light field's polarization is introduced, the filter's complex transfer function can be synthesized.

In connection with the optical filtration of signals, it is frequently necessary to synthesize both alternating and complex functions. The basic feature of the realization of complex spatial filters is that in any recording medium, only signals described by real non-negative functions can be recorded. When the widely known methods for synthesizing such filters in analog and discrete form are used, they make it possible to obtain a useful response located outside a system's optical axis, which creates definite difficulties during processing [1,2].

The method proposed in [3] for carrying out complex spatial filtration on the basis of the properties of polarized light forms a filtered image on the optical axis and has the advantage of a large format, but it requires the use of special film of the "Polaroid Vectograph" type, which has low resolution.

In this article we discuss a method for synthesizing complex spatial filters in polarized light that does not require the use of special carriers for its realization.

A special but practically important case of spatial filtration is the obtaining of a filter with a real alternating transfer function. Let us discuss the possibility

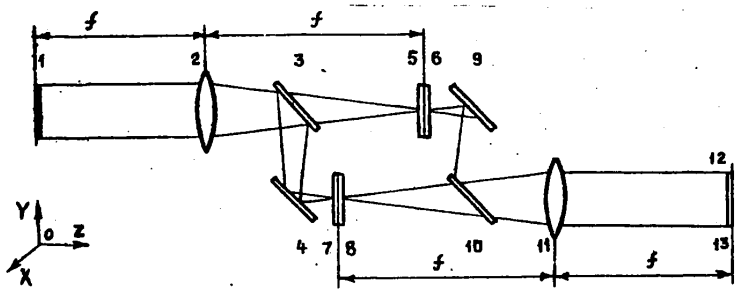

Figure 1. Optical diagram of filtration of alternating function: 1. plane of input image; 2, 11. Fourier lenses; 3, 10. semitransparent mirrors; 4, 9. mirrors; 5, 7. polarizers; 6, 8. frequency planes with optical transparencies; 12. analyzer; 13. plane of the output image.

of its realization, using as an example the system represented in Figure 1. A transparency with the amplitudinal transmission coefficient $\Psi(x,y)$ is located in the forward focal plane of lens 2.

Polarizers 5 and 7, the planes of transmission of which are parallel to the OX and OY axes, respectively, are set up in frequency planes 6 and 8 in front of the transparencies. In order to calculate optical devices in polarized light it is convenient to use matrix methods [4]. In our further analysis we will use (Dzhons's) method and limit ourselves to a quasimonochromatic approximation. In connection with this, the light beams at the outlets of polarizers 5 and 7 can be represented as Dzhons vectors:

$$\begin{bmatrix} E_x(x_f, y_f) \\ 0 \end{bmatrix} \text{ and } \begin{bmatrix} 0 \\ E_y(x_f, y_f) \end{bmatrix}, \tag{1}$$

where $E_x(x_f,y_f)$ = component of the beam that has passed through polarizer 5; $E_y(x_f,y_f)$ = component of the beam that has passed through polarizer 7. Let us assume that the moduli of these components are equal:

$$|E_x(x_f, y_f)| = |E_y(x_f, y_f)| = \frac{1}{2}\mathcal{F}\{\Psi(x,y)\}, \tag{2}$$

where $F\{\ \}$ = symbol of Fourier transformation. In the general case, the amplitude coefficient of the optical transparency's transmission coefficient can be represented as

$$t(x_f, y_f) = \frac{1}{2}[1 + g(x_f, y_f)], \tag{3}$$

where $g(x_f,y_f)$ = a real function limited by the values

$$-1 < g(x_f, y_f) < 1. \tag{4}$$

Optical transparencies 6 and 8, on which are recorded some functions $g_1(x_f,y_f)$ and $g_2(x_f,y_f)$ that satisfy condition (4), will have transmission coefficients $t_1(x_f,y_f)$ and $t_2(x_f,y_f)$. The light beams modulated by $t_1(x_f,y_f)$ and $t_2(x_f,y_f)$ can be represented as

$$\frac{1}{2}\begin{bmatrix} \mathcal{F}\{\Psi(x,y)\}\, t_1(x_f, y_f) \\ 0 \end{bmatrix} \text{ and } \begin{bmatrix} 0 \\ \mathcal{F}\{\Psi(x,y)\} t_2(x_f, y_f) \end{bmatrix}. \tag{5}$$

Provided that the state of polarization of the output beam is not taken into consideration, the operation of analyzer 12 can be described by the vector line [3]

$$[\cos\varphi \sin\varphi], \tag{6}$$

where ϕ = angle between the plane of transmission of analyzer 9 and the OX axis. In this case the resulting distribution of the scalar amplitudes in the plane 13 of the output image is

$$\Psi_1(-x_1-y_1) = \frac{1}{g}\mathcal{F}\{[\cos\varphi \sin\varphi]\begin{bmatrix}\mathcal{F}\{\Psi(x_f,y_f)\}t_1(x_f,y_f)\\ \mathcal{F}\{\Psi(x_f,y_f)\}t_2(x_f,y_f)\end{bmatrix}. \tag{7}$$

When (3) is taken into consideration, (7) can be written as

$$\Psi_1(-x_1-y_1) = \frac{1}{g}\mathcal{F}\{\mathcal{F}[\Psi(x,y)]\,[\cos\varphi + \sin\varphi + g_1(x_f,y_f)\cos\varphi + g_2(x_f,y_f)\sin\varphi]\}. \tag{8}$$

Let us assume that $\phi = -\pi/4$ and $g_1(x_f,y_f) = -g_2(x_f,y_f)$. In this case, $t_1(x_f,y_f)$ and $t_2(x_f,y_f)$ are the positive and negative recording of alternating function $g(x_f,y_f)$. Expression (8) then takes on the form

$$\Psi_1(-x_1-y_1) = \frac{1}{4}\mathcal{F}\{\mathcal{F}[\Psi(x,y)]\,g(x_f,y_f)\}. \tag{9}$$

Thus, the desired alternating transfer function of the filter can be realized quite simply in accordance with (4) and (9).

In order to synthesize the complex filter, let us represent the function describing the filter as the sum of real and imaginary parts, the signs of both of which can change:

$$H(x_f,y_f) = A(x_f,y_f) + iB(x_f,y_f). \tag{10}$$

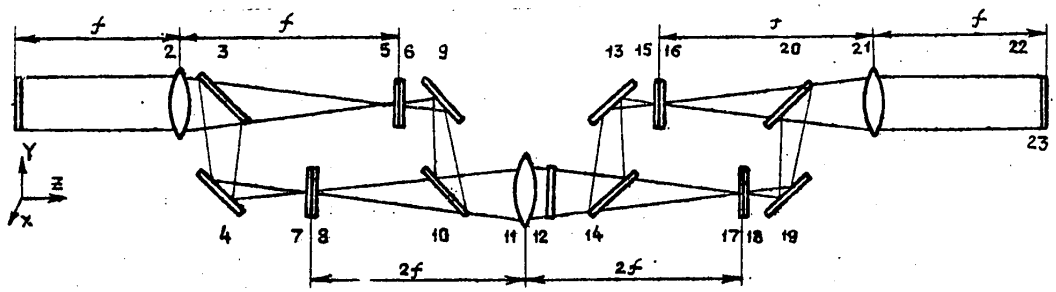

Figure 2. Optical diagram of complex spatial filtration: 1. plane of the input image; 2, 21. Fourier lenses; 3, 10, 14, 20. semitransparent mirrors; 4, 9, 13, 19. mirrors; 5, 7, 15, 17. polarizers; 6, 8, 16, 18. frequency planes with optical transparencies; 11. lens; 12. phase plate; 22. analyzer; 23. plane of the output image.

Let us discuss the possibility of realizing a function of this type with the help of the system depicted in Figure 2. It consists of two units, each of which synthesizes a real bipolar function according to the method previously discussed.

In order to obtain the imaginary part, between the units we introduce phase plate 12, which introduces a relative difference in phases between the polarization

components. Its matrix representation has the following form [3]:

$$\begin{bmatrix} \exp(i\vartheta) & 0 \\ 0 & \exp(-i\vartheta) \end{bmatrix}. \tag{11}$$

We will now discuss the possibility of realizing the complex function by turning pairs of polarizers 5, 7 and 15, 17 and phase plate 12, relative to their own optical axes, through angles w_1, θ and w_2, respectively.

In frequency planes 6 and 8, the distribution of the amplitudes can be represented as:

$$\frac{1}{4}\mathcal{F}[\Psi(x,y)]\begin{bmatrix}\cos w_1 \\ \sin w_1\end{bmatrix}[1-g(x_f,y_f)], \tag{12}$$

$$\frac{1}{4}\mathcal{F}[\Psi(x,y)]\begin{bmatrix}\cos(w_1+\frac{\pi}{2}) \\ \sin(w_1+\frac{\pi}{2})\end{bmatrix}[1+g(x_f,y_f)]. \tag{13}$$

The lenses and free space do not exert any effect on the polarization of the light beams. This makes it possible to examine, independently of each other, the scalar and polarization characteristics of the light beams between polarizers 5, 7 and 15, 17.

Lens 11 performs the function of transferring the images, it being the case that planes 6, 8 and 16, 18 are situated at a distance of double its focal length away from it.

The rotation of phase plate 12 through angle θ relative to the OX axis is determined by the product of three matrices [4]:

$$M_1 = \begin{bmatrix}\cos\theta & \sin\theta \\ -\sin\theta & \cos\theta\end{bmatrix}\begin{bmatrix}\exp(i\vartheta) & 0 \\ 0 & \exp(-i\vartheta)\end{bmatrix}\begin{bmatrix}\cos\theta & \sin\theta \\ -\sin\theta & \cos\theta\end{bmatrix}. \tag{14}$$

Let us assume, as before, that the amplitude transmission coefficients of transparencies 16 and 18 are

$$t_1'(x_f,y_f) = \frac{1}{2}[1-g'(x_f,y_f)],$$
$$t_2'(x_f,y_f) = \frac{1}{2}[1+g'(x_f,y_f)].$$

By analogy with (14), the matrix representation of the set of the second pair of polarizers 15 and 17, rotated relative to their respective optical axes through angle w_2, and transparencies 16 and 18 has the form

$$M_2 = \frac{1}{8}\cdot\begin{bmatrix}\cos w_2 & \sin w_2 \\ -\sin w_2 & \cos w_2\end{bmatrix}\begin{bmatrix}1-g'(x_f,y_f) & 0 \\ 0 & 1+g'(x_f,y_f)\end{bmatrix}\begin{bmatrix}\cos w_2 & \sin w_2 \\ -\sin w_2 & \cos w_2\end{bmatrix}.$$

The distribution of the scalar amplitudes in the rear focal plane 23 of lens 21 (which carries out the Fourier transform), allowing for the effect of analyzer 22, can then be represented as

$$\Psi_2(-x,-y) = \frac{1}{64}\mathcal{F}\{\mathcal{F}[\Psi(x,y)][\cos\varphi \sin\varphi]^{\times}, \tag{15}$$
$$\times M_2 M_1 \begin{bmatrix}\cos w_1 - \sin w_1 - g(x_f,y_f)(\cos w_1 + \sin w_1) \\ \cos w_1 + \sin w_1 + g(x_f,y_f)(\cos w_1 - \sin w_1)\end{bmatrix}\},$$

where

$$\frac{1}{64}\,[\cos\varphi \sin\varphi]\,M_2 M_1 \begin{bmatrix} \cos w_2 - \sin w_2 - g(x_f, y_f)(\cos w_2 + \sin w_2) \\ \cos w_2 + \sin w_2 + g(x_f, y_f)(\cos w_2 - \sin w_2) \end{bmatrix} \tag{16}$$

is nothing other than the filter's transfer function $H(x_f, y_f)$.

Assuming in (16) that $w_1 = -\pi/4$, $\theta = \pi/2$, $\delta = \pi/4$, $w_2 = \pi/4$, $\phi = \pi/2$, after the transformations we obtain

$$H(x_f, y_f) = \frac{1}{64}\{[g(x_f, y_f) - g'(x_f, y_f)] + i[g(x_f, y_f) + g'(x_f, y_f)]\} \tag{17}$$

For $w_1 = w_2 = \pi/4$, $\theta = \pi/2$, $\delta = \pi/4$, $\phi = 0$,

$$H(x_f, y_f) = \frac{1}{64}\{[g(x_f, y_f) - g'(x_f, y_f)] - i[g(x_f, y_f) + g'(x_f, y_f)]\}. \tag{18}$$

Thus, from (17) and (18) it follows that the system depicted in Figure 2 makes it possible to synthesize the filter's complex transfer function. The analysis that was made of expressions (16), (17) and (18) shows that for inaccuracy in the installation of the polarizers amounting to $\pm 1°$, the values of the factors entering the complex transfer function will change less than 0.01. Besides this, it should be mentioned that a change in the angle of rotation of phase plate 12 will have an effect only on the coefficients for the imaginary part of the complex transfer function, leaving the real part unchanged. This makes it possible to control, within certain limits, both the amplitude and phase of the filter's complex transfer function.

The filter that we have been discussing has a positive property: the capability of creating at its output a unique, axial, useful signal. In order to realize the filter it is possible to use such well-known recording mediums as photographic film or plates with high resolution.

BIBLIOGRAPHY

1. Gudmen, D., "Vvedeniye v fur'ye-optiku" [Introduction to Fourier Optics], Moscow, Izdatel'stvo "Mir", 1970.

2. Akayev, A.A., and Mayorov, S.A., "Kogerentnyye opticheskiye vychislitel'nyye mashiny" [Coherent Optical Computers], Leningrad, Izdatel'stvo "Mashinostroyeniye", 1977.

3. Marathay, A.S., "Realization of Complex Filters With Polarized Light," J. OPT. SOC. AMER., Vol 59, No 6, 1968.

4. Dzherrard, A., and Berch, Dzh., "Vvedeniye v matrichnuyu optiku" [Introduction to Matrix Optics], Moscow, Izdatel'stvo "Mir", 1978.

UDC 550.834

PROCESSING SEISMIC SIGNALS WITH DEPICTION OF DYNAMIC CHARACTERISTICS

Leningrad GOLOGRAFIYA I OPTICHESKAYA OBRABOTKA INFORMATSII V GEOLOGII in Russian 1980 (signed to press 19 Nov 80) pp 174-178

[Article by L.Ya. Maslina and L.P. Dunayeva from collection of works "Holography and Optical Information Processing in Geology", edited by Professor S.B. Gurevich and Candidate of Technical Sciences O.A. Potapov, Leningrad Physicotechnical Institute imeni A.F. Ioffe, USSR Academy of Sciences, 500 copies, 181 pages]

[Text] The authors explain a method for studying the dynamic characteristics of seismic waves that makes it possible to obtain additional information for the prediction of the presence of hydrocarbon deposits.

The use of coherent optical systems for the processing of geophysical information is an urgent problem [1]. In particular, the utilization of such systems for the processing of large volumes of seismic information is promising.

Let us discuss a method of processing seismic signals obtained by the reflected wave method during geophysical investigations for the purpose of finding gas and oil deposits.

Since reflecting boundaries coincide with the boundaries of lithological-stratigraphic horizons, a study of the nature of the reflections makes it possible to obtain data on the structure of the geological strata and, in particular, the presence of a nonuniformity of the deposit type.

Changes in the spectral composition of the waves and their intensity have various causes: absorption of high frequencies, a change in the shape of the vibrations at interfaces, interference from nearby boundaries and so on. Because of the diversity of the wave propagation and interference conditions, the problem of using seismic data to discover directly the effect of a deposit is quite complicated. In order to increase the nonambiguity of the decision made about the presence of an oil or gas deposit in a section, it is necessary to conduct an integrated examination of the diagnostic indicators inherent in a deposit, using various seismic (and geophysical) parameters [2,3].

The special feature of the proposed method is that information about the dynamic characteristics of the waves is depicted invariantly on an amplitude and time scale, which insures the possibility of using coherent optical systems for the operational

identification of anomalous effects caused by deposits. The effects are identified by the method of optical matched filtration, using standards obtained for surveyed deposits in the territory being investigated as the matched filters. As a result, it proves to be possible to make an operational evaluation, under field conditions (and on a real time scale), of the prospects of the section under investigation.

In the method for processing seismic signals that we are discussing, information is extracted from the relative change in the periods and amplitudes of seismic vibrations with respect to a section. Before this is done, we must synthesize the field of relative phase changes, which can be registered in any previously assigned scale invariantly to the amplitude and time scale of the incoming seismic signal [4,5].

The original signals are a seismic station's output signals, stored in analog or digital memory systems and read in the form of electrical signals.

In order to construct the field of relative phase changes, the seismic vibrations on each track are formalized in the form of pulses, the temporal position of which corresponds to the maximum (or minimum) amplitude of the vibration.

The distance between the pulses corresponds to the seismic vibrations' period. In the chosen time interval, the periods of the vibrations for each of the tracks are compared.

The field of the relative phase changes is synthesized in the form of signs on each track that characterize the relative change in the duration of each subsequent period of the vibrations relative to each preceding one along the track.

As a result of the comparison, the following decisions are made. If the duration of the subsequent period is greater than that of the preceding one, this situation is marked by the sign "+"; if it is less, it receives a "-" sign. A "·" sign corresponds to equality of the periods, while when there is a "malfunction"--that is, when the duration of the period being measured exceeds a given value--no sign is given. The sequence of signs is registered on a common scale for all the tracks and over a common interval of time. The signs for adjacent tracks are compared and the zones where identical signs are grouped along a profile are noted, along with their location with respect to the seismic section's depth. An alternation of signs characterizes a change in the wave field's phase, while continuity of tracking along a profile of identical signs indicates stability of the values of a reflected wave's periods over a given time interval.

The technique can be realized in the form of a structurally simple device that can be attached to a seismic station's equipment complex and that makes it possible to obtain a preliminary evaluation of the nature of a wave field, while performing field research, for the purpose of detecting anomalous effects caused by a deposit.

Visualization of the relative deviations of a wave field's phase can be carried out on a color television screen.

At the same time, the output data can be recorded on any information carrier, such as thermal paper, in the form of signs (with the help of a thermal printing head), in the matrix of liquid crystal memories, on standard or color photographic film and so forth.

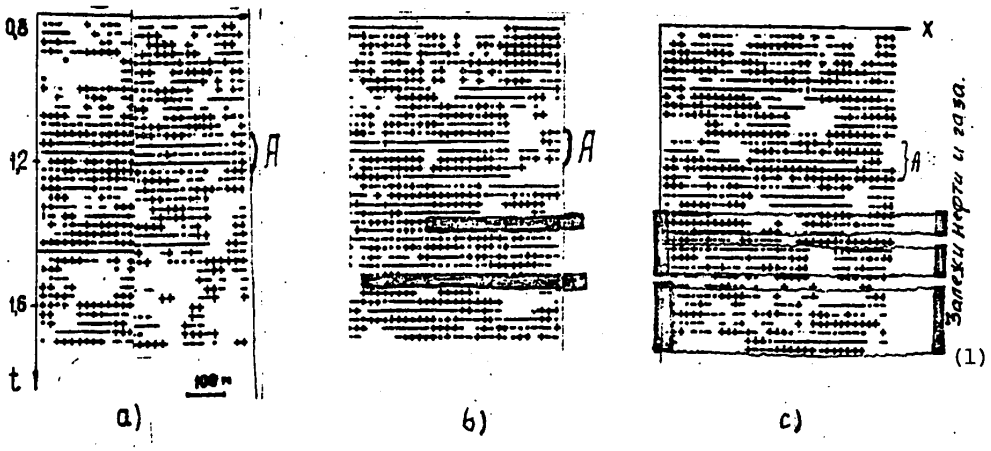

+1, -2, •3, 4

Figure 1. Fields of relative changes in periods of seismic vibrations outside a deposit (a), near a deposit (b) and within a deposit (c): 1. increase in the period; 2. decrease in the period; 3. equality of periods; 4. gas and oil deposit.
Key: 1. gas and oil deposit

Analogous transformations can also be made in order to obtain information about the nature of the change in amplitude of the seismic vibrations.

An experimental test of this processing technique was carried out on the basis of materials obtained in the Zhetybay gas and oil deposit (southern Mangyshlak), which is an area where there has b en intensive drilling. In Figure 1 we see the original material and the results of processing in three sections of the profile: outside the deposit (1a), near and on the edge of the deposit (1b), and inside the deposit (1c). It is obvious that in separate intervals in the section, at distances of up to 350 m, we can trace groups with similar sequences of phase changes (along the profile), such as group A at time 1.1-1.2 s. With some interruptions, the nature of the phase change in these groups is correlated along the profile and characterizes stable phase relationships caused by the reflecting boundaries. In the deposit section (Figure 1c), we can trace group A, but in the interval 1.4-1.7 s the traceability of the identical signs along the profile deteriorates and the field becomes less regular. In the vicinity of the deposit, on the section of the profile adjacent to its edge, we see a "column" of sequences with periodically changing signs, to the left of which the field is made much more complicated by interference. The traceability of the reflections improves over the productive bed.

These features, when used together with other anomalous parameters, can be used to predict the presence of deposits in a given region by modeling them in the form of standards of individual patterns and using a coherent optical system, the development of one of the variants of which is now taking place at MIREA [expansion unknown].

The automatic processing of seismic information, with depiction of the field of relative phase changes on a real time scale, determines the possibility of using the

model of a signal to isolate information about the presence of features determining the boundaries of a deposit.

BIBLIOGRAPHY

1. Potapov, O.A., "Opticheskaya obrabotka geofizicheskoy i geologicheskoy informatsii" [Optical Processing of Geophysical and Geological Information], Moscow, Izdate'stvo "Nedra", 1977, 184 pp.

2. Berezkin, V.M., Kirichek, M.A., and Kunarev, A.V., "Primeneniye geofizicheskikh metodov razvedki dlya pryamykh poiskov mestorozhdeniy nefti i gaza" [Using Geophysical Surveying Methods for Direct Searches for Gas and Oil Deposits], Moscow, Izdatel'stvo "Nedra", 1978.

3. Polshkov, M.K., et al., "Method for Processing Seismic Information," USSR Patent No 402841, B. IZOBR., No 42, 1973.

4. Maslina, L.Ya., and Yerofeyev, G.S., "Insuring Amplitude-Temporal Invariance of Quasiperiodic Signals in Order to Identify Them in Holographic Identification Systems," MEZHVUZOVSKIY SB. NAUCH. TR. "OPTICHESKAYA GOLOGRAFIYA", No 8, 1977.

5. Maslina, L.Ya., et al., "Sposob raspoznavaniya obrazov" [Method of Identifying Forms], USSR Patent No 533949, applied for 11 June 1974, granted 7 July 1976.

11746
CSO: 8144/1928

- END -